Accepted Manuscript

Modulation of the spacer in *N,N*-bis(alkanol)amine aryl ester heterodimers led to the discovery of a series of highly potent P-glycoprotein-based multidrug-resistance (MDR) modulators

Silvia Dei, Laura Braconi, Alfonso Trezza, Marta Menicatti, Marialessandra Contino, Marcella Coronnello, Niccolò Chiaramonte, Dina Manetti, Maria Grazia Perrone, Maria Novella Romanelli, Chatchanok Udomtanakunchai, Nicola Antonio Colabufo, Gianluca Bartolucci, Ottavia Spiga, Milena Salerno, Elisabetta Teodori

PII: S0223-5234(19)30282-X

DOI: https://doi.org/10.1016/j.ejmech.2019.03.054

Reference: EJMECH 11224

To appear in: *European Journal of Medicinal Chemistry*

Received Date: 26 November 2018

Revised Date: 21 March 2019

Accepted Date: 22 March 2019

Please cite this article as: S. Dei, L. Braconi, A. Trezza, M. Menicatti, M. Contino, M. Coronnello, Niccolò. Chiaramonte, D. Manetti, M.G. Perrone, M.N. Romanelli, C. Udomtanakunchai, N.A. Colabufo, G. Bartolucci, O. Spiga, M. Salerno, E. Teodori, Modulation of the spacer in *N,N*-bis(alkanol)amine aryl ester heterodimers led to the discovery of a series of highly potent P-glycoprotein-based multidrug-resistance (MDR) modulators, *European Journal of Medicinal Chemistry* (2019), doi: https://doi.org/10.1016/j.ejmech.2019.03.054.

Graphical abstract

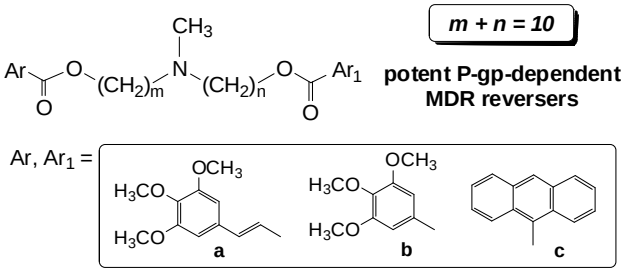

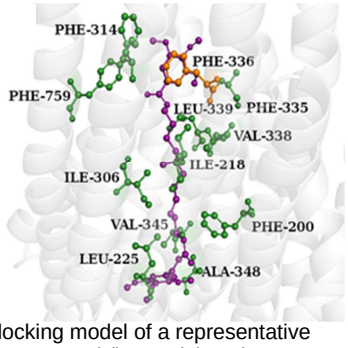

docking model of a representative compound (in purple) and P-gp

:

Modulation of the spacer in *N,N*-bis(alkanol)amine aryl ester heterodimers led to the discovery of a series of highly potent P-glycoprotein-based multidrug-resistance (MDR) modulators

Silvia Dei,[a]* Laura Braconi,[a] Alfonso Trezza,[b] Marta Menicatti,[a] Marialessandra Contino,[c] Marcella Coronnello,[d] Niccolò Chiaramonte,[a] Dina Manetti,[a] Maria Grazia Perrone,[c] Maria Novella Romanelli,[a] Chatchanok Udomtanakunchai,[e] Nicola Antonio Colabufo,[c] Gianluca Bartolucci,[a] Ottavia Spiga,[b] Milena Salerno,[f] Elisabetta Teodori[a]

[a] Department of Neuroscience, Psychology, Drug Research and Child's Health - Section of Pharmaceutical and Nutraceutical Sciences, University of Florence, via Ugo Schiff 6, 50019 Sesto Fiorentino (FI), Italy.
[b] Department of Biotechnology, Chemistry and Pharmacy, (Department of Excellence 2018-2022), University of Siena, via Aldo Moro 2, 53100 Siena, Italy
[c] Department of Pharmacy – Drug Sciences, University of Bari Aldo Moro, via Orabona 4, 70125, Bari, Italy.
[d] Department of Health Sciences - Section of Clinical Pharmacology and Oncology, University of Florence, Viale Pieraccini 6, 50139 Firenze, Italy.
[e] Department of Radiologic Technology, Faculty of Associated Medical Sciences, Chang Mai University, 50200, Thailand.
[f] University of Paris 13, Sorbonne Paris Cité, Laboratoire CSPBAT, CNRS (UMR 7244), UFR-SMBH, 74 rue Marcel Cachin, 93017 Bobigny, France

* corresponding author:
Silvia Dei, Department of Neuroscience, Psychology, Drug Research and Child's Health - Section of Pharmaceutical and Nutraceutical Sciences, University of Florence, via Ugo Schiff 6, 50019 Sesto Fiorentino (FI), Italy. Tel +39 055 4573689. Email: silvia.dei@unifi.it

Abstract

In this study, a new series of *N,N*-bis(alkanol)amine aryl ester heterodimers was synthesized and studied. The new compounds were designed based on the structures of our previous arylamine ester derivatives endowed with high P-gp-dependent multidrug resistance reversing activity on a multidrug-resistant leukemia cell line. All new compounds were active in the pirarubicin uptake assay on the doxorubicin–resistant erythroleukemia K562 cells (K562/DOX). Compounds bearing a linker made up of 10 methylenes showed unprecedented high reversal activities regardless of the combination of aromatic moieties. Docking results obtained by an *in silico* study supported the data obtained by the biological tests and a study devoted to establish the chemical stability in phosphate buffer solution (PBS) and human plasma showed that only a few compounds exhibited a significant degradation in the human plasma matrix. Ten selected non-hydrolysable derivatives were able to inhibit the P-gp-mediated rhodamine-123 efflux on K562/DOX cells, and the evaluation of their apparent permeability and ATP consumption on other cell lines suggested that the compounds can behave as unambiguous or not transported substrates. The activity of these the compounds on the transport proteins breast cancer resistance protein (BCRP) and multidrug resistance associated protein 1 (MRP1) was also analyzed. All tested derivatives displayed a moderate potency on the BCRP overexpressing cells; while only four molecules showed to be effective on MRP1 overexpressing cells, highlighting a clear structural requirement for selectivity. In conclusion, we have identified a new very powerful series of compounds which represent interesting leads for the development of new potent and efficacious P-gp-dependent MDR modulators.

Keywords
P-gp modulators; BCRP modulators; MRP1 modulators; MDR reversers; pirarubicin uptake; molecular docking; human plasma stability; rhodamine-123 efflux; ATPase activity; apparent permeability.

List of Abbreviations
P-gp, P-glycoprotein; DOX, Doxorubicin; EDCI, 1-(3-dimethylaminopropyl)-3-ethylcarbodiimmide hydrochloride; DMAP, 4-dimethylaminopyridine; TPSA, topological polar surface area; PDB, Protein Data Bank; PBS, phosphate buffer solution; KEE, ketoprofene ethylester; Rhd123, rhodamine-123; MDCK, Madin-Darby Canin Kidney; BCRP, Breast Cancer Resistance Protein; MRP1, Multidrug Resistance associated Protein 1; Caco-2 cells, colorectal adenocarcinoma cells.

1. Introduction

The resistance of cancer cells to cytotoxic drugs is a significant limitation to successful chemotherapy. Multidrug resistance (MDR) is a type of acquired drug resistance to multiple classes of structurally and mechanistically unrelated anticancer drugs [1].
MDR is a complex phenomenon which can derive from different biochemical mechanisms. In the case of the so called classical MDR, cells accumulate a lower intracellular concentration of drug as a result of an accelerated efflux of the antitumor agents mediated by an ATP-dependent process. The main mechanism responsible of this transport is the overexpression of integral membrane transporters such as P-glycoprotein (P-gp, ABCB1) [2], Breast Cancer Resistance Protein (BCRP, ABCG2) [3] and Multidrug Resistance associated protein 1 (MRP1, ABCC1) [4], belonging to the ABC (ATP Binding Cassette) protein family.
P-gp is a membrane glycoprotein present, beside cancer cells, in several important tissues and blood-tissue barriers, where it regulates some important physiological processes such as the secretion of lipophilic molecules and the extrusion of exogenous agents [5]. Unfortunately, this efflux protein is overexpressed in cancer cells as a result of the upregulation of the human MDR1 gene expression and it extrudes the chemotherapeutic drug from the cells, lowering its concentration below that necessary for anticancer action [6].
Since its discovery and the elucidation of the mechanism of action, P-gp has been considered a suitable target for circumventing transporter-dependent MDR. MDR reversers (chemosensitizers) are P-gp modulators that administered in combination with cytotoxic agents, which are substrates of the efflux pump, could restore their efficacy in resistant cancer cells [7,8].
Verapamil was the first compound showing P-gp modulating activity and, together with many other molecules, belongs to the first generation of P-gp modulators. However, the toxicity of this first series of compounds prevented their clinical use and, at present, verapamil is only used as gold standard in biological assays. Since then, many P-gp modulators, belonging to three generations of compounds have been identified [9,10]. Several of them have reached pre-clinical or clinical trials [11,12], but none of these compounds has been approved for therapy, because of their low potency, toxicity and inhibitory effect on isoforms of cytochrome [13], although some of the latest MDR reversing compounds show a safer profile.
The failure of pre-clinical and clinical investigational studies led to considerable pessimism regarding the validity of such therapeutic approach to overcome MDR [14]. Nevertheless, the search for new, safer, more potent and efficacious multidrug transporter modulators is still of interest. In fact, MDR occurs also in brain disorders such as epilepsy, depression, and schizophrenia: in these diseases, about 20-40 % of the patients develop resistance to current therapeutic drugs [15]. Another field of investigation regards Parkinson's and Alzheimer's diseases:

recent evidences suggest that a decrease in P-gp expression and function at blood brain barrier occur in these diseases [16]. Consequently, there are several reasons for medicinal chemists to continue the search for molecules that could be used to modulate P-gp.

Information on the interaction site of P-gp suggest that it is a large, flexible drug binding domain where molecules can accommodate in a plurality of binding modes, establishing π–π, ion-π, hydrogen bonds and hydrophobic interactions [17]. So, in the search for efficient P-gp modulating MDR reversers, in the last years we have designed and studied several families of basic molecules bearing suitably positioned aromatic rings, assuming that the presence of aromatic moieties and of one or more protonable nitrogen atoms is an important property for the P-gp interaction. In our drug design strategy, these molecular features have been connected by linkers of different length and flexibility [18,19]. In particular, a high structural flexibility would allow the molecules to choose the most productive binding mode within the P-gp recognition site. This approach, labeled as "polyvalency", had been already used successfully by other researchers, who synthesized several homodimers as MDR inhibitors [20-22].

Based on the polyvalency approach, we synthesized several *N*,*N*-bis(alkanol)amine aryl esters characterized by the presence of a basic nitrogen atom linked to two different aromatic ester portions by two polymethylenic chains of variable length as spacers. This approach provided good results since most of the synthesized compounds showed to be very potent MDR reversers in a human leukemia cell line [18,23,24].

The first series of compounds were characterized by different combinations of aromatic residues connected to the *N*-methylated basic portion by two identical polymethylenic chains of variable length as spacers [18,23,24]; best results were obtained by the combination of two chains constituted by 4 or 5 methylenes, with a spacer total length corresponding to 8 or 10 methylenes and one nitrogen atom. Then, we explored the consequences of varying the relative position of the nitrogen in the chain, abandoning the symmetry of the linkers. These derivatives conserved two aromatic ester portions, and a chain of nine components, eight methylenes and one nitrogen atom, but the position of the nitrogen atom was changed according to the length of the two linkers (3- and 5-methylenes long, structure A, Chart 1) [24]. In this way the nitrogen atom was at different distances from the two aromatic moieties, according to the length of the two different spacers. The new asymmetric compounds showed an outstanding potency if compared to the symmetric isomers; in particular the combination of the *(E)*-3-(3,4,5-trimethoxyphenyl)vinyl (also named *trans*-3,4,5-trimethoxycinnamyl) moiety with the 3,4,5-trimethoxyphenyl and anthracene residues (compounds **I-IV**, structure A, Chart 1) that were already present in the most potent of the previously synthesized compounds [18,23,24] gave rise to the best results of the series. On the bases of these unexpected results, in the present study we decided to widen the series of asymmetrical derivatives by synthesizing all the possible isomers obtained by the combination of different spacers of 2-8 units, for a total length of 8, 9 and 10 methylenes, bearing the aromatic moieties described above (compounds **1-28**, structure B, Chart 1).

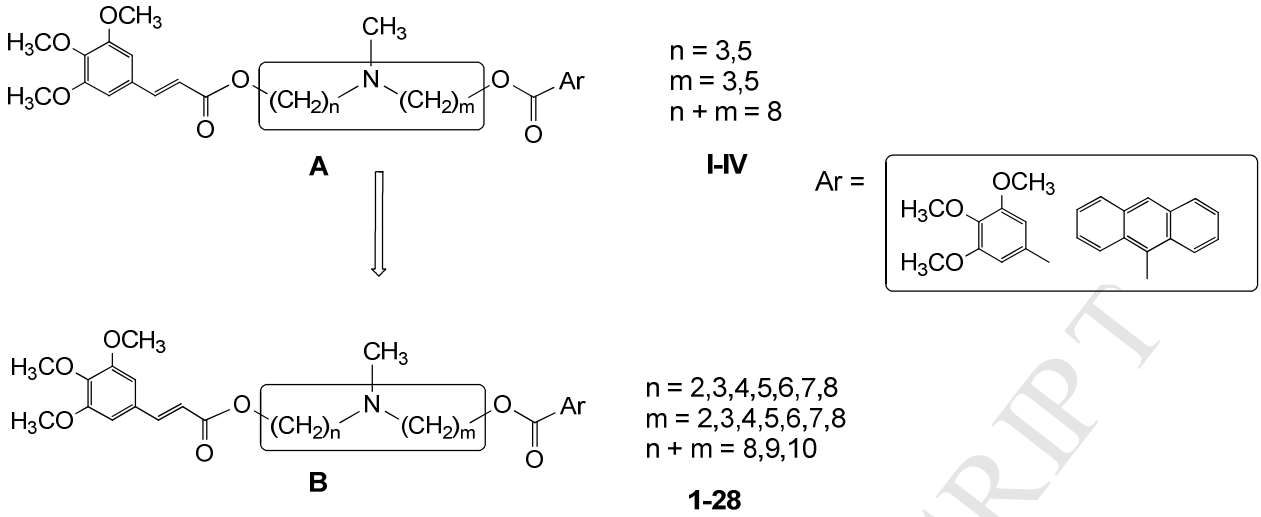

Chart 1. Structure of the reference compounds **I-IV** and of the derivatives **1-28** synthesized in this paper.

The reversal activity of the new compounds **1-28** was evaluated by the pirarubicin uptake assay in doxorubicin-resistant erythroleukemia K562 cells (K562/DOX). Moreover, a molecular docking simulation was performed to identify the potential binding poses of compounds and their mechanism of interaction within the P-gp binding pocket. Finally, a study devoted to establishing the chemical stability of these compounds was planned. In fact, it is well known that the ester group, present in the chemical structure of studied compounds, can be susceptible to hydrolysis by the plasma enzymes. Therefore, a series of experiments concerning the stability of these compounds were performed.

On the bases of the obtained results, the derivatives displaying the best activity on pirarubicin assay and a good chemical stability were tested to define their interacting mechanism *vs* P-gp by evaluating their effect on P-gp mediated rhodamine-123 efflux on K562/DOX cell line. Moreover, the activity of the same compounds was measured on another cell line overexpressing P-gp, the transfected Madin-Darby Canine Kidney-MDR1 (MDCK-MDR1) one, and on two cell lines overexpressing the sister pumps MRP1 and BCRP, MDCK-MRP1 and MDCK-BCRP respectively, to evaluate their selectivity. Finally, their apparent permeability on Caco-2 cells and their effect on ATP cell depletion on MDCK-MDR1 cells were also analyzed.

2. Chemistry

The reaction pathways used to synthesize the designed derivatives (**1-28**) are reported in Schemes 1 and 2. The haloesters **29-40** were synthesized by esterification of the suitable haloalkyl alcohol (2-bromoethan-1-ol, 3-bromopropan-1-ol, 4-chlorobutan-1-ol, 5-chloropentan-1-ol, 6-chlorohexan-1-ol, 7-bromoheptan-1-ol and 8-bromooctan-1-ol) with the commercially available (*E*)-3-(3,4,5-trimethoxyphenyl)acrylic acid, 3,4,5-trimethoxybenzoic acid or anthracene-9-carboxylic acid (Scheme 1). These esters were obtained by transformation of the carboxylic acid in the corresponding acyl chloride by reaction with $SOCl_2$ in ethanol-free $CHCl_3$ (for details, see the Experimental section). Derivatives **29**, **30**, **32**, **33**, **35** had already been described by our group [18, 24].

The chloroalkyl esters **31**- **34** were transformed in the corresponding iodo derivatives **41-44** with NaI in acetone, to achieve higher yields in the following reaction. The bromo esters **29-30, 35-40** and the iodo esters **41-44** were then transformed into the secondary amines **45-54** by reaction with the corresponding aminoalcohol using standard procedures (Scheme 2). These compounds were alkylated by reductive methylation with HCOOH/HCHO to give the corresponding tertiary amines **55-64**. In order to obtain the (2-hydroxyethyl)methylaminoesters **65-72**, the appropriate haloester

was reacted with the commercially available 2-methylaminoethan-1-ol, yielding directly the desired tertiary amines **65-72**.

Final compounds **1-28** were eventually obtained by reaction of **55-72** with the proper carboxylic acid using EDCI and DMAP in anhydrous CH_2Cl_2, or by transformation of the carboxylic acid in the corresponding acyl chloride as described before. The suitable acids are the same described previously: (*E*)-3-(3,4,5-trimethoxyphenyl)acrylic acid, 3,4,5-trimethoxybenzoic acid and anthracene-9-carboxylic acid.

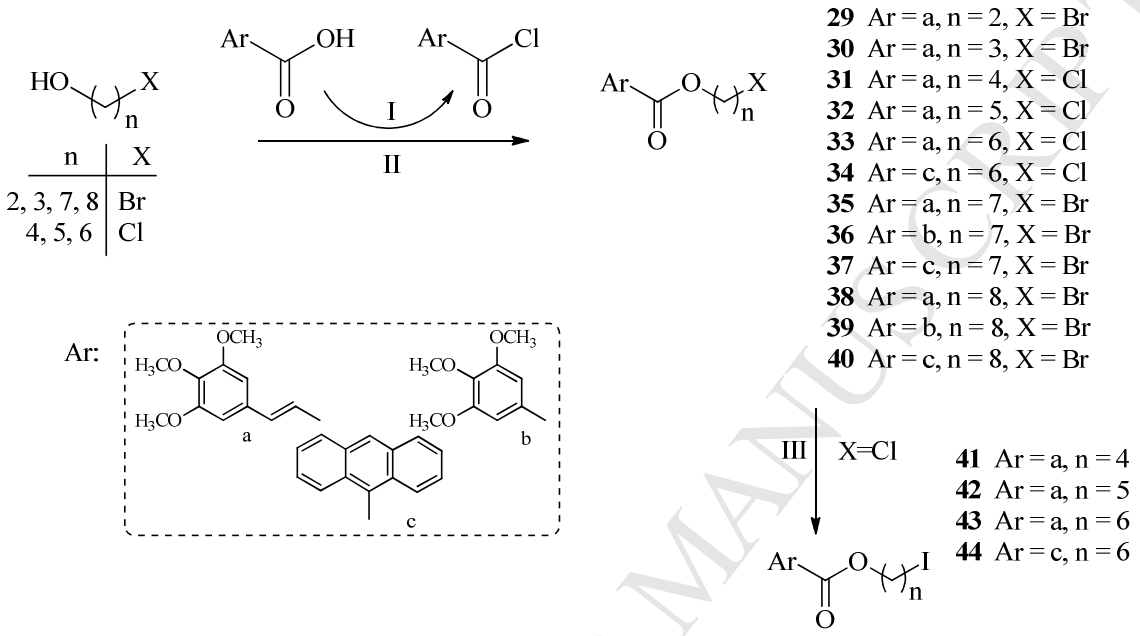

Scheme 1. Reagents and conditions: (I) $SOCl_2$, $CHCl_3$; (II) $CHCl_3$; (III) NaI, acetone.

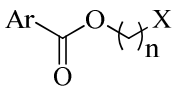

29-30
35-44

X = Br, I

I

II

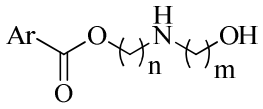

45 Ar = a, n = 2, m = 6
46 Ar = a, n = 4, m = 5
47 Ar = a, n = 5, m = 4
48 Ar = a, n = 3, m = 6
49 Ar = a, n = 6, m = 3
50 Ar = a, n = 4, m = 6
51 Ar = a, n = 6, m = 4
52 Ar = a, n = 7, m = 3
53 Ar = b, n = 7, m = 3
54 Ar = c, n = 7, m = 3

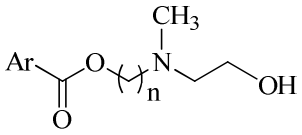

65 Ar = a, n = 6
66 Ar = c, n = 6
67 Ar = a, n = 7
68 Ar = b, n = 7
69 Ar = c, n = 7
70 Ar = a, n = 8
71 Ar = b, n = 8
72 Ar = c, n = 8

III

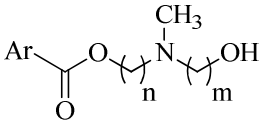

55 Ar = a, n = 2, m = 6
56 Ar = a, n = 4, m = 5
57 Ar = a, n = 5, m = 4
58 Ar = a, n = 3, m = 6
59 Ar = a, n = 6, m = 3
60 Ar = a, n = 4, m = 6
61 Ar = a, n = 6, m = 4
62 Ar = a, n = 7, m = 3
63 Ar = b, n = 7, m = 3
64 Ar = c, n = 7, m = 3

IV

IV

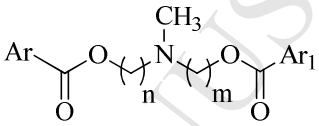

1-28

1 Ar = a, n = 6, m = 2, Ar_1 = b
2 Ar = b, n = 6, m = 2, Ar_1 = a
3 Ar = a, n = 6, m = 2, Ar_1 = c
4 Ar = c, n = 6, m = 2, Ar_1 = a
5 Ar = a, n = 5, m = 4, Ar_1 = b
6 Ar = b, n = 5, m = 4, Ar_1 = a
7 Ar = a, n = 5, m = 4, Ar_1 = c
8 Ar = c, n = 5, m = 4, Ar_1 = a
9 Ar = a, n = 6, m = 3, Ar_1 = b
10 Ar = b, n = 6, m = 3, Ar_1 = a
11 Ar = a, n = 6, m = 3, Ar_1 = c
12 Ar = c, n = 6, m = 3, Ar_1 = a
13 Ar = a, n = 7, m = 2, Ar_1 = b
14 Ar = b, n = 7, m = 2, Ar_1 = a
15 Ar = a, n = 7, m = 2, Ar_1 = c
16 Ar = c, n = 7, m = 2, Ar_1 = a
17 Ar = a, n = 6, m = 4, Ar_1 = b
18 Ar = b, n = 6, m = 4, Ar_1 = a
19 Ar = a, n = 6, m = 4, Ar_1 = c
20 Ar = c, n = 6, m = 4, Ar_1 = a
21 Ar = a, n = 7, m = 3, Ar_1 = b
22 Ar = b, n = 7, m = 3, Ar_1 = a
23 Ar = a, n = 7, m = 3, Ar_1 = c
24 Ar = c, n = 7, m = 3, Ar_1 = a
25 Ar = a, n = 8, m = 2, Ar_1 = b
26 Ar = b, n = 8, m = 2, Ar_1 = a
27 Ar = a, n = 8, m = 2, Ar_1 = c
28 Ar = c, n = 8, m = 2, Ar_1 = a

Ar, Ar_1:

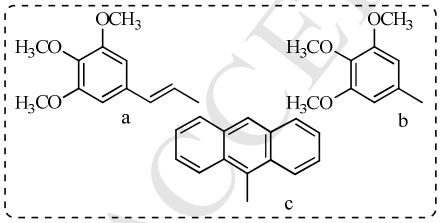

Scheme 2. Reagents and conditions: (I) $H_2N(CH_2)_mOH$ (m= 3, 4, 5, 6), an. CH_3CN; (II) $CH_3NH(CH_2)_2OH$, an. CH_3CN; (III) $HCOOH/CH_2O$, EtOH; (IV) Ar_1COCl, $CHCl_3$ or EDCI, DMAP, an. CH_2Cl_2.

3. Results and discussion

3.1. Modulation of pirarubicin uptake on K562 cells

The P-gp modulating ability of compounds **1-28** was evaluated on K562/DOX doxorubicin resistant cells. K562 is a human leukemia cell line established from a patient with chronic myelogenous leukemia in blast transformation [25]. K562/DOX cells overexpress almost exclusively the membrane glycoprotein P-gp [26-29]. P-gp expression in both sensitive K562 and K562/DOX cells was checked by cytometric analysis with a P-gp-specific antibody (JSB-1 monoclonal antibody); the obtained results showed an increase in the fluorescence ratio of about 3 times in the resistant line. Moreover, application of a second methodology, the Real-time PCR analysis, indicated a substantial increase in mRNA expression level of the ATP binding cassette transporter ABCB1 (175 folds) in the resistant cell line compared with the parental one, confirming an increased presence of P-gp in the K562/DOX resistant cell line. Details are reported in the Experimental Section and in the Supplementary Data (Figures S34 and S35).

The uptake of THP-adriamycin (pirarubicin) was measured by a continuous spectrofluorometric signal of anthracycline at 590 nm (λ_{ex} = 480 nm) after cell incubation, following the protocols reported in previous papers [30,31]. The P-gp modulating activity of the studied compounds on the pirarubicin uptake test is expressed by: *i*) $[I]_{0.5}$, which measures the potency of the modulator and represents the concentration that causes a half-maximal increase (α = 0.5) in the nuclear concentration of pirarubicin, and *ii*) α_{max}, which represents the efficacy of the modulator and is the maximum increase in the nuclear concentration of pirarubicin in resistant cells that can be obtained with a given compound. The value of α varies between 0 (in the absence of the modulator) and 1 (when the amount of pirarubicin in resistant cells is the same as in sensitive cells).

The results obtained are reported in Table 1 together with those of verapamil, the gold standard of P-gp activity inhibition, used as reference compound. 3,4,5-Trimethoxyphenyl derivatives **I** and **II** and their anthracene analogs **III** (GDE6) and **IV** (FRA77) [24] have been added for comparison, since they are the previously obtained asymmetric derivatives.

All the newly synthesized compounds were able to inhibit the activity of P-gp; their potencies and efficacies were higher than those of verapamil. In fact, all molecules showed potency values ($[I]_{0.5}$) in the submicromolar or nanomolar range and in many cases were able to completely reverse P-gp-dependent pirarubicin extrusion (α_{max} close to 1).

A thorough evaluation of the potency values indicated that both the chain length and the combination of the aromatic residues have some influence on the activity of our compounds. In fact, in the case of derivatives **1**-**4**, which carried a total spacer of 8-methylenes due to the combination of two chains of 2 and 6 methylenes, the anthracene derivative **3** showed the best result, with an $[I]_{0.5}$ value of 0.04 μM, as it happened for the two anthracene regioisomers **III** and **IV** which were used as lead compounds. The other compounds of the set, **1**, **2** and **4**, had lower potencies.

In the case of a total length of 9 methylenes, which can be obtained by three different combinations of spacers, the presence of the anthracene residue conferred excellent properties to the molecules: all the isomers, except for compound **16**, showed a nanomolar activity (compounds **7**, **8**, **11, 12** and **15** with $[I]_{0.5}$ values between 0.02 and 0.04 μM). The corresponding derivatives carrying the combination of *trans*-3,4,5-trimethoxycinnamyl moiety with the 3,4,5-trimethoxyphenyl residue showed a similar nanomolar activity only in the case of the two regioisomers **13** and **14**.

The best results were obtained with the isomers with a total spacer of 10 methylenes; remarkably, all the compounds (the three series **17**-**20**, **21**-**24**, **25**-**28**) showed outstanding potencies in the nanomolar range, regardless of the combination of aromatic moieties, with unprecedented results in these series of derivatives.

As regards the efficacy values, almost all the compounds were able to completely reverse P-gp-dependent pirarubicin extrusion (α_{max} = 0.90-0.99). In a little number of derivatives, some lower efficacies can be highlighted (compounds **1**, **4**, and **14** with α_{max} values of 0.77 or 0.79).

Altogether, these data seem to confirm our previous results [23,24] that the MDR modulating activity of this family of molecules can be related on the one hand to the nature of the aromatic moieties and on the other to two characteristics of the linker, both the position of the nitrogen and the total length of the tether. More interestingly, however, from these results it also comes to light that the compounds which present a total spacer of 10 methylenes (**17-28**) are a new series of very potent and efficacious compounds, regardless of the combination of aromatic moieties and of chain lengths. In these series, only the total distance of the aromatic esters seems to be the crucial factor for the activity. Therefore, we compared the potencies of these asymmetric compounds **17-28** with the results obtained by the corresponding symmetric isomers **V** and **VI** already described by us [18]. As shown in Table 1 these two analogs, particularly the 3,4,5-trimethoxyphenyl derivative **V**, showed a lower potency and efficacy. This comparison confirms the result already found in our previous paper [24]. In fact, although the nitrogen position has not a clear influence on the activity, if this atom is at the center of the spacer the activity of the compounds decreases.

Table 1

MDR-reversing activity and predictor parameters for binding free energy, drug transport properties and lipophilicity of compounds **1-28**.

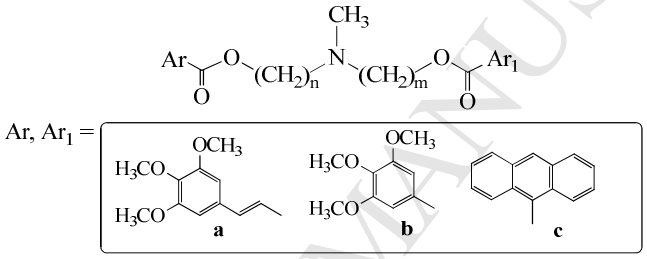

total number of methylenes in the spacer	compd	n	m	Ar	Ar_1	$[I]_{0.5}$ µM[a]	α_{max}[b]	ΔG (Kcal/ mol)[c]	TPSA (Å²)[d]	$logP_{o/w}$[e]
8	**I**[f]	5	3	a	b	0.12±0.02	0.99 ±0.01	-7	111.22	6.30
	II[f]	5	3	b	a	0.27±0.05	0.97±0.02	-6.2	111.22	6.26
	III GDE6[f]	5	3	a	c	0.04±0.01	0.98 ±0.02	-7.4	83.53	6.42
	IV FRA77[f]	5	3	c	a	0.04±0.02	0.94±0.03	-8.3	83.53	6.38
8	**1**	6	2	a	b	0.19±0.07	0.77±0.04	-6.4	111.22	6.31
	2	6	2	b	a	0.46±0.07	0.91±0.03	-6.3	111.22	6.38
	3	6	2	a	c	0.04±0.01	0.94±0.03	-7.9	83.53	6.30
	4	6	2	c	a	0.20±0.08	0.79±0.06	-6.9	83.53	5.86
9	**5**	5	4	a	b	0.10 ± 0.04	0.94± 0.05	-7	111.22	6.26
	6	5	4	b	a	0.27 ± 0.12	0.99 ± 0.01	-6.9	111.22	6.60
	7	5	4	a	c	0.03 ± 0.01	0.99 ± 0.01	-7	83.53	6.11
	8	5	4	c	a	0.04 ± 0.01	0.94 ± 0.02	-7.8	83.53	6.21
9	**9**	6	3	a	b	0.24 ± 0.08	0.90 ± 0.04	-6.8	111.22	6.53
	10	6	3	b	a	0.39 ± 0.12	0.99 ± 0.01	-6.5	111.22	6.56
	11	6	3	a	c	0.03 ± 0.001	0.99 ± 0.01	-8	83.53	6.35
	12	6	3	c	a	0.04 ± 0.01	0.92 ± 0.03	-8.4	83.53	6.22
9	**13**	7	2	a	b	0.04 ± 0.01	0.99 ± 0.01	-7	111.22	6.23
	14	7	2	b	a	0.07±0.02	0.79±0.04	-7.5	111.22	6.58
	15	7	2	a	c	0.02 ± 0.01	0.98 ± 0.02	-7.5	83.53	6.31
	16	7	2	c	a	0.17±0.08	0.88±0.08	-7	83.53	6.11
10	**17**	6	4	a	b	0.01±0.001	0.99±0.01	-8	111.22	6.91
	18	6	4	b	a	0.07 ± 0.002	0.99 ± 0.01	-7.4	111.22	6.89

	19	6	4	a	c	0.02±0.005	0.94±0.05	-8.7	83.53	6.66
	20	6	4	c	a	0.01 ± 0.002	0.95 ± 0.05	-7.7	83.53	6.74
10	**21**	7	3	a	b	0.06 ± 0.02	0.99 ± 0.01	-7	111.22	6.90
	22	7	3	b	a	0.08 ± 0.03	0.97±0.03	-7.4	111.22	6.95
	23	7	3	a	c	0.01 ± 0.003	0.93 ± 0.04	-8	83.53	6.67
	24	7	3	c	a	0.04 ± 0.01	0.88 ± 0.08	-8.3	83.53	6.71
10	**25**	8	2	a	b	0.02 ± 0.01	0.93 ± 0.03	-7.3	111.22	6.91
	26	8	2	b	a	0.04 ± 0.01	0.91 ± 0.02	-7.5	111.22	6.89
	27	8	2	a	c	0.05 ± 0.02	0.99 ± 0.01	-8.1	83.53	6.81
	28	8	2	c	a	0.04 ± 0.01	0.96 ± 0.02	-7.2	83.53	6.80
10	**V**[g]	5	5	a	b	0.80 ± 0.20	0.84 ± 0.09	-6.7	111.22	6.80
	VI[g]	5	5	a	c	0.10 ± 0.02	0.80 ± 0.07	-6.9	83.53	6.90
	Verapamil[h]					1.60 ± 0.30	0.70 ± 0.07	-7.8	63.95	4.50

[a] Concentration of the inhibitor that causes a 50% increase in nuclear concentration of pirarubicin ($\alpha = 0.5$). [b] Efficacy of MDR-modulator and maximum increase that can be obtained in the nuclear concentration of pirarubicin in resistant cells. Results are expressed as the mean ± SE of three independent experiments done at least three times. [c] Predicted binding affinity. [d] Predicted topological polar surface area (TPSA). [e] The n-octanol/water partition coefficient (log $P_{o/w}$) was obtained by using implicit log P method (iLOGP) [f] See within ref. [24]: compounds **I**, **II**, **III** and **IV** are labelled as 13, 12, 16, and 15 respectively. [g] See within ref. [18]: compounds **V** and **VI** are labelled as 11 and 12 respectively. [h] see ref. [24].

3.2. Molecular modeling studies

In order to elucidate the binding mode of the compounds in the P-gp interaction site, and possibly to explain their remarkable inhibitory activity, an *in silico* study was performed. Therefore, since the computational analysis provides a reliable structural basis to undertake structural investigations of drug binding, we chose to study the capacity of the compounds to interact with P-gp using *in silico* docking techniques. To validate and strengthen the computational modelling approach [32,33], we first performed docking calculations with all our compounds on the basis of their *in vitro* activity. Briefly, using Autodock Vina XB scoring function [34], we found, for all the compounds, the binding energy for the best docking poses, which were all located within the inner chamber of the protein. The good correlation between in *vitro* and *in silico* calculations (Figure S33, Supplementary Data) provided confidence for using our modelling strategy to investigate putative interactions with P-gp. The crystal structure of human P-gp (PDB code 6C0V) was used as Molecular docking target [35], while, to identify the potential binding pocket of our compounds, we referred to the 3D structure of Mus musculus P-gp in complex with BDE-100 (PDB code 4XWK) [36,37]. As a matter of fact, this compound showed to be a P-gp inhibitor with a IC_{50} of 23.2±2.9 μM [37]. Compounds were clustered into sets "1" and "2", based on the presence (set 1) or absence (set 2) of the anthracene group. The ligand binding mode was visually analyzed: all compounds docked with similar poses (Figure 1), showing interactions that appeared similar to those established by verapamil with the binding site residues. The computation of docking energies shows that all molecules can interact with the binding site, displaying a good thermodynamic affinity. Nevertheless, some differences can be highlighted, depending on the aromatic residues and the total length of the spacer, which modify the binding profiles. The docking results showed that the more active compounds, which show a calculated binding free energy (ΔG value) smaller than -7.8, are decorated in most cases by the anthracene ester group; in addition, the compounds characterized by a linker of 10 methylenes never exhibit ΔG higher than -7.

Also, the analyses of predicted lipophilicity (logP) and of the topological polar surface area (TPSA), by using SwissADME [38] were performed. The parameter TPSA is defined as the sum of surfaces of polar atoms in the molecule and is useful to identify the druggability of ligands, since it can be a measure of the ability of the compounds to permeate cells. Molecules with a TPSA value greater

than 140 Å² tend to be poor in permeation of cell membranes and are considered poor drug-like compounds [39].

These parameters may explain the differences between $[I]_{0.5}$ and efficacy values against ΔG, in particular as regard the standard verapamil. In fact, comparing the new synthesized compounds with verapamil, it can be observed how, despite a similar ΔG value, verapamil displays lower potency and efficacy with respect to the derivatives described in the paper. This behavior could be related to its lower lipophilicity and permeability.

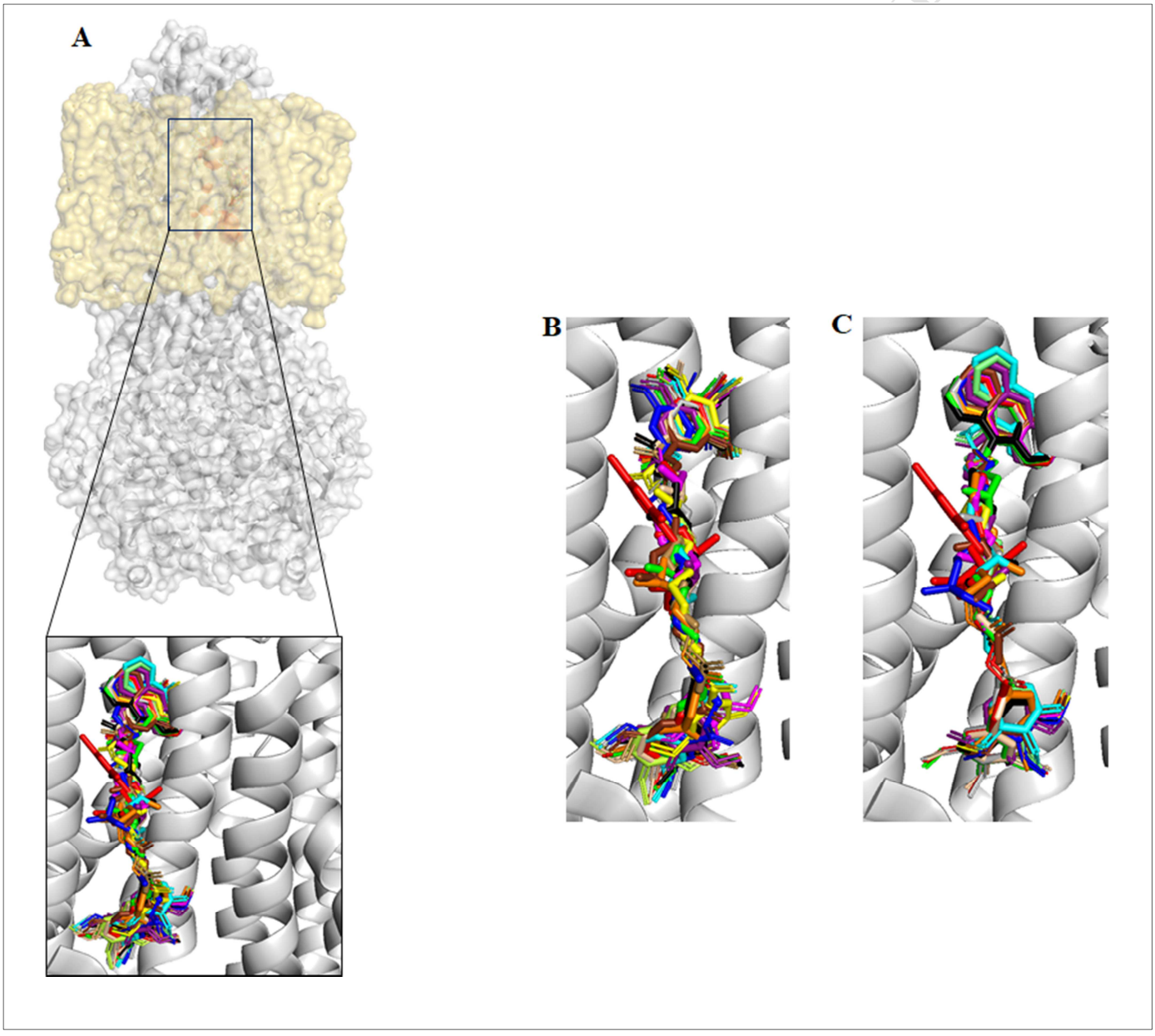

Fig. 1. Overview of the best poses of compounds **1-28** within the P-gp binding pocket. A) The P-gp 3D structure is shown in grey cartoon and surface representation. The bilayer is reported in yellow surface. BDE100 (red), Verapamil (black) and the studied ligands (coloured) are shown inside the P-gp binding pocket with stick models. B) and C) show a closer view of the binding mode of set "1" and set "2", respectively.

To gain more information on the remarkable inhibitory activity of the new compounds, we also carried out a ligand-binding-site interaction network analyses on derivatives **17** and **23,** which are two very potent compounds representative of the two clusters**.** In fact, it could be interesting to evaluate which type of interactions could be established between the protein and these active compounds, identifying the involved residues, and making a comparison with those formed by other well-known inhibitors.

Crystal structure of the mouse P-gp complexed with BDE-100 compound (PDB code 4XWK), was used as reference point to study protein binding interactions [34]. BDE-100 forms hydrophobic interactions with different aromatic residues but only one π-stacking bond with Tyr-303; this is enough for its inhibitory capacity. Additionally, in a recent work a P-gp modulator was showed to bind two sites of internal protein cavity also identified in co-crystal structures in both the inward-open and the inward-closed transporter [40], showing the same binding region of our docking results.

Figure 2 shows the 3D molecular docking models of the interaction between P-gp and the standard verapamil (pointed up in panel B), and the very active compounds **23** and **17**, which are representative of cluster "1" and "2", respectively (panel C and D). Verapamil docked into the human P-gp (PDB code 6C0V) [35], is surrounded by several lipophilic or aromatic residues, but as well as BDE-100, is able to form only one π-stacking interaction. On the contrary, compounds **17** and **23** can form a higher number of interactions with different residues of the binding site: the presence of long polymethylenic chains allows numerous hydrophobic interactions within the binding pocket, in addition to the capability to form stronger aromatic interactions compared to BDE-100 and verapamil. For instance, for **23** the presence of the anthracene group favors the formation of three π-stacking bonds between the three rings of the aromatic moiety and Phe-335, Phe-728 and Phe-759 residues of the P-gp binding site, while both BDE-100 and verapamil can form only one π-stacking interaction. As regard compound **17**, the higher number of hydrophobic interactions of the spacers, compared to verapamil, stabilizes its binding into the active pocket despite the formation of only one π-stacking bond.

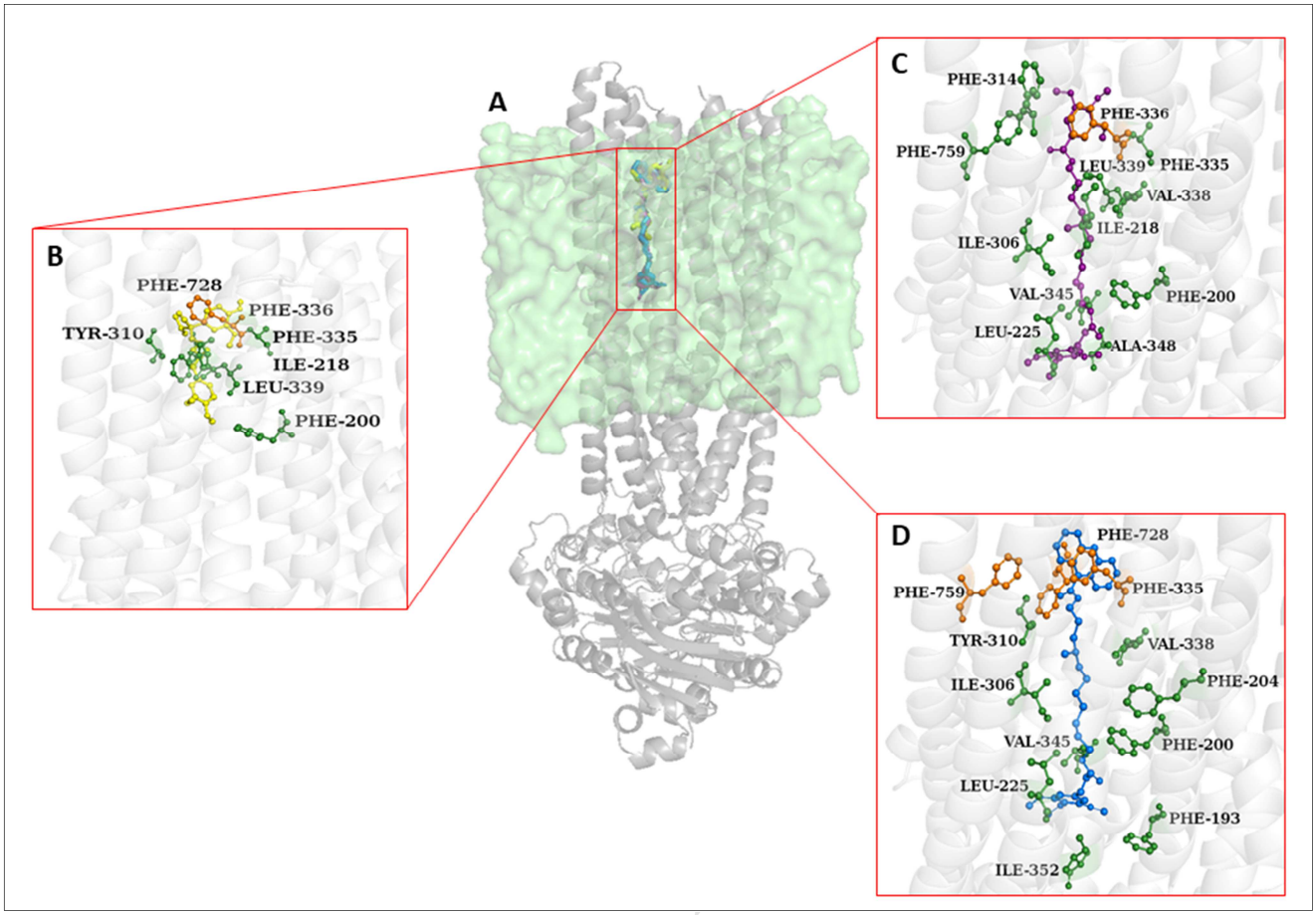

Fig. 2: 3D Molecular docking models of the interaction between compounds and P-gp. A) The P-gp 3D structure is shown in grey cartoon and the bilayer is reported as green surface. B) Verapamil in yellow, C) Compound **23** in purple, D) Compound **17** in blue. For clarity only interacting residues are displayed, with hydrophobic residues in green and π-stacking in orange respectively.

In summary, the docking results supported the data obtained by the biological tests: all molecules are able to interact with the binding site with a good thermodynamic affinity: the differences in the activity can be related to the ΔG values. The good activity of the compounds bearing an anthracene ester group can be partially explained by the higher number of π-stacking bonds that these molecules are able to establish with the protein.

3.3. Chemical stability tests

The chemical stability tests on these compounds were carried out both in phosphate buffer solution (PBS) and in human plasma, to distinguish between spontaneous or enzymatic hydrolysis respectively.

The stability analyses were performed by LC-MS/MS methods operating in product ion scan mode, in the appropriate m/z range to ensure the fragment ions detection. The LC-MS/MS system and the parameters used in this study were reported in the Supplementary Data section.

The stability of each compound, in both reported matrices, was evaluated by monitoring the variation of its concentration at different incubation times. By plotting these data (analyte concentrations vs the incubation time) their respective degradation profiles were obtained. Generally, when the substrate concentration is smaller than its Michaelis–Menten constant (K_M), the enzymatic degradation rate is described by a first-order kinetic.

Therefore, plotting the natural logarithm of the quantitative data versus the incubation time, a linear function can be used, and its slope represents the degradation rate constant (*k*). Therefore, the half-life ($t_{1/2}$) of each tested compound can be calculated as follows:

$$t_{1/2} = \ln(0.50\,\mu M) / k$$

The plots of the natural logarithm of the quantitative data versus the incubation time of all the studied compounds were analysed. The obtained results demonstrated that all the compounds were stable in PBS and most of them also in human plasma. In fact, only the degradation plots of **II**, **10**, **18** and **22** in human plasma showed a significant decay rate (*k* value), and their calculated half-life values ($t_{1/2}$ values between 39 min. and 123 min), were reported in Table 2. Furthermore, the half-life value of ketoprofene ethylester (KEE), used as reference compound, demonstrated that the employed human batch was enzymatically active (half-life < 2 h) [30]. At the contrary, the *k* values of the other studied compounds were close to 0; consequently, for these derivatives, extremely high $t_{1/2}$ values can be calculated. Since under the proposed experimental conditions a half-life over 240 min is not measurable, it is reasonable to consider that their half-life values could be equal or greater than 240 min. The human plasma degradation profiles of compound **22** and of its stable isomer **21** are reported as an example (Figure 3); the plots of the other compounds are reported in the Supplementary Data section.

Table 2
Half-life values of reference and studied compounds.

Comp.	PBS $t_{1/2}$ ± error (min)	Human plasma $t_{1/2}$ ± error (min)
KEE	n.d.	107 ± 16
1	>240	>240
2	>240	>240
3	>240	>240
4	>240	>240
5	>240	>240
6	>240	>240
7	>240	>240
8	>240	>240
9	>240	>240
10	>240	39 ± 6
11	>240	>240
12	>240	>240
13	>240	>240
14	>240	>240
15	>240	>240
16	>240	>240
17	>240	>240
18	>240	123 ± 53
19	>240	>240
20	>240	>240
21	>240	>240
22	>240	45 ± 13
23	>240	>240
24	>240	>240
25	>240	>240
26	>240	>240
27	>240	>240
28	>240	>240
I	>240	>240
II	>240	41 ± 19
V	>240	>240

n.d.: not determined

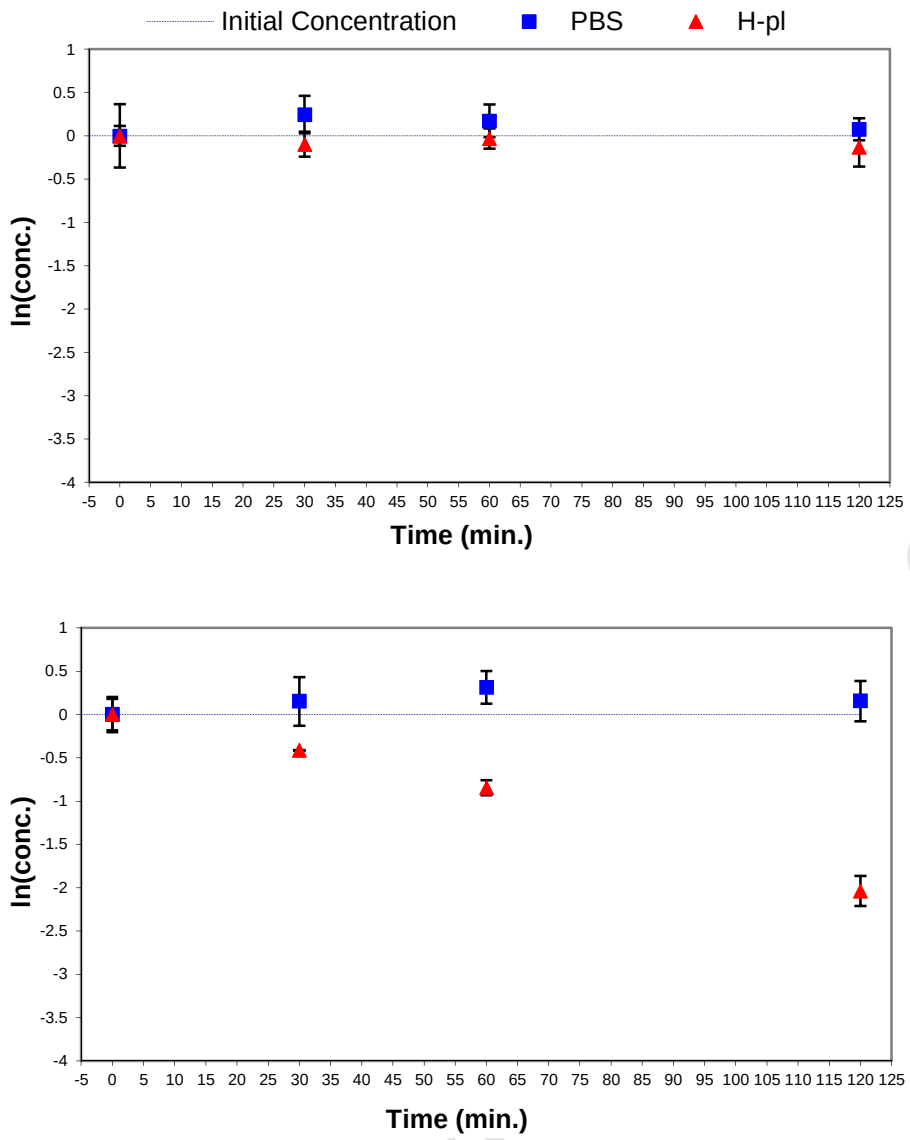

Fig. 3: Degradation profiles in PBS (blue) and human plasma (red) of compound **21** (top) and compound **22** (bottom).

The degradation products of **II**, **10**, **18** and **22** compounds were also investigated to establish the possible enzyme hydrolytic mechanism. The results confirmed that these compounds were degraded for hydrolysis of the ester group linked to the *trans*-3,4,5-trimethoxycinnamyl moiety, with formation of the corresponding *N*-alkyl alcohol and of the free trimethoxycinnamic acid. As an example, the chromatograms of compound **22** in human plasma at two incubation times (0 and 120 min respectively) is reported in Figure 4.

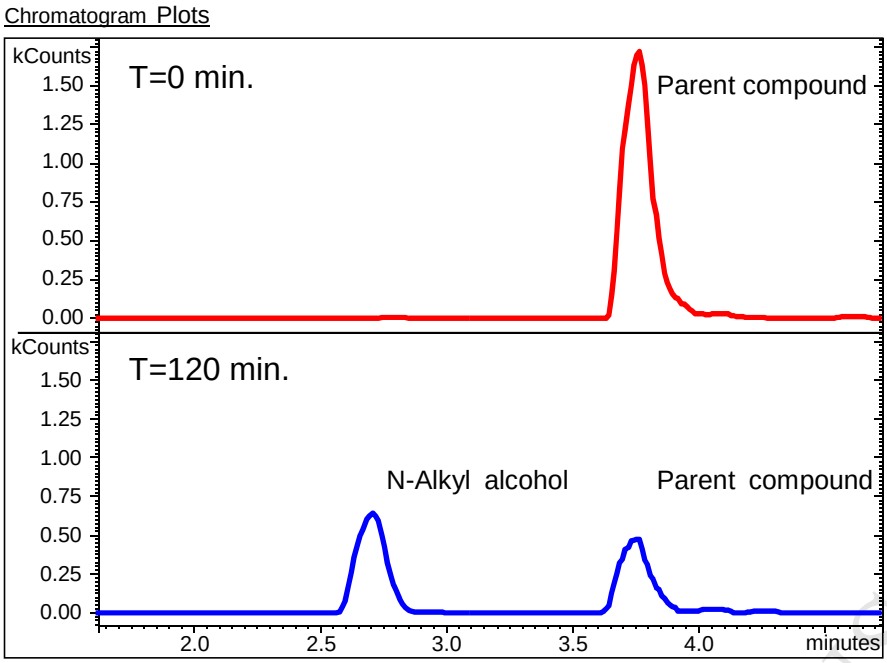

Fig. 4: LC-MS/MS chromatographic profiles of compound **22** in human plasma at the initial (up) and final (bottom) incubation time.

Interestingly, the hydrolysis occurs only when the *trans*-3,4,5-trimethoxycinnamic ester is combined with the 3,4,5-trimethoxybenzoic moiety, while the combination with the anthracene group prevents the enzyme activity (i.e. anthracene analogues **24** and/or **12**). Furthermore, hydrolysis occurs only when the *N*-alkyl chain length of the *trans*-3,4,5-trimethoxycinnamyl portion is of three methylenes: different values prevent the hydrolysis (i.e. **26** and/or **V**). Only **18**, bearing a *N*-alkyl chain length of four methylenes in the cinnamyl portion, shows an appraisable degradation, but its *k* value is three times lower with respect to the analogues carrying a chain with three methylene units. Compound **6**, characterized by the same structural feature of **18**, is instead completely stable in human plasma, indicating that the chain composed by 4 methylenes confers a higher stability.

3.4 Inhibition of P-gp-mediated rhodamine-123 (Rhd 123) efflux on K562/DOX cells

Based on the interesting results obtained, the effect of the most active compounds was further evaluated on the P-gp function. For this test, all the compounds which presented a total spacer of 10 methylenes, apart from the hydrolysable derivatives **18** and **22**, were selected. The ability of compounds **17**, **19-21**, and **23-28** to inhibit the transport activity of the pump was measured evaluating the P-gp specific substrate rhodamine-123 intracellular accumulation on the resistant K562/DOX cell lines as described in the Experimental Section. Cells were loaded with rhodamine-123 for 30 min; after this accumulation period, the efflux of the fluorochrome was evaluated after 10 min more, both in the presence and in the absence of modulators tested at 1.0 μM concentration. The intracellular accumulation of Rhd 123 was also evaluated on the parental line K562 (Experimental Section). Because of the low level of P-gp present in this cell line, the rhodamine-123 accumulated in the uptake phase was completely retained by the cell after 15 and 30 min of efflux time (Figure S36 Supplementary Data).Therefore, the inhibiting activity of the selected compounds was not evaluated on the parental cell line.

The inhibition of P-gp-mediated Rhd 123 efflux of compounds **17**, **19-21**, and **23-28** on K562/DOX cells is reported in Figure 5. In Figure 5A, the effect of Rhd 123 alone and of the compounds added at 1.0 μM concentrations is reported, expressed as fluorescence ratio value, that is the ratio between median fluorescence intensity value acquired at the end of the efflux phase, and that acquired at the

end of the uptake phase. The values were expressed as percentage. The calculated ratios are reported in the Supplementary Data (Table S4). Verapamil, tested at 3.0 µM concentration, was used as reference compound. In Figure 5B, some typical fluorescence curves are reported, obtained in the absence (panel a) or in the presence of verapamil (panel b) or of two representative compounds, the potent isomers **19** and **20** (panels c-d). The fluorescence curves of the other tested compounds are reported in the Supplementary Data (Figure S37).

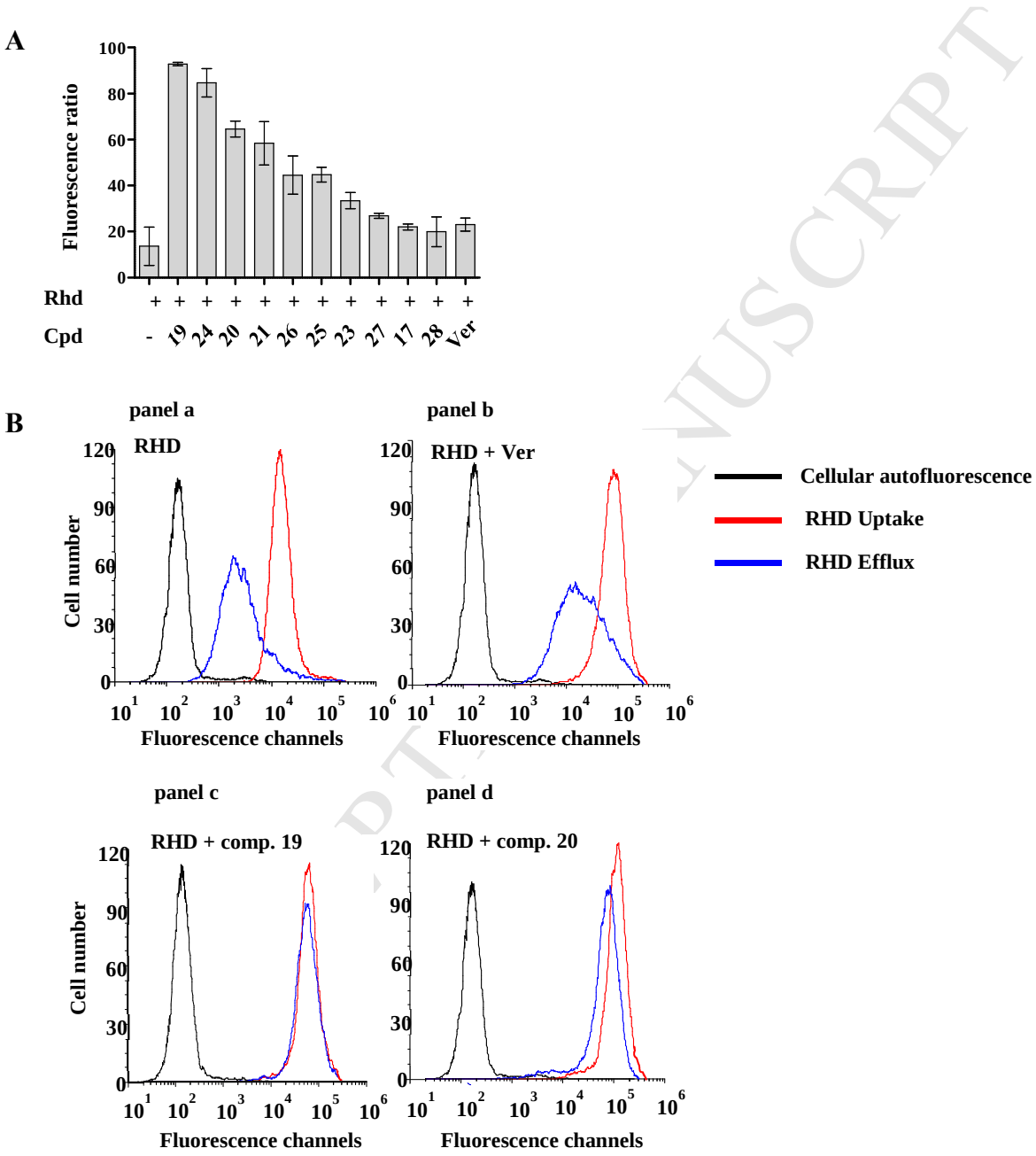

Fig. 5. Inhibition of P-gp-mediated Rhd 123 efflux of compounds **17**, **19-21** and **23-28** on K562/DOX cells. (A) Fluorescence ratio values in K562/DOX cells incubated with Rhd 123 in the absence (control) and in the presence of compounds **17**, **19-21** and **23-28** tested at 1.0 µM concentration. The efflux of the fluorochrome was evaluated after 10 min as reported in Experimental Section. The data were expressed as the mean ± SE of three independent experiments done at least three times. The figure also shows the reference compound, verapamil tested at 3.0 µM concentration. (B) The fluorescence curves were calculated after 30 min Rhd 123 uptake and 10 min of efflux in Rhd 123-free medium. Each peak is identified by a fluorescence channel number and designates the amount of intracellular Rhd 123 in each sample in the absence and in presence of the tested compounds. Autofluorescence histogram (black line): cells incubated in media alone. Uptake

histogram (red line): cells incubated 30 minutes in media with 5 μM rhodamine-123. Efflux histogram (blue line): cells incubated 30 minutes in media with 5 μM rhodamine-123 in the absence (panel a) or in the presence of verapamil (panel b), compound **19** (panel c), or **20** (panel d), then washed and incubated in rhodamine-free media in the absence (panel a) and in presence of compounds (panels b-d) for 10 minutes.

The fluorescence ratio values showed that all the compounds were able to inhibit the efflux of Rhd 123, although to different extent. The most potent compounds were in order **19**, **24**, **20**, **21**, **26**, **25**; derivatives **23**, **27**, **17** and **28** were slightly more or equally active with respect to verapamil, although tested at lower concentration than the reference (1 and 3 μM, respectively).
In particular, the anthracene derivatives **19** and **24** showed an outstanding activity, and were able to maintain a high Rhd 123 intracellular fluorescence, showing an efflux of the fluorochrome of just 7.2% and 15.3% respectively; **20** the regioisomer of **19,** and the 3,4,5-trimethoxybenzoic derivative **21** were able to maintain 64.6% and 58.4% of the intracellular fluorescence after 10 minutes of efflux, still showing a considerable ability in inhibiting the efflux of Rhd123.
The same result is highlighted by analyzing the fluorescence curves. The treatment with the regioisomers **19** and **20** caused a Rhd 123 intracellular retention higher than the untreated sample (panel a), as evidenced by the blue curves overlaid on the red ones of the uptake. These derivatives were able to retain almost all the Rhd 123 in the cells showing a P-gp inhibiting activity much higher than verapamil.

3.5 Transfected MDCK cells: characterization of P-gp interacting mechanism and selectivity vs the other MDR transporters

The effect of the most active compounds on K562/DOX cells, already selected for the inhibition of the P-gp-mediated rhodamine-123 efflux test, was further evaluated. The potency of compounds **17**, **19-21**, and **23-28** was tested on a different cell line overexpressing P-gp, the Madin-Darby Canine Kidney-MDR1 (MDCK-MDR1) cells, measuring their inhibiting activity of the transport of a profluorescent probe, Calcein-AM, that is a P-gp substrate (Table 3).
The P-gp interacting profile was also investigated combining other two biological assays: the apparent permeability (P_{app}) determination in Caco-2 cell monolayer, and the ATP cell depletion in MDCK-MDR1 cells [41]. The first assay measures the ratio between two fluxes: 1) BA, representative of passive diffusion from the basolateral to apical compartments; 2) AB, representative of active transport, from the apical to basolateral compartments. If the ratio BA/AB is < 2, the compound is classified as an inhibitor (also considering the results of the ATPase activity). If the ratio is > 2, the compound is classified as a substrate.
The detection of the ATP consumption in cells overexpressing P-gp measures the transport of the tested compound. Only a P-gp unambiguous substrate, as transported, induces a depletion of ATP while a P-gp inhibitor, as not transported, does not induce ATP consumption. Moreover, another substrate category, known as category IIB_3, displaying a P_{app} value > 2 but not inducing an ATP cell depletion is also reported [42]**.**
At last, the activity of the compounds *vs* two other sister proteins, MRP1 and BCRP, was tested (Table 3) by evaluating the ability of the ligands to inhibit the transport of Calcein-AM (MRP1 substrate) in cells overexpressing MRP1 (MDCK-MRP1) and of the fluorescent probe Hoechst 33342 (BCRP substrate) in cells overexpressing BCRP (MDCK-BCRP cells).
Expression levels of P-gp, MRP1 and BCRP were periodically analyzed by immunoblotting analysis in MDCK-MDR1, MDCK-MRP1 and MDCK-BCRP cells respectively, as described in the Experimental Section. Tubulin was used as control of equal protein loading. A representative western blot analysis is reported in the Supplementary Data (Figure S38).

Table 3
Biological evaluation of derivatives **17**,**19**-**21**,**23**-**28**: inhibition activity on MDCK-MDR1, MDCK-MRP1 and MDCK-BCRP cells overexpressing each transporter, ATP cell depletion in MDCK-MDR1 and apparent permeability (P_{app}) determination (BA/AB) in Caco-2 cell monolayer.

	EC_{50} μM[a]				
Compd	***P-gp***	***MRP1***	***BCRP***	***ATP cell depletion***	P_{app} [b]
17	0.20±0.03	5.08±1.01	16.0±2.9	Y	7.5
19	0.52±0.10	NA	3.8±0.72	N	11
20	0.85±0.17	NA	3.3±0.55	Y	27
21	0.21±0.11	3.0±0.60	8.1±1.59	N	5.2
23	0.23±0.05	NA	3.9±0.78	N	11
24	0.26±0.05	NA	3.0±0.49	N	25
25	0.30±0.10	4.5±0.89	3.8±0.70	N	7.1
26	0.22±0.04	2.2±0.42	4.5±0.87	N	6.8
27	0.34±0.07	NA	5.4±1.06	N	14.4
28	0.92±0.20	NA	5.1±1.02	N	4.6
verapamil	0.50±0.10	6.8±3.0	NT	Y[c]	18

[a] Values are the mean ±SEM of two independent experiments, with samples in triplicate. [b] Apparent permeability estimation: values are from two independent experiments, with samples in duplicate. [c] Percentage of the effect at a concentration of 1 μM (20%). NA = not active. NT = not tested.

As shown in Table 3, on MDCK-MDR1 cells the compounds displayed good activities *vs* P-gp (EC_{50} ranging from 0.20 μM to 0.92 μM). More in details, compounds **17**, **23**, **24** and **26** showed the higher potency (EC_{50}=0.20 μM, 0.23 μM, 0.26 μM and 0.22 μM respectively). The trend in potency is slightly different from that shown in the pirarubicin uptake test, but it is not surprising since the cell lines are different. However, it is interesting to note that derivatives **17** and **23** were among the most active compounds also in the pirarubicin uptake assay. Moreover, all the compounds showed a moderate activity *vs* BCRP (EC_{50} ranging from 3.0 μM to 16.0 μM); however, in this test they were at least 10-fold less active with respect to P-gp assay. Finally, only derivatives **17**, **21**, **25** and **26** showed some activity *vs* MRP1, while the other ligands were completely inactive. These four compounds share the same combination of aromatic moieties, namely the (*E*)-3-(3,4,5-trimethoxyphenyl)vinyl residue and the 3,4,5-trimethoxyphenyl one; it can be concluded that the presence of the anthracene moiety is not favorable for the activity on this pump. So, a structural requirement for the selectivity *vs* MRP1 could be highlighted.
The apparent permeability determination P_{app} (BA/AB) in Caco-2 cell monolayer indicated that all compounds had a BA/AB ratio > 2; thus, considering also the results of the ATP consumption test, compounds **17** and **20** can be defined unambiguous substrates while all the other compounds were classified as substrate belonging to category IIB_3, as above reported.

4. Conclusions

In the present study, we designed and synthesized several new *N*,*N*-bis(alkanol)amine aryl ester heterodimers by modulating the combination of aromatic moieties and the length of the methylenic chain. We achieved all the possible isomers obtained by the combination of different spacers of 2-8 units, for a total length of 8, 9 and 10 methylenes, bearing the aromatic moieties described above. These derivatives were as first evaluated for their P-gp inhibitory activity on doxorubicin-resistant erythroleukemia K562 cell line (K562/DOX). The new compounds showed good P-gp modulating ability in the pirarubicin assay: all molecules showed potency values ($[I]_{0.5}$) in the submicromolar or nanomolar range and in many cases were able to completely reverse P-gp-dependent pirarubicin extrusion (α_{max} close to 1).

The best results were obtained with the isomers showing a total spacer of 10 methylenes; in fact, all the compounds showed outstanding potencies in the nanomolar range, regardless of the combination of aromatic moieties, with unprecedented results in these series of derivatives. In this group of compounds, the nitrogen position and therefore the distance of this atom from the combined aromatic residues have not a clear influence on the activity. So, the total distance of the aromatic esters seems to be the crucial factor for the activity. However, comparing the potencies of the compounds **17-28** with the activities obtained by two already described symmetric isomers **V** and **VI** [18] (Table 1), the same result already found in our previous paper [24] was confirmed: the nitrogen position has not a clear influence on the activity, but if this atom is at the center of the spacer the activity of the compounds decreases.

To explain the remarkable activity of the new compounds, we carried out a ligand-binding-site interaction network analyses on all the derivatives. Using a computational approach, we highlighted that all the molecules can interact with the protein binding site, displaying a good thermodynamic affinity. Some compounds however showed better binding outlines, characterized by smallest binding energies (ΔG) that showed a certain correlation with the experimental activities. The good activity of the compounds bearing an anthracene ester group could be partially explained by the higher number of π-stacking bond that these molecules are able to establish with the protein.

Interesting information was obtained from the stability experiments performed on these new series of MDR inhibitors both in phosphate buffer solution (PBS) and in human plasma. The compounds, despite the presence of two ester groups, were stable in both the tested matrices. Only four compounds (**II**, **10**, **18** and **22**) exhibited a significant degradation in the human plasma matrix, showing the hydrolysis of the ester group present on the 3,4,5-trimethoxycinnamyl moiety of the molecule. Interestingly, these compounds presented a common characteristic in their chemical structures which reasonably favors the enzymatic activity. In fact, it was observed that the hydrolysis occurs only in the presence of the 3,4,5-trimethoxyphenyl moiety and when the *N*-alkyl chain linked with *trans*-3,4,5-trimethoxycinnamyl portion has a length of three methylenes. Therefore, the substitution of aromatic moiety (e.g. in the case of anthracene analogues) or the modification of the length of the *N*-alkyl chain, prevents the enzymatic activity.

The compounds which present a total spacer of 10 methylenes, apart from the hydrolysable derivatives **18** and **22,** were selected to further characterize the biological profile of the series. The chosen molecules were tested on another resistant cell line which overexpresses P-gp, the transfected MDCK-MDR1 cell line. The obtained results confirmed that our derivatives showed a good P-gp inhibiting activity also in these cells. To deepen the evaluation of their effect on P-gp function, three different tests were performed. The ability of the compounds of inhibiting the efflux of rhodamine-123 was tested at 1 μM concentration on K562/DOX cells; all the derivatives were able to inhibit the P-gp-mediated efflux with a noteworthy efficacy, which was at least the same of verapamil tested at 3 μM concentration. Evaluation of apparent permeability on Caco-2 cells and ATP consumption on MDCK-MDR1 cell line suggested that compounds **17** and **20** behave as unambiguous substrates, while the other derivatives can be classified as IIB_3 substrates.

The selectivity profile of the compounds *vs* two sister proteins was also analyzed, evaluating their effect on cells overexpressing MRP1 and BCRP (MDCK-MRP1 and MDCK-BCRP cell lines respectively). Our derivatives displayed a moderate potency on the BCRP overexpressing cells; since this efflux transporter BCRP is often co-expressed with MDR1, the presence of some activity also on this pump could be an interesting property of these series of derivatives. On the contrary, only four molecules showed to be effective on MDCK-MRP1 cell line, and a clear structural requirement for the selectivity *vs* MRP1 could be highlighted.

In conclusion, we have identified a new very powerful series of P-gp-dependent MDR inhibitors showing a *N*,*N*-bis(alkanol)amine aryl ester scaffold. Interestingly, all the compounds carrying a linker composed by 10 methylenes in different combination showed an excellent pharmacological profile. Docking studies confirmed that these molecules can interact in a fruitful manner with the P-gp binding pocket, and evaluation of their chemical stability in PBS and human plasma confirmed

that these compounds are in most cases stable in both media, allowing us to predict their *in vivo* bioavailability. In this series, derivatives bearing the 3,4,5-trimethoxyphenyl moiety appear very active in inhibiting P-gp both in K562/DOX and in MDCK-MDR1 cell lines, but maintain a moderate activity on BCRP and MRP1 overexpressing cells; derivatives bearing the anthracene residue instead show a good profile of activity on P-gp overexpressing cells and on MDCK- BCRP cell line but do not present any activity on MDCK-MRP1, highlighting interesting differences in their selectivity profile.

5. Experimental

5.1. Chemistry

All melting points were taken on a Büchi apparatus and are uncorrected. NMR spectra were recorded on a Bruker Avance 400 spectrometer (400 MHz for ^{1}H-NMR, 100 MHz for ^{13}C-NMR). Chromatographic separations were performed on a silica gel column by gravity chromatography (Kieselgel 40, 0.063-0.200 mm; Merck) or flash chromatography (Kieselgel 40, 0.040-0.063 mm; Merck). Yields are given after purification, unless otherwise stated.

ESI-MS spectra were obtained using a Varian 1200L triple quadrupole system (Palo Alto, CA, USA) equipped by Elettrospray Source (ESI) operating in both positive and negative ions.

The data were acquired in scan mode between the range 150-800 m/z by introducing the sample solution, via syringe pump at 10 μL min^{-1}. The sample solution of each analyte was freshly prepared by diluting its stock solution (1 mg mL^{-1} in acetonitrile) up to a concentration of 1.0 μg mL^{-1} in mixture of mQ water: acetonitrile 50:50 (v/v).

In the used instrumental conditions, the most abundant signal for the analytes showed to be the protonated ($[M+H]^+$) or deprotonated ($[M-H]^-$) molecule ion species.

Compounds **1-28** were obtained in a purity ≥ 95%. Their combustion analyses are indicated by symbols, and the analytical results are within ±0.4% of the theoretical values. Compounds were named following IUPAC rules as applied by ChemBioDraw Ultra 14.0 software. When reactions were performed in anhydrous conditions, the mixtures were maintained under nitrogen. Free bases **1-28** were transformed into the hydrochloride by treatment with a solution of acetyl chloride (1.1 eq) in anhydrous CH_3OH. The salts were crystallized from abs. ethanol/petroleum ether.

*5.1.1. General procedure for the synthesis of haloesters **29-40***

A 1 mmol portion of the appropriate carboxylic acid (*trans*-3-(3,4,5-trimethoxyphenyl)acrylic acid, 3,4,5-trimethoxybenzoic acid or anthracene-9-carboxylic acid) was transformed into the acyl chloride by reaction with $SOCl_2$ (2 mmol) in 5 mL of $CHCl_3$ (free of ethanol) at 60 °C for 4-5 h.

The reaction mixture was cooled to rt, and the solvent was removed under reduced pressure; the mixture was then treated twice with cyclohexane and the solvent removed under reduce pressure. The acyl chloride obtained was dissolved in $CHCl_3$ (free of ethanol), and the suitable alcohol (2-bromoethan-1-ol, 3-bromopropan-1-ol, 4-chlorobutan-1-ol, 5-chloropentan-1-ol, 6-bromoexan-1-ol, 7-bromeptan-1-ol or 8-bromooctan-1-ol) (0.9 eq) was added. The mixture was heated to 60 °C. After 4 h, the reaction mixture was cooled to rt, and treated with CH_2Cl_2. The resulting organic layer was washed with 10% NaOH solution, dried with Na_2SO_4, and the solvent was removed under reduced pressure. The substances obtained were purified by flash chromatography in the case of **31**, **38**, **39** and **40**, otherwise were used as such for the next reaction. Compounds **29**, **30**, **32**, **33** and **35** were already synthesized by our group with the same procedure [18,24].

*5.1.1.1. **(E)-4-chlorobutyl 3-(3,4,5-trimethoxyphenyl)acrylate 31***

Pale yellow oil. Chromatographic eluent: cyclohexane/ethyl acetate70:30. Yield: 68.0%. ^{1}H-NMR ($CDCl_3$) δ: 7.60 (d, J=16.0 Hz, 1H, *CH*=CH); 6.75 (s, 2H, CH arom.); 6.33 (d, J=16.0 Hz, 1H, CH=*CH*); 4.24 (t, J=6.0 Hz, 2H, CH_2O); 3.89 (s, 6H, OCH_3); 3.88 (s, 3H, OCH_3); 3.60 (t, J=6.0 Hz, 2H, CH_2Cl); 1.98-1.82 (m, 4H, CH_2) ppm. ^{13}C APT NMR **($CDCl_3$) δ:** 153.46 (C=O); 144.90

(CH=CH); 129.85 (C); 117.17 (CH=CH); 105.29 (CH arom.); 63.67 (CH_2); 60.97 (OCH_3); 56.18 (OCH_3); 44.50 (CH_2); 29.23 (CH_2); 26.21 (CH_2) ppm.

5.1.1.2. ***6-chlorohexyl anthracene-9-carboxylate 34***

Yellow oil. Yield: 87.1 %. ^{1}H-NMR ($CDCl_3$) δ: 8.52 (s, 1H, CH arom.); 8.15-7.97 (m, 4H, CH arom.); 7.62-7.42 (m, 4H, CH arom.); 4.63 (t, J=6.8 Hz, 2H, CH_2O); 3.54 (t, J=4.8 Hz, 2H, CH_2Cl); 1.96-1.85 (m, 2H, CH_2); 1.85-1.76 (m 2H, CH_2); 1.63-1.46 (m, 4H, CH_2) ppm.

5.1.1.3. ***7-bromoheptyl 3,4,5-trimethoxybenzoate 36***

Pale yellow oil. Yield: 37.8%. ^{1}H-NMR ($CDCl_3$) δ: 7.28 (s, 2H, CH arom.); 4.29 (t, J=6.8 Hz, 2H, CH_2O); 3.90 (s, 6H, OCH_3); 3.89 (s, 3H, OCH_3); 3.39 (t, J=6.8 Hz, 2H, CH_2Br); 1.90-1.81 (m, 2H, CH_2); 1.80-1.70 (m, 2H, CH_2); 1.50-1.32 (m, 6H, CH_2) ppm. ^{13}C APT NMR ($CDCl_3$) δ: 166.22 (C=O); 152.91 (C); 142.16 (C); 125.46 (C); 106.79 (CH arom.); 62.21 (CH_2); 60.88 (OCH_3); 56.24 (OCH_3); 33.80 (CH_2); 32.65 (CH_2); 28.63 (CH_2); 28.38 (CH_2); 28.02 (CH_2); 25.82 (CH_2) ppm.

5.1.1.4. ***7-bromoheptyl anthracene-9-carboxylate 37***

Orange oil. Yield: 41.2%. ^{1}H-NMR ($CDCl_3$) δ: 8.49 (s, 1H, CH arom.); 8.08 (d, J=8.4 Hz, 2H, CH arom.); 8.05 (d, J=8.4 Hz, 2H, CH arom.); 7.60-7.40 (m, 4H, CH arom.); 4.62 (t, J=6.4 Hz, 2H, CH_2O); 3.38 (t, J=6.8 Hz, 2H, CH_2Br); 1.92-1.78 (m, 4H, CH_2); 1.60-1.30 (m, 6H, CH_2) ppm. ^{13}C APT NMR ($CDCl_3$) δ: 169.74 (C=O); 131.02 (C); 129.26 (CH arom.); 128.66 (CH arom.); 128.41 (C); 129.96 (CH arom.); 125.48 (CH arom.); 125.02 (CH arom.); 65.81 (CH_2); 33.88 (CH_2); 32.66 (CH_2); 29.13 (CH_2); 28.77 (CH_2); 28.70 (CH_2); 26.06 (CH_2) ppm.

5.1.1.5. ***(E)-8-bromooctyl 3-(3,4,5-trimethoxyphenyl)acrylate 38***

Yellow oil. Chromatographic eluent: cyclohexane/ethyl acetate70:30. Yield: 40.2%. ^{1}H-NMR ($CDCl_3$) δ: 7.55 (d, J=16.0 Hz, 1H, *CH*=CH); 6.72 (s, 2H, CH arom.); 6.31 (d, J=16.0 Hz, 1H, CH=*CH*); 4.16 (t, J=6.8 Hz, 2H, CH_2O); 3.85 (s, 6H, OCH_3); 3.84 (s, 3H, OCH_3); 3.37 (t, J=6.8 Hz, 2H, CH_2Br); 1.90-1.81 (m, 2H, CH_2); 1.76-1.65 (m, 2H, CH_2); 1.44-1.24 (m, 8H, CH_2) ppm. ^{13}C APT NMR ($CDCl_3$) δ: 167.07 (C=O); 153.43 (C); 144.61 (CH=CH); 129.96 (C); 117.48 (CH=CH); 105.20 (CH arom.); 64.64 (CH_2); 60.98 (OCH_3); 56.16 (OCH_3); 33.98 (CH_2); 32.74 (CH_2); 29.07 (CH_2); 28.70 (CH_2); 28.63 (CH_2); 28.05 (CH_2); 25.87 (CH_2) ppm. ESI-MS *m/z* (%): 429 (100) $[M+H]^+$.

5.1.1.6. ***8-bromooctyl 3,4,5-trimethoxybenzoate 39***

Pale yellow oil. Chromatographic eluent: cyclohexane/ethyl acetate 80:20. Yield: 37.3%. ^{1}H-NMR ($CDCl_3$) δ: 7.27 (s, 2H, CH arom.); 4.28 (t, J=6.8 Hz, 2H, CH_2O,); 3.88 (s, 6H, OCH_3); 3.87 (s, 3H, OCH_3); 3.37 (t, J=6.4 Hz, 2H, CH_2Br); 1.86-1.80 (m, 2H, CH_2); 1.78-1.69 (m, 2H, CH_2); 1.43-1.22 (m, 8H, CH_2) ppm.

5.1.1.7. ***8-bromooctyl anthracene-9-carboxylate 40***

Yellow oil. Chromatographic eluent: cyclohexane/ethyl acetate 80:20. Yield:79.6%. ^{1}H-NMR ($CDCl_3$) δ: 8.50 (s, 1H, CH arom.); 8.07 (d, J=8.8 Hz, 2H, CH arom.); 8.00 (d, J=8.4 Hz, 2H, CH arom.,); 7.57-7.48 (m, 4H, CH arom.); 4.63 (t, J=6.8 Hz, 2H, CH_2O); 3.38 (t, J=4.8 Hz, 2H, CH_2Br); 1.95-1.77 (m, 4H, CH_2); 1.47-1.38 (m, 8H, CH_2) ppm. ^{13}C APT NMR **($CDCl_3$) δ:** 169.78 (C=O); 131.03 (C); 129.25 (CH arom.); 128.66 (CH arom.); 128.41 (C); 126.95 (CH arom.); 125.49 (CH arom.); 125.04 (CH arom.); 70.92 (CH_2); 65.91 (CH_2); 33.99 (CH_2); 32.76 (CH_2); 29.16 (CH_2); 28.66 (CH_2); 28.07 (CH_2); 26.02 (CH_2) ppm.

5.1.2. General procedure for the synthesis of iodoesters ***41-44***

A 1 mmol portion of the suitable chloroester (**31-34**) was dissolved in acetone. To this solution NaI (4 eq) was added, and the resulting mixture was maintained 24 h at reflux in the dark. The reaction mixture was cooled to room temperature, and the solvent was removed under reduced pressure; the residue was dissolved in CH_2Cl_2 and washed with water. The organic layer was dried with Na_2SO_4, and the solvent was removed under reduced pressure yielding a yellow oil which was used as such for the next reaction. Compound **42** was already synthesized by our group with the same procedure [24].

5.1.2.1. ***(E)-4-iodobutyl 3-(3,4,5-trimethoxyphenyl)acrylate 41***
Yield: 94.7%. ^{1}H-NMR ($CDCl_3$) δ: 7.57 (d, J=16.0 Hz, 1H, *CH*=CH); 6.73 (s, 2H, CH arom.); 6.31 (d, J=16.0 Hz, 1H, CH=*CH*); 4.20 (t, J=6.0 Hz, 2H, CH_2O); 3.86 (s, 6H, OCH_3); 3.85 (s, 3H, OCH_3); 3.21 (t, J=6.8 Hz, 2H, CH_2I); 1.98-1.87 (m, 2H, CH_2); 1.84-1.74 (m, 2H, CH_2) ppm.
5.1.2.2. ***(E)-6-iodohexyl 3-(3,4,5-trimethoxyphenyl)acrylate 43***
Yield: 95.9%. ^{1}H-NMR ($CDCl_3$) δ: 7.58 (d, J=16.0 Hz, 1H, CH=CH); 6.74 (s, 2H, CH arom.); 6.33 (d, J=15.6 Hz, 1H, CH=CH); 4.19 (t, J=6.8 Hz, 2H, CH_2O); 3.88 (s, 6H, OCH_3); 3.87 (s, 3H, OCH_3); 3.19 (t, J=6.8 Hz, 2H, CH_2I); 1.91-1.79 (m, 2H, CH_2); 1.86-1.68 (m, 2H, CH_2); 1.50-1.38 (m, 4H, CH_2) ppm. ^{13}C APT NMR ($CDCl_3$) δ: 166.98 (C=O); 153.44 (C); 144.66 (*CH*=CH); 140.16 (C); 129.92 (C); 117.40 (CH=*CH*); 105.28 (CH arom.); 64.61 (CH_2); 60.95 (OCH_3); 56.18 (OCH_3); 33.13 (CH_2); 29.83 (CH_2); 26.54 (CH_2); 25.10 (CH_2); 6.79 (CH_2) ppm.
5.1.2.3. ***6-iodohexyl anthracene-9-carboxylate 44***
Yield: 90.4%. ^{1}H-NMR ($CDCl_3$) δ: 8.52 (s, 1H, CH arom.); 8.15-7.97 (m, 4H, CH arom.); 7.65-7.42 (m, 4H, CH arom.); 4.63 (t, J=6.4 Hz, 2H, CH_2O); 3.17 (t, J=6.8 Hz, 2H, CH_2I); 1.99-1.73 (m, 4H, CH_2); 1.60-1.37 (m, 4H, CH_2) ppm.

5.1.3. General procedure for the synthesis of hydroxyaminoesters ***45-54***
The appropriate haloester (**29, 30, 35-37, 41-43**) (1 mmol) and the suitable aminoalkylalcohol (3-aminopropan-1-ol, 4-aminobutan-1-ol, 5-aminopentan-1-ol or 6-aminohexan-1-ol) (2 mmol) were dissolved in 1 mL of anhydrous CH_3CN. The mixture was heated at 80 °C for 5-10 h. The reaction mixture was cooled to room temperature, treated with CH_2Cl_2 and the organic layer was washed with 10% NaOH solution. After drying with Na_2SO_4, the solvent was removed under reduced pressure and the residue purified by flash chromatography, yielding a pale-yellow oil. **52** was used as such in the next reaction.

5.1.3.1. ***(E)-2-((6-Hydroxyhexyl)amino)ethyl 3-(3,4,5- trimethoxyphenyl)acrylate 45***
Chromatographic eluent: CH_2Cl_2/MeOH/NH_4OH 90:10:1. Yield: 26.3%. ^{1}H-NMR ($CDCl_3$) δ: 7.56 (d, J=16.0 Hz, 1H, *CH*=CH); 6.71 (s, 2H, CH arom.); 6.33 (d, J=16.0 Hz, 1H, CH=*CH*); 4.27 (t, J=4.8 Hz, 2H, CH_2OH); 3.85 (s, 6H, OCH_3); 3.83 (s, 3H, OCH_3); 3.61-3.53 (m, 2H, CH_2O); 2.89 (t, J=4.8 Hz, 2H, NCH_2,); 2.61 (t, J=6.4 Hz, 2H, NCH_2); 1.59-1.41 (m, 4H, CH_2); 1.40-1.23 (m, 4H, CH_2) ppm. ESI-MS *m/z* (%): 382 (100) $[M+H]^+$.
5.1.3.2. ***(E)-4-((5-Hydroxypentil)amino)butyl 3-(3,4,5- trimethoxyphenyl)acrylate 46***
Chromatographic eluent: CH_2Cl_2/MeOH/NH_4OH 90:10:1. Yield: 35.6%. ^{1}H-NMR ($CDCl_3$) δ: 7.53 (d, J=15.6 Hz, 1H, *CH*=CH); 6.70 (s, 2H, CH arom.); 6.29 (d, J=15.6 Hz, 1H, CH=*CH*); 4.14 (t, J=6.8 Hz, 2H, CH_2O); 3.83 (s, 6H, OCH_3); 3.82 (s, 3H, OCH_3); 3.56 (t, J=6.4 Hz, 2H, CH_2OH); 3.21 (bs, 1H, OH); 2.64-2.57 (m, 4H, NCH_2); 1.78-1.68 (m, 2H, CH_2); 1.68-1.42 (m, 6H, CH_2); 1.42-1.32 (m, 2H, CH_2) ppm. ^{13}C APT NMR ($CDCl_3$) δ: 166.95 (C=O); 153.38 (C); 144.63 (CH=CH); 140.05 (C); 129.87 (C); 117.37 (CH=CH); 105.19 (CH arom.); 64.26 (CH_2); 62.19 (CH_2); 60.91 (OCH_3); 56.12 (OCH_3); 49.52 (CH_2); 49.26 (CH_2); 29.53 (CH_2); 29.06 (CH_2); 28.57 (CH_2); 28.24 (CH_2); 26.55 (CH_2) ppm.
5.1.3.3. ***(E)-5-((4-Hydroxybutyl)amino)pentyl 3-(3,4,5- trimethoxyphenyl)acrylate 47***
Chromatographic eluent: abs. ethanol/ CH_2Cl_2/petroleum ether/NH_4OH 65:340:60:8. Yield: 72.5%. ^{1}H-NMR ($CDCl_3$) δ: 7.53 (d, J=16.0 Hz, 1H, *CH*=CH); 6.71 (s, 2H, CH arom.); 6.29 (d, J=16.0 Hz, 1H, CH=*CH*); 4.13 (t, J=6.8 Hz, 2H, CH_2O); 3.83 (s, 6H, OCH_3); 3.82 (s, 3H, OCH_3); 3.51 (t, J=5.0 Hz, 2H, CH_2OH); 3.44 (bs, 1H, OH); 2.61-2.56 (m, 4H, NCH_2); 1.72-1.48 (m, 8H, CH_2); 1.49-1.32 (m, 2H, CH_2) ppm. ^{13}C APT NMR ($CDCl_3$) δ: 166.98 (C=O); 153.38 (C); 144.61 (CH=CH); 140.04 (C); 129.91 (C); 117.39 (CH=CH); 105.21 (CH arom.); 64.36 (CH_2); 62.44 (CH_2); 60.90 (OCH_3); 56.12 (OCH_3); 49.64 (CH_2); 49.32 (CH_2); 32.39 (CH_2); 29.31 (CH_2); 26.59 (CH_2); 26.44 (CH_2); 23.73 (CH_2) ppm.
5.1.3.4. ***(E)-3-((6-Hydroxyhexyll)amino)propyl 3-(3,4,5-trimethoxyphenyl)acrylate 48***

Chromatographic eluent: abs. ethanol/ CH_2Cl_2/petroleum ether/NH_4OH 65:340:60:8. Yield: 51.3%. ^{1}H-NMR ($CDCl_3$) δ: 7.60 (d, J=16.0 Hz, 1H, *CH*=CH); 6.74 (s, 2H, CH arom.); 6.32 (d, J=16.0 Hz, 1H, CH=*CH*); 4.26 (t, J=6.0 Hz, 2H, CH_2O); 3.87 (s, 6H, OCH_3); 3.86 (s, 3H, OCH_3); 3.61 (t, J=6.8 Hz, 2H, CH_2OH); 2.72 (t, J=7.2 Hz, 2H, NCH_2); 2.61 (t, J=7.2 Hz, 2H, NCH_2); 1.96-1.85 (m, 2H, CH_2); 1.83 (bs, 1H, NH); 1.61-1.58 (m, 4H, CH_2); 1.40-1.30 (m, 4H, CH_2) ppm. ^{13}C APT NMR ($CDCl_3$) δ: 166.99 (C=O); 153.43 (C); 144.81 (CH=CH); 140.16 (C); 129.87 (C); 117.25 (CH=CH); 105.26 (CH arom.); 62.80 (CH_2); 62.68 (CH_2); 60.96 (OCH_3); 56.17 (OCH_3); 49.81 (CH_2); 46.61 (CH_2); 32.65 (CH_2); 29.88 (CH_2); 29.22 (CH_2); 27.04 (CH_2); 25.62 (CH_2) ppm.

5.1.3.5. ***(E)-6-((3-Hydroxypropyl)amino)hexyl 3-(3,4,5-trimethoxyphenyl)acrylate 49***

Chromatographic eluent: abs. ethanol/ CH_2Cl_2/petroleum ether/NH_4OH 65:340:60:8. Yield: 80.3%. ^{1}H-NMR ($CDCl_3$) δ: 7.50 (d, J=15.6 Hz, 1H, *CH*=CH); 6.78 (s, 2H, CH arom.); 6.27 (d, J=15.6 Hz 1H, CH=*CH*); 4.11 (t, J=6.8 Hz, 2H, CH_2O); 3.80 (s, 6H, OCH_3); 3.79 (s, 3H, OCH_3); 3.69 (t, J=5.6 Hz, 2H, CH_2OH); 3.51 (bs, 2H, NH+OH); 2.79 (t, J=6.0 Hz, 2H, NCH_2); 2.56 (t, J=6.8 Hz, 2H, NCH_2); 1.69-1.57 (m, 4H, CH_2); 1.52-1.41 (m, 2H, CH_2); 1.40-1.22 (m, 4H, CH_2) ppm. ^{13}C APT NMR ($CDCl_3$) δ: 166.98 (C=O); 153.35 (C); 144.57 (CH=CH); 140.01 (C); 129.89 (C); 117.37 (CH=CH); 105.20 (CH arom.); 64.43 (CH_2); 63.48 (CH_2); 60.86 (OCH_3); 56.10 (OCH_3); 49.49 (CH_2); 49.37 (CH_2); 30.48 (CH_2); 29.42 (CH_2); 28.61 (CH_2); 28.81 (CH_2); 25.78 (CH_2) ppm.

5.1.3.6. ***(E)-4-((6-Hydroxyhexyl)amino)butyl 3-(3,4,5-trimethoxyphenyl)acrylate 50***

Chromatographic eluent: CH_2Cl_2/MeOH/NH_4OH 90:10:1. Yield: 57.4%. ^{1}H-NMR ($CDCl_3$) δ: 7.50 (d, J=16.0 Hz, 1H, *CH*=CH); 6.67 (s, 2H, CH arom.); 6.25 (d, J=16.0 Hz, 1H, CH=*CH*); 4.13 (t, J=6.8 Hz, 2H, CH_2O); 3.80 (s, 6H, OCH_3); 3.78 (s, 3H, OCH_3); 3.50 (t, J=6.4 Hz, 2H, CH_2OH); 2.57 (t, J=6.8 Hz, 2H, NCH_2); 2.53 (t, J=7.2 Hz, 2H, NCH_2); 2.45 (bs, 2H, OH+NH); 1.71-1.60 (m, 2H, CH_2); 1.59-1.49 (m, 2H, CH_2); 1.58-1.45 (m, 4H, CH_2); 1.33-1.20 (m, 4H, CH_2) ppm. ^{13}C APT NMR ($CDCl_3$) δ: 166.92 (C=O); 153.35 (C); 144.63 (CH=CH); 140.04 (C); 129.85 (C); 117.29 (CH=CH); 105.20 (CH arom.); 64.28 (CH_2); 62.24 (CH_2); 60.86 (OCH_3); 56.09 (OCH_3); 49.74 (CH_2); 49.40 (CH_2); 32.64 (CH_2); 29.75 (CH_2); 27.05 (CH_2); 26.55 (CH_2); 26.31 (CH_2); 25.67 (CH_2) ppm.

5.1.3.7. ***(E)-6-((4-Hydroxybutyl)amino)hexyl 3-(3,4,5-trimethoxyphenyl)acrylate 51***

Chromatographic eluent: CH_2Cl_2/MeOH/NH_4OH 95:5:0.5. Yield: 70.3%. ^{1}H-NMR ($CDCl_3$) δ: 7.58 (d, J=15.6 Hz, 1H, *CH*=CH); 6.75 (s, 2H, CH arom.); 6.34 (d, J=15.6 Hz, 1H, CH=*CH*); 4.19 (t, J=6.4 Hz, 2H, CH_2O); 3.89 (s, 6H, OCH_3); 3.87 (s, 3H, OCH_3); 3.57 (t, J=6.4 Hz, 2H, CH_2OH); 2.68-2.58 (m, 4H, NCH_2); 1.72-1.58 (m, 6H, CH_2); 1.60-1.51 (m, 2H, CH_2); 1.47-1.32 (m, 4H, CH_2) ppm. ^{13}C APT NMR ($CDCl_3$) δ: 167.27 (C=O); 153.44 (C); 144.61 (CH=CH); 129.96 (C); 117.48 (CH=CH); 105.27 (CH arom.); 64.52 (CH_2); 62.58 (CH_2); 60.97 (OCH_3); 56.18 (OCH_3); 49.66 (CH_2); 49.39 (CH_2); 32.60 (CH_2); 29.53 (CH_2); 28.83 (CH_2); 28.66 (CH_2); 26.93 (CH_2); 25.85 (CH_2) ppm.

5.1.3.8. ***(E)-6-((3-Hydroxypropyl)amino)hexyl 3-(3,4,5-trimethoxyphenyl)acrylate 52***

Yield: 72.3%. ^{1}H-NMR ($CDCl_3$) δ: 7.53 (d, J=16.0 Hz, 1H, *CH*=CH); 6.71 (s, 2H, CH arom.); 6.29 (d, J=16.0 Hz, 1H, CH=*CH*); 4.14 (t, J=6.8 Hz, 2H, CH_2O); 3.83 (s, 6H, OCH_3); 3.82 (s, 3H, OCH_3); 3.73 (t, J=5.6 Hz, 2H, CH_2OH); 2.91 (bs, 2H, NH+OH); 2.80 (t, J=6.0 Hz, 2H, NCH_2); 2.55 (t, J=7.2 Hz, 2H, NCH_2); 1.72-1.62 (m, 4H, CH_2); 1.50-1.38 (m, 2H, CH_2); 1.38-1.25 (m, 6H, CH_2) ppm. ^{13}C APT NMR ($CDCl_3$) δ: 167.05 (C=O); 153.42 (C); 144.58 (CH=CH); 140.10 (C); 129.95 (C); 117.48 (CH=CH); 105.27 (CH arom.); 64.61 (CH_2); 64.19 (CH_2); 60.93 (OCH_3); 56.16 (OCH_3); 49.87 (CH_2); 49.71 (CH_2); 30.56 (CH_2); 29.74 (CH_2); 29.12 (CH_2); 28.68 (CH_2); 27.12 (CH_2); 25.88 (CH_2) ppm.

5.1.3.9. ***6-((3-Hydroxypropyl)amino)hexyl 3,4,5-trimethoxybenzoate 53***

Chromatographic eluent: abs. ethanol/ CH_2Cl_2/petroleum ether/NH_4OH 65:340:60:8. Yield: 71.4%. ^{1}H-NMR ($CDCl_3$) δ: 7.24 (s, 2H, CH arom.); 4.24 (t, J=6.8 Hz, 2H, CH_2O); 3.85 (s, 6H, OCH_3); 3.84 (s, 3H, OCH_3); 3.73 (t, J=5.6 Hz, 2H, CH_2OH); 3.21 (bs, 1H, OH); 2.80 (t, J=6.0 Hz, 2H, NCH_2); 2.55 (t, J=6.8 Hz, 2H, NCH_2); 1.76-1.67 (m, 2H, CH_2); 1.67-61 (m, 2H, CH_2); 1.48-1.23 (m, 8H, CH_2) ppm. ^{13}C APT NMR ($CDCl_3$) δ: 166.21 (C=O); 152.87 (C); 142.12 (C); 125.48 (C);

106.78 (CH arom.); 65.15 (CH_2); 64.00 (CH_2); 60.84 (OCH_3); 56.20 (OCH_3); 49.76 (CH_2); 49.70 (CH_2); 30.64 (CH_2); 29.74 (CH_2); 29.30 (CH_2); 28.65 (CH_2); 27.11 (CH_2); 25.89 (CH_2) ppm.

5.1.3.10. ***6-((3- Hydroxypropyl)amino)hexyl anthracene-9-carboxylate 54***

Chromatographic eluent: abs. ethanol/ CH_2Cl_2/petroleum ether/NH_4OH 65:340:60:8. Yield: 48.4%. ^{1}H-NMR ($CDCl_3$) δ: 8.50 (s, 1H, CH arom.); 8.03 (d, J=8.8 Hz, 2H, CH arom.); 8.00 (d, J=8.4 Hz, 2H, CH arom.); 7.55-7.40 (m, 4H, CH arom.); 4.60 (t, J=6.8 Hz, 2H, CH_2O); 3.78 (t, J=5.2 Hz, 2H, CH_2OH); 3.21 (bs, 1H, OH); 2.82 (t, J=5.6 Hz, 2H, NCH_2); 2.56 (t, J=7.2 Hz, 2H, NCH_2); 1.90-1.81 (m, 2H, CH_2); 1.72-1.61 (m, 2H, CH_2); 1.50-1.20 (m, 8H, CH_2) ppm.

5.1.4. General procedure for the synthesis of (hydroxyalkyl)methylaminoesters ***55-64***

A 1 mmol portion of the appropriate hydroxyaminoester (**45-54**) was dissolved in 5 mL of anhydrous ethanol and HCOOH (17 mmol) and 37% HCHO solution (5 mmol) were added. The mixture was heated to 80 °C for 4-5 h and concentrated in vacuo. The residue was then dissolved in CH_2Cl_2 and the organic layer was washed with 10% NaOH solution. After drying with Na_2SO_4, the solvent was removed under reduced pressure, giving a pure compound as yellow oil which was used as such for the next reaction.

5.1.4.1. ***(E)-2-((6-Hydroxyhexyl)(methyl)amino)ethyl 3-(3,4,5-trimethoxyphenyl)acrylate 55***

Yield: 80.7%. ^{1}H-NMR ($CDCl_3$) δ: 7.61 (d, J=16.0 Hz, 1H, *CH*=CH); 6.75 (s, 2H, CH arom.); 6.37 (d, J=16.0 Hz, 1H, CH=*CH*); 4.33 (t, J=6.0 Hz, 2H, CH_2O); 3.88 (s, 6H, OCH_3); 3.87 (s, 3H, OCH_3); 3.62 (t, J=6.4 Hz, 2H, CH_2O); 2.75 (t, J=6.0 Hz, 2H, NCH_2); 2.47 (t, J=7.2 Hz, 2H, NCH_2); 2.36 (s, 3H, NCH_3); 1.63 -1.48 (m, 4H, CH_2); 1.46-1.28 (m, 4H, CH_2) ppm.

5.1.4.2. ***(E)-4-((5-Hydroxypentyl)(methyl)amino)butyl 3-(3,4,5-trimethoxyphenyl)acrylate 56***

Yield: 92.0%. ^{1}H-NMR ($CDCl_3$) δ: 7.54 (d, J=16.0 Hz, 1H, *CH*=CH); 6.71 (s, 2H, CH arom.); 6.30 (d, J=16.0 Hz, 1H, CH=*CH*); 4.17 (t, J=6.8 Hz, 2H, CH_2O); 3.84 (s, 6H, OCH_3); 3.83 (s, 3H, OCH_3); 3.58 (t, J=6.8 Hz, 2H, CH_2O); 2.40-2.25 (m, 4H, NCH_2); 2.16 (s, 3H, NCH_3); 1.74-1.50 (m, 6H, CH_2); 1.50-1.40 (m, 2H, CH_2); 1.40-1.32 (m, 2H, CH_2) ppm. ^{13}C APT NMR ($CDCl_3$) δ: 166.99 (C=O); 153.39 (C); 144.62 (CH=CH); 140.05 (C); 129.91 (C); 117.40 (CH=CH); 105.20 (CH arom.); 64.43 (CH_2); 62.62 (CH_2); 60.92 (OCH_3); 57.68 (CH_2); 57.35 (CH_2); 56.13 (OCH_3); 41.11 (NCH_3); 32.48 (CH_2); 28.88 (CH_2); 26.76 (CH_2); 24.14 (CH_2); 23.91 (CH_2) ppm.

5.1.4.3. ***(E)-5-((4-Hydroxybutyl)(methyl)amino)pentyl 3-(3,4,5-trimethoxyphenyl)acrylate 57***

Yield: 85.0%. ^{1}H-NMR ($CDCl_3$) δ: 7.54 (d, J=16.0 Hz, 1H, *CH*=CH); 6.71 (s, 2H, CH arom.); 6.30 (d, J=16.0 Hz, 1H, CH=*CH*); 4.15 (t, J=6.8 Hz, 2H, CH_2O); 3.84 (s, 6H, OCH_3); 3.83 (s, 3H, OCH_3); 3.51 (m, J=5.6 Hz, 2H, CH_2O); 2.41-2.30 (m, 4H, NCH_2); 2.19 (s, 3H, NCH_3); 1.74-1.51 (m, 6H, CH_2); 1.51-1.50 (m, 2H, CH_2); 1.48-1.32 (m, 2H, CH_2) ppm. ^{13}C APT NMR ($CDCl_3$) δ: 166.96 (C=O); 153.39 (C); 144.57 (CH=CH); 140.06 (C); 129.93 (C); 117.42 (CH=CH); 105.22 (CH arom.); 64.39 (CH_2); 62.60 (CH_2); 60.90 (OCH_3); 58.17 (CH_2); 57.74 (CH_2); 56.13 (OCH_3); 41.21 (NCH_3); 32.54 (CH_2); 28.62 (CH_2); 26.45 (CH_2); 26.14 (CH_2); 23.89 (CH_2) ppm.

5.1.4.4. ***(E)-3-((6-Hydroxyhexyl)(methyl)amino)propyl 3-(3,4,5-trimethoxyphenyl)acrylate 58***

Yield: 91.1%. ^{1}H-NMR ($CDCl_3$) δ: 7.54 (d, J=16.0 Hz, 1H, *CH*=CH); 6.71 (s, 2H, CH arom.); 6.29 (d, J=16.0 Hz, 1H, CH=*CH*); 4.19 (t, J=6.8 Hz, 2H, CH_2O); 3.84 (s, 6H, OCH_3); 3.82 (s, 3H, OCH_3); 3.56 (t, J=6.8 Hz, 2H, CH_2O); 2.42 (t, J=7.2 Hz, 2H, NCH_2); 2.30 (t, J=7.6 Hz, 2H, NCH_2); 2.18 (s, 3H, NCH_3); 1.89-1.77 (m, 2H, CH_2); 1.54-1.49 (m, 2H, CH_2); 1.49-1.40 (m, 2H, CH_2); 1.40-1.20 (m, 4H, CH_2) ppm. ^{13}C APT NMR ($CDCl_3$) δ: 166.95 (C=O); 153.40 (C); 144.68 (CH=CH); 140.11 (C); 129.88 (C); 117.31 (CH=CH); 105.25 (CH arom.); 63.03 (CH_2); 62.56 (CH_2); 60.91 (OCH_3); 57.58 (CH_2); 56.14 (OCH_3); 54.18 (CH_2); 42.09 (NCH_3); 32.67 (CH_2); 27.16 (CH_2); 27.08 (CH_2); 26.54 (CH_2); 25.64 (CH_2) ppm.

5.1.4.5. ***(E)-6-((3-Hydroxypropyl)(methyl)amino)hexyl 3-(3,4,5-trimethoxyphenyl)acrylate 59***

Yield: 96.3%. ^{1}H-NMR ($CDCl_3$) δ: 7.49 (d, J=15.6 Hz, 1H, *CH*=CH); 6.67 (s, 2H, CH arom.); 6.26 (d, J=15.6 Hz, 1H, CH=*CH*); 4.10 (t, J=6.4 Hz, 2H, CH_2O); 3.79 (s, 6H, OCH_3); 3.78 (s, 3H, OCH_3); 3.69 (t, J=5.6 Hz, 2H, CH_2O); 2.48 (t, J=6.0 Hz, 2H, NCH_2); 2.27 (t, J=7.2 Hz, 2H, NCH_2);

2.14 (s, 3H, NCH_3); 1.68-1.58 (m, 4H, CH_2); 1.48-1.20 (m, 6H, CH_2) ppm. ^{13}C APT NMR ($CDCl_3$) δ: 166.91 (C=O); 153.34 (C); 144.50 (CH=CH); 140.01 (C); 129.89 (C); 117.41 (CH=CH); 105.19 (CH arom.); 64.45 (CH_2); 64.42 (CH_2); 60.83 (OCH_3); 58.30 (CH_2); 57.97 (CH_2); 56.07 (OCH_3); 41.88 (NCH_3); 28.62 (CH_2); 27.78 (CH_2); 27.09 (CH_2); 26.91 (CH_2); 22.66 (CH_2) ppm.

5.1.4.6. ***(E)-4-(6-Hydroxyhexyl(methyl)amino)butyl 3-(3,4,5-trimethoxyphenyl)acrylate 60***

Yield: 96.9%. ^{1}H-NMR ($CDCl_3$) δ: 7.50 (d, J=16.0 Hz, 1H, *CH*=CH); 6.68 (s, 2H, CH arom.); 6.26 (d, J=16.0 Hz, 1H, CH=*CH*); 4.13 (t, J=6.4 Hz, 2H, CH_2O); 3.80 (s, 6H, OCH_3); 3.79 (s, 3H, OCH_3); 3.51 (t, J=6.8 Hz, 2H, CH_2O); 2.86 (bs, 1H, OH); 2.30-2.22 (m, 4H, NCH_2); 2.12 (s, 3H, NCH_3); 1.65-1.59 (m, 2H, CH_2); 1.54-1.44 (m, 4H, CH_2); 1.43-1.33 (m, 2H, CH_2); 1.32-1.18 (m, 4H, CH_2) ppm. ^{13}C APT NMR ($CDCl_3$) δ: 166.97 (C=O); 153.34 (C); 144.61 (CH=CH); 139.99 (C); 129.87 (C); 118.00 (CH=CH); 105.17 (CH arom.); 64.39 (CH_2); 62.40 (CH_2); 60.87 (OCH_3); 57.66 (CH_2); 57.25 (CH_2); 56.08 (OCH_3); 42.10 (NCH_3); 32.66 (CH_2); 27.25 (CH_2); 27.06 (CH_2); 26.73 (CH_2); 25.67 (CH_2); 23.63 (CH_2) ppm.

5.1.4.7. ***(E)-6-(4-Hydroxybutyl(methyl)amino)hexyl 3-(3,4,5-trimethoxyphenyl)acrylate 61***

Yield: 93.1%. ^{1}H-NMR ($CDCl_3$) δ: 7.53 (d, J=16.0 Hz, 1H, *CH*=CH); 6.71 (s, 2H, CH arom.); 6.30 (d, J=16.0 Hz, 1H, CH=*CH*); 4.14 (t, J=6.4 Hz, 2H, CH_2O); 3.84 (s, 6H, OCH_3); 3.83 (s, 3H, OCH_3); 3.52-3.47 (m, 2H, CH_2O); 2.36-2.24 (m, 4H, NCH_2); 2.17 (s, 3H, NCH_3); 1.70-1.55 (m, 6H, CH_2); 1.54-1.44 (m, 2H, CH_2); 1.53-1.23 (m, 4H, CH_2) ppm. ^{13}C APT NMR ($CDCl_3$) δ: 166.96 (C=O); 153.40 (C); 144.51 (CH=CH); 140.07 (C); 129.94 (C); 117.47 (CH=CH); 105.23 (CH arom.); 64.49 (CH_2); 62.63 (CH_2); 60.88 (OCH_3); 58.23 (CH_2); 57.87 (CH_2); 56.12 (OCH_3); 41.23 (NCH_3); 32.66 (CH_2); 28.64 (CH_2); 27.09 (CH_2); 26.74 (CH_2); 26.30 (CH_2); 25.88 (CH_2) ppm.

5.1.4.8. ***(E)-6-((3-Hydroxypropyl(methyl)amino)hexyl 3-(3,4,5-trimethoxyphenyl)acrylate 62***

Yield: 97.6%. ^{1}H-NMR ($CDCl_3$) δ: 7.56 (d, J=15.6 Hz, 1H, *CH*=CH); 6.73 (s, 2H, CH arom.); 6.31 (d, J=15.6 Hz, 1H, CH=*CH*); 4.16 (t, J=6.4 Hz, 2H, CH_2O); 3.86 (s, 6H, OCH_3); 3.85 (s, 3H, OCH_3); 3.76 (t, J=5.2 Hz, 2H, CH_2O); 2.56 (t, J=5.6 Hz, 2H, NCH_2); 2.33 (t, J=7.2 Hz, 2H, NCH_2); 2.21 (s, 3H, NCH_3); 1.72-1.63 (m, 4H, CH_2); 1.50-1.42 (m, 2H, CH_2); 1.42-1.25 (m, 6H, CH_2) ppm.

5.1.4.9. ***6-((3-Hydroxypropyl)(methyl)amino)hexyl 3,4,5-trimethoxybenzoate 63***

Yield: 79.8%. ^{1}H-NMR ($CDCl_3$) δ: 7.26 (s, 2H, CH arom.); 4.27 (t, J=6.8 Hz, 2H, CH_2O); 3.87 (s, 6H, OCH_3); 3.86 (s, 3H, OCH_3); 3.75 (t, J=5.4 Hz, 2H, CH_2O); 2.47 (t, J=5.6 Hz, 2H, NCH_2); 2.32 (t, J=7.6 Hz, 2H, NCH_2); 2.20 (s, 3H, NCH_3); 1.80-1.69 (m, 2H, CH_2); 1.68-1.62 (m, 2H, CH_2); 1.50-1.23 (m, 8H, CH_2) ppm. ^{13}C APT NMR ($CDCl_3$) δ: 166.24 (C=O); 152.88 (C); 142.10 (C); 125.50 (C); 106.77 (CH arom.); 65.18 (CH_2); 64.59 (CH_2); 60.86 (OCH_3); 58.50 (CH_2); 58.06 (CH_2); 56.21 (OCH_3); 41.85 (NCH_3); 29.16 (CH_2); 28.67 (CH_2); 27.65 (CH_2); 27.17 (CH_2); 27.10 (CH_2); 25.92 (CH_2) ppm.

5.1.4.10. ***6-((3-Hydroxypropyl)(methyl)amino)hexyl anthracene-9-carboxylate 64***

Yield: 87.2%. ^{1}H-NMR ($CDCl_3$) δ: 8.50 (s, 1H, CH arom.); 8.03 (d, J=8.8 Hz, 2H, CH arom.); 8.00 (d, J=8.4 Hz, 2H, CH arom.); 7.55-7.42 (m, 4H, CH arom.); 4.61 (t, J=6.8 Hz, 2H, CH_2O); 3.78 (t, J=5.2 Hz, 2H, CH_2O); 2.56 (t, J=5.6 Hz, 2H, NCH_2); 2.34 (t, J=7.2 Hz, 2H, NCH_2); 2.21 (s, 3H, NCH_3); 1.93-1.86 (m, 2H, CH_2); 1.70-1.64 (m, 2H, CH_2); 1.50-1.20 (m, 8H, CH_2) ppm. ^{13}C APT NMR ($CDCl_3$) δ: 169.77 (C=O); 131.01 (C); 129.20 (CH arom.); 128.61 (CH arom.); 128.39 (C); 129.92 (CH arom.); 125.46 (CH arom.); 125.02 (CH arom.); 65.91 (CH_2); 64.61 (CH_2); 58.45 (CH_2); 58.07 (CH_2); 41.85 (NCH_3); 29.15 (CH_2); 28.72 (CH_2); 27.65 (CH_2); 27.18 (CH_2); 27.03 (CH_2); 26.03 (CH_2) ppm.

5.1.5. ***General procedure for the synthesis of (2-hydroxyethyl)methylaminoesters 65-72***

The appropriate haloester (**35-40**, **43**, **4**) (1 mmol) and 2-methylaminoethan-1-ol (2 mmol) were dissolved in 3 mL of anhydrous CH_3CN. The mixture was maintained at rt for 48 h. The reaction mixture was treated with CH_2Cl_2 and the organic layer was washed with 10% NaOH solution. After drying with Na_2SO_4, the solvent was removed under reduced pressure.

The substances obtained were used as such for the next reaction (**65**, **66**, **67**), or were purified by flash chromatography in the case of **68**, **69**, **70**, **71** and **72**.

5.1.5.1. ***(E)-6-((2- Hydroxyethyl) methylamino)hexyl 3-(3,4,5- trimethoxyphenyl)acrylate 65***
Yellow oil. Yield: 91.0%. ^{1}H-NMR ($CDCl_3$) δ: 7.56 (d, J=16.0 Hz, 1H, *CH*=CH); 6.73 (s, 2H, CH arom.); 6.32 (d, J=16.0 Hz, 1H, CH=*CH*); 4.17 (t, J=6.8 Hz, 2H, CH_2O); 3.86 (s, 6H, OCH_3); 3.85 (s, 3H, OCH_3); 3.55 (t, J=5.6 Hz, 2H, CH_2OH); 2.99 (bs, 1H, OH); 2.49 (t, J=5.6 Hz, 2H, NCH_2); 2.37 (t, J=7.2 Hz, 2H, NCH_2);2.21 (s, 3H, NCH_3); 1.77-1.60 (m, 2H, CH_2); 1.53-1.42 (m, 2H, CH_2); 1.41-1.26 (m, 4H, CH_2) ppm.
5.1.5.2. ***6-((2-Hydroxyethyl)methylamino)hexyl anthracene-9-carboxylate 66***
Yellow oil. Yield: 94.9%. ^{1}H-NMR ($CDCl_3$) δ: 8.48 (s, 1H, CH arom.); 8.05-7.87 (m, 4H, CH arom.); 7.56-7.40 (m, 4H, CH arom.); 4.62 (t, J=6.8 Hz, 2H, CH_2O); 3.57 (t, J=5.6 Hz, 2H, CH_2OH); 2.50 (t, J=5.6 Hz, 2H, NCH_2); 2.39 (t, J=6.8 Hz, 2H, NCH_2); 2.23 (s, 3H, NCH_3); 1.95-1.86 (m, 2H, CH_2); 1.57-1.43 (m, 4H, CH_2); 1.42-1.30 (m, 2H, CH_2) ppm.
5.1.5.3. ***(E)-7-((2- Hydroxyethyl)methylamino)heptyl 3-(3,4,5- trimethoxyphenyl)acrylate 67***
Yellow-orange oil. Yield 93.2%.^{1}H-NMR ($CDCl_3$) δ: 7.52 (d, J=16.0 Hz, 1H, *CH*=CH); 6.69 (s, 2H, CH arom.); 6.28 (d, J=16.0 Hz, 1H, CH=*CH*); 4.13 (t, J=6.4 Hz, 2H, CH_2O); 3.82 (s, 6H, OCH_3); 3.81 (s, 3H, OCH_3); 3.51 (t, J=5.6 Hz, 2H, CH_2OH); 2.99 (bs, 1H, OH); 2.44 (t, J=5.6 Hz, 2H, NCH_2); 2.32 (t, J=7.2 Hz, 2H, NCH_2); 2.16 (s, 3H, NCH_3); 1.69-1.59 (m, 2H, CH_2); 1.48-1.20 (m, 8H, CH_2) ppm. ^{13}C APT NMR ($CDCl_3$) δ: 166.98 (C=O); 153.37 (C); 144.52 (CH=CH); 140.05 (C); 129.92 (C); 117.44 (CH=CH); 105.23 (CH arom.); 64.56 (CH_2); 60.86 (OCH_3); 58.86 (CH_2); 58.41 (CH_2); 57.72 (CH_2); 56.10 (OCH_3); 41.63 (NCH_3); 29.13 (CH_2); 28.66 (CH_2); 27.14 (CH_2); 25.89 (CH_2) ppm.
5.1.5.4. ***7-((2-Hydroxyethyl)methylamino)heptyl 3,4,5-trimethoxybenzoate 68***
Oil. Chromatographic eluent: CH_2Cl_2/MeOH/NH_4OH 95:5:0.5. Yield: 77.3%. ^{1}H-NMR ($CDCl_3$) δ: 7.27 (s, 2H, CH arom.); 4.28 (t, J=6.8 Hz, 2H, CH_2O); 3.89 (s, 6H, OCH_3); 3.88 (s, 3H, OCH_3); 3.55 (t, J=5.6 Hz, 2H, CH_2OH); 2.92 (bs, 1H, OH); 2.50 (t, J=5.6 Hz, 2H, NCH_2); 2.38 (t, J=7.6 Hz, 2H, NCH_2); 2.22 (s, 3H, NCH_3); 1.81-1.70 (m, 2H, CH_2); 1.50-1.28 (m, 8H, CH_2) ppm.
5.1.5.5. ***7-((2-Hydroxyethyl)methylamino)heptyl anthracene-9-carboxylate 69***
Pale yellow oil. Chromatographic eluent: CH_2Cl_2/MeOH/NH_4OH 96:4:0.4. Yield: 66%. ^{1}H-NMR ($CDCl_3$) δ: 8.51 (s, 1H, CH arom.); 8.04 (d, J=8.8 Hz, 2H, CH arom.); 8.05 (d, J=8.4 Hz, 2H, CH arom.); 7.58-7.40 (m, 4H, CH arom.); 4.61 (t, J=6.8 Hz, 2H, CH_2O); 3.57 (t, J=5.6 Hz, 2H, CH_2OH); 2.92 (bs, 1H, OH); 2.51 (t, J=5.6 Hz, 2H, NCH_2); 2.39 (t, J=7.6 Hz, 2H, NCH_2; 2.25 (s, 3H, NCH_3); 1.94-1.83 (m 2H, CH_2); 1.50-1.20 (m, 8H, CH_2) ppm.
5.1.5.6. ***(E)-8-(2- Hydroxyethyl)methylamino)octyl 3-(3,4,5-trimethoxyphenyl)acrylate 70***
Pale yellow oil. Chromatographic eluent: CH_2Cl_2/MeOH/NH_4OH 90:10:1. Yield: 56.1%. ^{1}H-NMR ($CDCl_3$) δ: 7.54 (d, J=16.0 Hz, 1H, *CH*=CH); 6.71 (s, 2H, CH arom.); 6.30 (d, J=16.0 Hz, 1H, CH=*CH*); 4.15 (t, J=6.8 Hz, 2H, CH_2O); 3.84 (s, 6H, OCH_3); 3.83 (s, 3H, OCH_3); 3.54 (t, J=5.6 Hz, 2H, CH_2OH); 2.96 (bs, 1H, OH); 2.47 (t, J=5.6 Hz, 2H, NCH_2); 2.35 (t, J=7.2 Hz, 2H, NCH_2); 2.19 (s, 3H, NCH_3); 1.70-1.59 (m, 2H, CH_2); 1.47-1.38 (m, 2H, CH_2); 1.37-1.19 (m, 8H, CH_2) ppm. ^{13}C APT NMR ($CDCl_3$) δ: 167.02 (C=O); 153.39 (C); 144.54 (CH=CH); 140.01 (C); 129.94 (C); 117.47 (CH=CH); 105.18 (CH arom.); 64.64 (CH_2); 60.91 (OCH_3); 58.81 (CH_2); 58.33 (CH_2); 57.74 (CH_2); 56.11 (OCH_3); 41.60 (NCH_3); 29.40 (CH_2); 29.22 (CH_2); 28.71 (CH_2); 27.21 (CH_2); 27.18 (CH_2); 25.91 (CH_2) ppm.
5.1.5.7. ***8-(2- Hydroxyethyl)methylamino)octyl 3-(3,4,5- trimethoxybenzoate 71***
Pale yellow oil. Chromatographic eluent: CH_2Cl_2/MeOH/NH_4OH 95:5:0.5. Yield: 75.6%. ^{1}H-NMR ($CDCl_3$) δ: 7.28 (s, 2H, CH arom.); 4.29 (t, J=6.8 Hz, 2H, CH_2O); 3.89 (s, 6H, OCH_3); 3.88 (s, 3H, OCH_3); 3.56 (t, J=5.2 Hz, 2H, CH_2OH); 2.50 (t, J=5.2 Hz, 2H, CH_2N); 2.37 (t, J=7.2 Hz, 2H, CH_2N); 2.22 (s, 3H, NCH_3); 1.81-1.70 (m, 2H, CH_2); 1.50-1.22 (m, 10H, CH_2) ppm.
5.1.5.8. ***8-(2- Hydroxyethyl)methylamino)octyl anthracene-9-carboxylate 72***
Yellow oil. Chromatographic eluent: CH_2Cl_2/MeOH/NH_4OH 90:10:0.1. Yield: 32.4%.
^{1}H-NMR ($CDCl_3$) δ: 8.50 (s, 1H, CH arom.); 8.05-8.00 (m, 4H, CH arom.); 7.61-7.47 (m, 4H, CH arom.); 4.61 (t, J=6.8 Hz, 2H, CH_2O); 3.57 (t, J=5.2 Hz, 2H, CH_2OH); 2.50 (t, J=5.2 Hz, 2H,

NCH_2); 2.37 (t, J=7.2 Hz, 2H, NCH_2); 2.20 (s, 3H, NCH_3); 1.93-1.82 (m, 2H, CH_2); 1.53-1.42 (m, 2H, CH_2); 1.51-1.20 (m, 8H, CH_2) ppm.

5.1.6. General procedures for the synthesis of diester compounds ***1-28***

Diester compounds were synthesized using two different general procedures.

General procedure A.

A solution of the suitable (hydroxyalkyl)methylaminoester (0.250 mmol) in 5 mL of an. CH_2Cl_2 was cooled at 0 °C and 0.360 mmol of the appropriate carboxylic acid, 0.083 mmol of 4-dimethylaminopiridine (DMAP) and 0.500 mmol of 1-(3-dimethylaminopropyl)-3-ethylcarbodiimide hydrochloride (EDCl) were added. The reaction mixture was stirred for 1 h at 0 °C and 48 h at room temperature. Then CH_2Cl_2 was added and the organic layer was washed twice with a saturated solution of $NaHCO_3$. After drying with Na_2SO_4, the solvent was removed under reduced pressure. The crude product was then purified by flash chromatography using the appropriate eluting system, yielding the desired compound as an oil. All the compounds were transformed into the corresponding hydrochloride as white solid. The salts were crystallized from abs. ethanol/petroleum ether.

General procedure B.

A 0.250 mmol portion of the appropriate carboxylic acid ((*E*)-3-(3,4,5-trimethoxyphenyl)acrylic acid, 3,4,5-trimethoxybenzoic acid or anthracene-9-carboxylic acid) was transformed into the acyl chloride by reaction with $SOCl_2$ (2 eq) in 3 mL of $CHCl_3$ (free of ethanol) at 60 °C for 4-5 h.

The reaction mixture was cooled to rt, and the solvent was removed under reduced pressure; the mixture was then treated twice with cyclohexane and the solvent removed under reduce pressure. The acyl chloride obtained was dissolved in $CHCl_3$ (free of ethanol), and the suitable (hydroxyalkyl)methylaminoester (1 eq) was added. The mixture was heated to 60 °C. After 4 h, the reaction mixture was cooled to rt, and treated with CH_2Cl_2. The resulting organic layer was washed with 10% NaOH solution, dried with Na_2SO_4, and the solvent was removed under reduced pressure. The substances obtained were purified by flash chromatography using the appropriate eluting system, yielding the desired compound as an oil. All the compounds were transformed into the corresponding hydrochloride as white solid. The salts were crystallized from abs. ethanol/petroleum ether.

5.1.6.1. ***(E)-2-(Methyl-(6-((3-(3,4,5-trimethoxyphenyl)acryloyl)oxy))hexyl)amino)ethyl 3,4,5-trimethoxybenzoate 1***

Procedure A, starting from **65** and 3,4,5-trimethoxybenzoic acid.

Free base: chromatographic eluent: CH_2Cl_2/MeOH/NH_4OH 98:2:0.2. Yield: 69.1.%.

^{1}H-NMR ($CDCl_3$) δ: 7.52 (d, J=16.0 Hz, 1H, *CH*=CH); 7.23 (s, 2H, CH arom.); 6.69 (s, 2H, CH arom.); 6.28 (d, J=16.0 Hz, 1H, CH=*CH*); 4.35 (t, J=6.0 Hz, 2H, CH_2O); 4.11 (t, J=6.8 Hz, 2H, CH_2O); 3.82 (s, 9H, OCH_3); 3.81 (s, 6H, OCH_3); 3.80 (s, 3H, OCH_3); 2.73 (t, J=6.0 Hz, 2H, NCH_2); 2.41 (t, J=7.6 Hz, 2H, NCH_2); 2.29 (s, 3H, NCH_3); 1.65-1.58 (m, 2H, CH_2); 1.50-1.40 (m, 2H, CH_2); 1.40-1.23 (m, 4H, CH_2) ppm. ^{13}C APT NMR ($CDCl_3$) δ: 166.90 (C=O); 166.05 (C=O); 153.36 (C); 152.86 (C); 144.53 (CH=CH); 142.20 (C); 140.02 (C); 129.88 (C); 125.16 (C); 117.39 (CH=CH); 106.84 (CH arom.); 105.18 (CH arom.); 64.44 (CH_2); 62.92 (CH_2); 60.85 (OCH_3); 60.81 (OCH_3); 57.83 (NCH_2); 56.16 (OCH_3); 56.08 (OCH_3); 55.57 (NCH_2); 42.67 (NCH_3); 28.67 (CH_2); 27.19 (CH_2); 26.96 (CH_2); 25.86 (CH_2) ppm.

Hydrochloride: mp 90-92 °C**. Anal:** $C_{31}H_{44}ClNO_{10}$ (C, H, N).

5.1.6.2. ***(E)-6-(Methyl-(2-((3-(3,4,5-trimethoxyphenyl)acryloyl)oxy)ethyl)amino)hexyl 3,4,5-trimethoxybenzoate 2***

Procedure A, starting from **55** and 3,4,5-trimethoxybenzoic acid.

Free base: chromatographic eluent: CH_2Cl_2/MeOH/NH_4OH 98:2:0.2. Yield: 68.8.%.

^{1}H-NMR ($CDCl_3$) δ: 7.58 (d, J=16.0 Hz, 1H, *CH*=CH); 7.26 (s, 2H, CH arom.); 6.72 (s, 2H, CH arom.); 6.35 (d, J=16.0 Hz, 1H, CH=*CH*); 4.32-4.25 (m, 4H, CH_2O); 3.87 (s, 6H, OCH_3); 3.86 (s,

3H, OCH_3); 3.85 (s, 6H, OCH_3); 3.84 (s, 3H, OCH_3); 2.72 (t, J=6.0 Hz, 2H, NCH_2); 2.45 (t, J=7.6 Hz, 2H, NCH_2); 2.33 (s, 3H, NCH_3); 1.78-1.71 (m, 2H, CH_2); 1.58-1.30 (m, 6H, CH_2) ppm. ^{13}C APT NMR ($CDCl_3$) δ: 166.85 (C=O); 166.21 (C=O); 153.42 (C); 152.91 (C); 144.97 (CH=CH); 142.16 (C); 140.17(C); 129.83 (C); 125.46 (C); 117.15 (CH=CH); 106.84 (CH arom.); 105.31 (CH arom.); 65.07 (CH_2); 61.88 (CH_2); 60.92 (OCH_3); 60.87 (OCH_3); 57.80 (NCH_2); 56.23 (OCH_3); 56.14 (OCH_3); 55.60 (NCH_2); 42.53 (NCH_3); 28.72 (CH_2); 27.03 (CH_2); 26.87 (CH_2); 25.92 (CH_2) ppm.

Hydrochloride: mp 97-98 °C**. Anal:** $C_{31}H_{44}ClNO_{10}$ (C, H, N).

5.1.6.3. ***(E)-2-(Methyl-(6-((3-(3,4,5-trimethoxyphenyl)acryloyl)oxy)hexyl)amino)ethyl anthracene-9- carboxylate 3***

Procedure B, starting from **65** and anthracene-9-carboxylic acid.

Free base: chromatographic eluent: CH_2Cl_2/MeOH/NH_4OH 98:2:0.2. Yield: 32.8.%.

^{1}H-NMR ($CDCl_3$) δ: 8.49 (s, 1H, CH arom.); 8.14 (d, J=8.8 Hz, 2H, CH arom.); 7.99 (d, J=8.4 Hz, 2H, CH arom.); 7.58 (d, J=16.0 Hz, 1H, *CH*=CH); 7.54-7.44 (m, 4H, CH arom.); 6.73 (s, 2H, CH arom.); 6.33 (d, J=16.0 Hz, 1H, CH=*CH*); 4.75 (t, J=5.6 Hz, 2H, CH_2O); 4.14 (t, J=6.4 Hz, 2H, CH_2O); 3.87 (s, 3H, OCH_3); 3.85 (s, 6H, OCH_3); 2.90 (t, J=5.6 Hz, 2H, NCH_2); 2.51 (t, J=7.6 Hz, 2H, NCH_2); 2.39 (s, 3H, NCH_3); 1.69-1.51 (m, 4H, CH_2); 1.43-1.21 (m, 4H, CH_2) ppm. ^{13}C APT NMR ($CDCl_3$) δ: 169.45 (C=O); 167.02 (C=O); 153.42 (C); 144.59 (CH=CH); 140.07 (C); 130.97 (C); 129.95 (C); 129.37 (CH arom.); 128.58 (CH arom.); 128.47 (C); 127.86 (C); 126.91 (CH arom.); 125.46 (CH arom.); 125.23 (CH arom.); 117.48 (CH=CH); 105.22 (CH arom.); 64.54 (CH_2); 62.98 (CH_2); 60.97 (OCH_3); 57.79 (CH_2); 56.14 (OCH_3); 55.91 (CH_2); 42.37 (NCH_3); 28.68 (CH_2); 27.03 (CH_2); 25.90 (CH_2) ppm.

Hydrochloride: mp 84-86 °C**. Anal:** $C_{36}H_{42}ClNO_7$ (C, H, N).

5.1.6.4. ***(E)-6-(Methyl-(2-((3-(3,4,5-trimethoxyphenyl)acryloyl)oxy)ethyl)amino)hexyl anthracene-9- carboxylate 4***

Procedure A, starting from **66** and (*E*)-3-(3,4,5-trimethoxyphenyl)acrylic acid.

Free base: chromatographic eluent: CH_2Cl_2/MeOH/NH_4OH 99:1:0.1. Yield: 39.7.%.

^{1}H-NMR ($CDCl_3$) δ**:** 8.47 (s, 1H, CH arom.); 8.02 (d, J=8.8 Hz, 2H, CH arom.); 7.97 (d, J=8.4 Hz, 2H, CH arom.); 7.60 (d, J=16.0 Hz, 1H, *CH*=CH); 7.55-7.43 (m, 4H, CH arom.); 6.72 (s, 2H, CH arom.); 6.38 (d, J=16.0 Hz, 1H, CH=*CH*); 4.59 (t, J=6.8 Hz, 2H, CH_2O); 4.29 (t, J=6.0 Hz, 2H, CH_2O); 3.85 (s, 3H, OCH_3); 3.82 (s, 6H, OCH_3); 2.68 (t, J=5.6 Hz, 2H, NCH_2); 2.40 (t, J=7.2 Hz, 2H, NCH_2); 2.29 (s, 3H, NCH_3); 1.90-1.83 (m, 2H, CH_2); 1.54-1.41 (m, 4H, CH_2); 1.41-1.33 (m, 2H, CH_2) ppm. ^{13}C APT NMR ($CDCl_3$) δ: 169.69 (C=O); 166.93 (C=O); 153.41 (C); 144.86 (CH=CH); 140.11 (C); 130.97 (C); 129.89 (C); 129.22 (CH arom.); 128.62 (CH arom.); 128.36 (C); 128.15 (C); 126.92 (CH arom.); 125.45 (CH arom.); 124.98 (CH arom.); 117.30 (CH=CH); 105.24 (CH arom.); 65.80 (CH_2); 62.15 (CH_2); 60.94 (OCH_3); 57.86 (CH_2); 56.11 (OCH_3); 55.72 (CH_2); 42.66 (NCH_3); 28.75 (CH_2); 27.04 (CH_2); 26.05 (CH_2) ppm.

Hydrochloride: mp 61-63 °C**. Anal:** $C_{36}H_{42}ClNO_7$ (C, H, N).

5.1.6.5. ***(E)-4-(Methyl-(5-((3-(3,4,5-trimethoxyphenyl)acryloyl)oxy)pentyl)amino)butyl 3,4,5-trimethoxybenzoate 5***

Procedure B, starting from **57** and 3,4,5-trimethoxybenzoic acid.

Free base: chromatographic eluent: CH_2Cl_2/MeOH/NH_4OH 95:5:0.5. Yield: 83.1.%.

^{1}H-NMR ($CDCl_3$) δ: 7.58 (d, J=16.0 Hz, 1H, *CH*=CH); 7.28 (s, 2H, CH arom.); 6.74 (s, 2H, CH arom.); 6.33 (d, J=16.0 Hz, 1H, CH=*CH*); 4.31 (t, J=6.8 Hz, 2H, CH_2O); 4.19 (t, J=6.4 Hz, 2H, CH_2O); 3.89 (s, 3H, OCH_3); 3.88 (s, 6H, OCH_3); 3.87 (s, 6H, OCH_3); 3.86 (s, 3H, OCH_3); 2.41-2.33 (m, 4H, NCH_2); 2.21 (s, 3H, NCH_3); 1.82-1.75 (m, 2H, CH_2); 1.75-1.67 (m, 2H, CH_2); 1.64-1.56 (m, 2H, CH_2); 1.55-1.48 (m, 2H, CH_2); 1.44-1.36 (m, 2H, CH_2) ppm. ^{13}C APT NMR ($CDCl_3$) δ: 166.96 (C=O); 166.20 (C=O); 153.41 (C); 152.90 (C); 144.58 (CH=CH); 142.19 (C); 140.10 (C); 129.91 (C); 125.41 (C); 117.42 (CH=CH); 106.82 (CH arom.); 105.23 (CH arom.); 65.03 (CH_2); 64.50 (CH_2); 60.91 (OCH_3); 60.86 (OCH_3); 57.68 (CH_2); 57.30 (CH_2); 56.22 (OCH_3); 56.13

(OCH_3); 42.10 (NCH_3); 28.70 (CH_2); 26.96 (CH_2); 26.75 (CH_2); 23.95 (CH_2); 23.80 (CH_2) ppm. ESI-MS *m/z* (%): 604 (100) $[M+H]^+$.

Hydrochloride: mp 98-100 °C**. Anal:** $C_{32}H_{46}ClNO_{10}$ (C, H, N).

5.1.6.6. ***(E)-5-(Methyl-(4-((3-(3,4,5-trimethoxyphenyl)acryloyl)oxy)butyl)amino)pentyl 3,4,5-trimethoxybenzoate 6***

Procedure A, starting from **56** and 3,4,5-trimethoxybenzoic acid.

Free base: chromatographic eluent: CH_2Cl_2/MeOH/NH_4OH 96:4:0.4. Yield: 89.2.%.

^{1}H-NMR ($CDCl_3$) δ: 7.55 (d, J=16.0 Hz, 1H, *CH*=CH); 7.25 (s, 2H, CH arom.); 6.72 (s, 2H, CH arom.); 6.30 (d, J=16.0 Hz, 1H, *CH*=CH); 4.31-4.26 (m, 2H, CH_2O); 4.19-4-14 (m, 2H, CH_2O); 3.86 (s, 9H, OCH_3); 3.84 (s, 6H, OCH_3); 3.83 (s, 3H, OCH_3); 2.39-2.30 (m, 4H, NCH_2); 2.19 (s, 3H, NCH_3); 1.80-1.63 (m, 4H, CH_2); 1.63-1.45 (m, 4H, CH_2); 1.44-1.32 (m, 2H, CH_2) ppm. ^{13}C APT NMR ($CDCl_3$) δ: 166.95 (C=O); 166.21 (C=O); 153.40 (C); 152.89 (C); 144.63 (CH=CH); 142.29 (C); 140.08 (C); 129.90 (C); 125.44 (C); 117.38 (CH=CH); 106.80 (CH arom.); 105.21 (CH arom.); 65.09 (CH_2); 64.36 (CH_2); 60.92 (OCH_3); 60.87 (OCH_3); 57.65 (CH_2); 57.29 (CH_2); 56.22 (OCH_3); 56.13 (OCH_3); 42.05 (NCH_3); 28.70 (CH_2); 26.91 (CH_2); 26.73 (CH_2); 23.94 (CH_2); 23.75 (CH_2) ppm. ESI-MS *m/z* (%): 604.2 (100) $[M+H]^+$.

Hydrochloride: mp 89-91 °C**. Anal:** $C_{32}H_{46}ClNO_{10}$ (C, H, N).

5.1.6.7. ***(E)-4-(Methyl-(5-((3-(3,4,5-trimethoxyphenyl)acryloyl)oxy)pentyl)amino)butyl anthracene-9-carboxylate 7***

Procedure B, starting from **57** and anthracene-9-carboxylic acid.

Free base: chromatographic eluent: CH_2Cl_2/MeOH/NH_4OH 97:3:0.3. Yield: 23.1.%.

^{1}H-NMR ($CDCl_3$) δ: 8.51 (s, 1H, CH arom.); 8.04-8.00 (m, 4H, CH arom.); 7.58 (d, J=16.0 Hz, 1H, *CH*=CH); 7.55-7.46 (m, 4H, CH arom.); 6.74 (s, 2H, CH arom.); 6.33 (d, J=16.0 Hz, 1H, CH=*CH*); 4.64 (t, J=6.4 Hz, 2H, CH_2O); 4.18 (t, J=6.8 Hz, 2H, CH_2O); 3.87 (s, 3H, OCH_3); 3.86 (s, 6H, OCH_3); 2.44 (t, J=7.2 Hz, 2H, NCH_2); 2.36 (t, J=7.6 Hz, 2H, NCH_2); 2.23 (s, 3H, NCH_3); 1.94-1.87 (m, 2H, CH_2); 1.73-1.62 (m, 4H, CH_2); 1.56-1.48 (m, 2H, CH_2); 1.43-1.34 (m, 2H, CH_2) ppm. ESI-MS *m/z* (%): 614.2 (100) $[M+H]^+$.

Hydrochloride: ^{13}C APT NMR ($CDCl_3$) δ: 169.36 (C=O); 166.97 (C=O); 153.46 (C); 145.04 (CH=CH); 140.18 (C); 130.96 (C); 129.81 (C); 129.59 (CH arom.); 128.79 (CH arom.); 128.38 (C); 127.48 (C); 127.29 (CH arom.); 125.61 (CH arom.); 124.80 (CH arom.); 117.14 (CH=CH); 105.22 (CH arom.); 64.70 (CH_2); 63.74 (CH_2); 60.99 (OCH_3); 56.27 (OCH_3); 55.94 (CH_2); 55.62 (CH_2); 40.11 (NCH_3); 28.18 (CH_2); 26.24 (CH_2); 23.42 (CH_2); 20.99 (CH_2) ppm. mp 112-114 °C**. Anal:** $C_{37}H_{44}ClNO_7$ (C, H, N).

5.1.6.8. ***(E)-5-(Methyl-(4-((3-(3,4,5-trimethoxyphenyl)acryloyl)oxy)butyl)amino)pentyl anthracene-9-carboxylate 8***

Procedure B, starting from **56** and anthracene-9-carboxylic acid.

Free base: chromatographic eluent: CH_2Cl_2/MeOH/NH_4OH 97:3:0.3. Yield: 51.3.%.

^{1}H-NMR ($CDCl_3$) δ: 8.48 (s, 1H, CH arom.); 7.99 (d, J=8.8 Hz, 2H, CH arom.); 7.98 (d, J=6.8 Hz, 2H, CH arom.); 7.56 (d, J=16.0 Hz, 1H, *CH*=CH); 7.52-7.43 (m, 4H, CH arom.); 6.71 (s, 2H, CH arom.); 6.30 (d, J=16.0 Hz, 1H, CH=*CH*); 4.62-4.57 (m, 2H, CH_2O); 4.18-4.13 (m 2H, CH_2O); 3.84 (s, 3H, OCH_3); 3.83 (s, 6H, OCH_3); 2.50-2.34 (m, 4H, NCH_2); 2.22 (s, 3H, NCH_3); 1.91-1.84 (m, 2H, CH_2); 1.70-1.35 (m, 8H, CH_2) ppm. ^{13}C APT NMR ($CDCl_3$) δ: 169.73 (C=O); 167.01 (C=O); 153.41 (C); 144.72 (CH=CH); 130.98 (C); 129.92 (C); 129.27 (CH arom.); 128.65 (CH arom.); 128.37 (C); 126.96 (CH arom.); 125.48 (CH arom.); 124.97 (CH arom.); 117.35 (CH=CH); 105.17 (CH arom.); 65.77 (CH_2); 64.30 (CH_2); 60.99 (OCH_3); 57.46 (CH_2); 57.15 (CH_2); 56.15 (OCH_3); 41.89 (NCH_3); 28.67 (CH_2); 26.68 (CH_2); 24.02 (CH_2); 23.90 (CH_2); 23.55 (CH_2) ppm. ESI-MS *m/z* (%): 614.3 (100) $[M+H]^+$.

Hydrochloride: mp 70-72°C**. Anal:** $C_{37}H_{44}ClNO_7$ (C, H, N).

5.1.6.9. ***(E)-3-(Methyl-(6-((3-(3,4,5-trimethoxyphenyl)acryloyl)oxy)hexyl)amino)propyl 3,4,5-trimethoxybenzoate 9***

Procedure A, starting from **59** and 3,4,5-trimethoxybenzoic acid.

Free base: chromatographic eluent: CH_2Cl_2/MeOH/NH_4OH 97:3:0.3. Yield: 62.2.%.
^{1}H-NMR ($CDCl_3$) δ: 7.54 (d, J=16.0 Hz, 1H, *CH*=CH); 7.24 (s, 2H, CH arom.); 6.70 (s, 2H, CH arom.); 6.30 (d, J=16.0 Hz, 1H, CH=*CH*); 4.31 (t, J=6.4 Hz, 2H, CH_2O); 4.14 (t, J=6.4 Hz, 2H, CH_2O); 3.85 (s, 3H, OCH_3); 3.84 (s, 6H, OCH_3); 3.83 (s, 6H, OCH_3); 3.82 (s, 3H, OCH_3); 2.45 (t, J=7.2 Hz, 2H, NCH_2); 2.32 (t, J=7.2 Hz, 2H, NCH_2); 2.20 (s, 3H, NCH_3); 1.94-1.85 (m, 2H, CH_2); 1.68-1.61 (m, 2H, CH_2); 1.49-1.40 (m, 2H, CH_2); 1.39-1.25 (m, 4H, CH_2) ppm. ^{13}C APT NMR ($CDCl_3$) δ: 166.96 (C=O); 166.14 (C=O); 153.38 (C); 152.88 (C); 144.55 (CH=CH); 142.15 (C); 140.03 (C); 129.91 (C); 125.36 (C); 117.42 (CH=CH); 106.76 (CH arom.); 105.18 (CH arom.); 64.50 (CH_2); 63.52 (CH_2); 60.85 (OCH_3); 57.67 (CH_2); 56.19 (OCH_3); 56.11 (OCH_3); 54.16 (CH_2); 42.14 (NCH_3); 28.70 (CH_2); 27.18 (CH_2); 27.11 (CH_2); 26.64 (CH_2); 25.90 (CH_2) ppm.
Hydrochloride: mp 78-80 °C**. Anal:** $C_{32}H_{46}ClNO_{10}$ (C, H, N).

5.1.6.10. ***(E)-6-(Methyl-(3-((3-(3,4,5-trimethoxyphenyl)acryloyl)oxy)propyl)amino)hexyl 3,4,5-trimethoxybenzoate 10***

Procedure A, starting from **58** and 3,4,5-trimethoxybenzoic acid.
Free base: chromatographic eluent: CH_2Cl_2/MeOH/NH_4OH 97:3:0.3. Yield: 71.2.%.
^{1}H-NMR ($CDCl_3$) δ: 7.54 (d, J=16.0 Hz, 1H, *CH*=CH); 7.24 (s, 2H, CH arom.); 6.70 (s, 2H, CH arom.); 6.29 (d, J=16.0 Hz, 1H, CH=*CH*); 4.25 (t, J=6.4 Hz, 2H, CH_2O); 4.20 (t, J=6.4 Hz, 2H, CH_2O); 3.85 (s, 3H, OCH_3); 3.84 (s, 6H, OCH_3); 3.83 (s, 6H, OCH_3); 3.82 (s, 3H, OCH_3); 2.42 (t, J=7.2 Hz, 2H, NCH_2); 2.31 (t, J=7.2 Hz, 2H, NCH_2); 2.18 (s, 3H, NCH_3); 1.87-1.79 (m, 2H, CH_2); 1.78-1.68 (m, 2H, CH_2); 1.46-1.30 (m, 6H, CH_2) ppm. ^{13}C APT NMR ($CDCl_3$) δ: 166.88 (C=O); 166.18 (C=O); 153.40 (C); 152.88 (C); 144.64 (CH=CH); 142.13 (C); 140.10 (C); 129.87 (C); 125.47 (C); 117.31 (CH=CH); 106.78 (CH arom.); 105.22 (CH arom.); 65.10 (CH_2); 62.95 (CH_2); 60.89 (OCH_3); 60.84 (OCH_3); 57.63 (CH_2); 56.20 (OCH_3); 56.11 (OCH_3); 54.22 (CH_2); 42.08 (NCH_3); 28.70 (CH_2); 27.18 (CH_2); 27.10 (CH_2); 26.66 (CH_2); 25.94 (CH_2) ppm.
Hydrochloride: mp 95-97 °C**. Anal:** $C_{32}H_{46}ClNO_{10}$ (C, H, N).

5.1.6.11. ***(E)-3-(Methyl-(6-((3-(3,4,5-trimethoxyphenyl)acryloyl)oxy)hexyl)amino)propyl anthracene-9-carboxylate 11***

Procedure B, starting from **59** and anthracene-9-carboxylic acid.
Free base: chromatographic eluent: CH_2Cl_2/MeOH/NH_4OH 98:2:0.2. Yield: 50.9.%.
^{1}H-NMR ($CDCl_3$) δ: 8.48 (s, 1H, CH arom.); 8.04 (d, J=8.8 Hz, 2H, CH arom.); 7.98 (d, J=8.4 Hz, 2H, CH arom.); 7.59 (d, J=16.0 Hz, 1H, *CH*=CH); 7.54-7.44 (m, 4H, CH arom.); 6.73 (s, 2H, CH arom.); 6.34 (d, J=16.0 Hz, 1H, CH=*CH*); 4.67 (t, J=6.4 Hz, 2H, CH_2O); 4.17 (t, J=6.8 Hz, 2H, CH_2O); 3.87 (s, 3H, OCH_3); 3.84 (s, 6H, OCH_3); 2.53 (t, J=7.2 Hz, 2H, NCH_2); 2.35 (t, J=7.6 Hz, 2H, NCH_2); 2.24 (s, 3H, NCH_3); 2.08-2.01 (m, 2H, CH_2); 1.69-1.63 (m, 2H, CH_2); 1.52-1.44 (m, 2H, CH_2); 1.43-1.30 (m, 4H, CH_2) ppm. ^{13}C APT NMR ($CDCl_3$) δ: 169.65 (C=O); 167.02 (C=O); 153.43 (C); 144.57 (CH=CH); 130.99 (C); 129.95 (C); 129.25 (CH arom.); 128.62 (CH arom.); 128.39 (C); 128.09 (C); 126.91 (CH arom.); 125.46 (CH arom.); 125.02 (CH arom.); 117.50 (CH=CH); 105.24 (CH arom.); 64.59 (CH_2); 64.20 (CH_2); 60.95 (OCH_3); 57.80 (CH_2); 56.14 (OCH_3); 54.18 (CH_2); 42.17 (NCH_3); 28.74 (CH_2); 27.24 (CH_2); 27.15 (CH_2); 26.68 (CH_2); 25.96 (CH_2) ppm.
Hydrochloride: mp 57-58°C**. Anal:** $C_{37}H_{44}ClNO_7$ (C, H, N).

5.1.6.12. ***(E)-6-(Methyl-(3-((3-(3,4,5-trimethoxyphenyl)acryloyl)oxy)propyl)amino)hexyl anthracene-9-carboxylate 12***

Procedure B, starting from **58** and anthracene-9-carboxylic acid.
Free base: chromatographic eluent: CH_2Cl_2/MeOH/NH_4OH 96:4:0.4. Yield: 51.8.%.
^{1}H-NMR ($CDCl_3$) δ: 8.50 (s, 1H, CH arom.); 8.04-8.00 (m, 4H, CH arom.); 7.59 (d, J=16.0 Hz, 1H, *CH*=CH); 7.55-7.45 (m, 4H, CH arom.); 6.73 (s, 2H, CH arom.); 6.34 (d, J=16.0 Hz, 1H, CH=*CH*); 4.61 (t, J=6.4 Hz, 2H, CH_2O); 4.24 (t, J=6.8 Hz, 2H, CH_2O); 3.87 (s, 3H, OCH_3); 3.85 (s, 6H, OCH_3); 2.45 (t, J=7.2 Hz, 2H, NCH_2); 2.34 (t, J=7.2 Hz, 2H, NCH_2); 2.22 (s, 3H, NCH_3); 1.92-1.83 (m, 4H, CH_2); 1.54-1.47 (m, 4H, CH_2); 1.46-1.35 (m, 2H, CH_2) ppm. ^{13}C APT NMR ($CDCl_3$) δ: 169.73 (C=O); 166.96 (C=O); 153.43 (C); 144.70 (CH=CH); 140.12 (C); 131.00 (C); 129.91 (C);

129.22 (CH arom.); 128.62 (CH arom.); 128.38 (C); 128.17 (C); 126.92 (CH arom.); 125.46 (CH arom.); 125.00 (CH arom.); 117.36 (CH=CH); 105.24 (CH arom.); 65.84 (CH_2); 63.02 (CH_2); 60.96 (OCH_3); 57.63 (CH_2); 56.15 (OCH_3); 54.29 (CH_2); 42.11 (NCH_3); 28.76 (CH_2); 27.16 (CH_2); 27.11 (CH_2); 26.68 (CH_2); 26.06 (CH_2) ppm.
Hydrochloride: mp 72-73°C**. Anal:** $C_{37}H_{44}ClNO_7$ (C, H, N).

5.1.6.13. ***(E)-2-(Methyl-(7-((3-(3,4,5-trimethoxyphenyl)acryloyl)oxy))heptyl)amino)ethyl 3,4,5-trimethoxybenzoate 13***

Procedure B, starting from **67** and 3,4,5-trimethoxybenzoic acid.
Free base: chromatographic eluent: CH_2Cl_2/MeOH/NH_4OH 97:3:0.3. Yield: 69.2.%.
^{1}H-NMR ($CDCl_3$) δ: 7.55 (d, J=15.6 Hz, 1H, *CH*=CH); 7.27 (s, 2H, CH arom.); 6.72 (s, 2H, CH arom.); 6.31 (d, J=15.6 Hz, 1H, CH=*CH*); 4.38 (t, J=6.0 Hz, 2H, CH_2O); 4.15 (t, J=6.8 Hz, 2H, CH_2O); 3.86 (s, 9H, OCH_3); 3.85 (s, 6H, OCH_3); 3.84 (s, 3H, OCH_3); 2.75 (t, J=6.0 Hz, 2H, NCH_2); 2.42 (t, J=7.2 Hz, 2H, NCH_2); 2.31 (s, 3H, NCH_3); 1.70-1.61 (m, 2H, CH_2); 1.50-1.40 (m, 2H, CH_2); 1.40-1.20 (m, 6H, CH_2) ppm. ^{13}C APT NMR ($CDCl_3$) δ: 166.98 (C=O); 166.13 (C=O); 153.42 (C); 152.90 (C); 144.54 (CH=CH); 142.27 (C); 140.11 (C); 129.93 (C); 125.24 (C); 117.46 (CH=CH); 106.92 (CH arom.); 105.25 (CH arom.); 64.57 (CH_2); 63.10 (CH_2); 60.91 (OCH_3); 60.86 (OCH_3); 58.02 (CH_2); 56.20 (OCH_3); 56.14 (OCH_3); 55.66 (CH_2); 42.78 (NCH_3); 29.18 (CH_2); 28.69 (CH_2); 27.35 (CH_2); 27.26 (CH_2); 25.91 (CH_2) ppm.
Hydrochloride: mp 111-113 °C**. Anal:** $C_{32}H_{46}ClNO_{10}$ (C, H, N).

5.1.6.14. ***(E)-7-(Methyl-(2-((3-(3,4,5-trimethoxyphenyl)acryloyl)oxy)ethyl)amino)heptyl 3,4,5-trimethoxybenzoate 14***

Procedure A, starting from **68** and (*E*)-3-(3,4,5-trimethoxyphenyl)acrylic acid.
Free base: chromatographic eluent: CH_2Cl_2/MeOH/NH_4OH 98:2:0.2. Yield: 71.1.%.
^{1}H-NMR ($CDCl_3$) δ: 7.54 (d, J=16.0 Hz, 1H, *CH*=CH); 7.23 (s, 2H, CH arom.); 6.69 (s, 2H, CH arom.); 6.33 (d, J=16.0 Hz, 1H, CH=*CH*); 4.26-4.21 (m, 4H, CH_2O); 3.84 (s, 6H, OCH_3); 3.83 (s, 3H, OCH_3); 3.82 (s, 6H, OCH_3); 3.81 (s, 3H, OCH_3); 2.64 (t, J=6.0 Hz, 2H, NCH_2); 2.36 (t, J=7.2 Hz, 2H, NCH_2); 2.26 (s, 3H, NCH_3); 1.72-1.65 (m, 2H, CH_2); 1.48-1.25 (m, 8H, CH_2) ppm. ^{13}C APT NMR ($CDCl_3$) δ: 166.84 (C=O); 166.16 (C=O); 153.39 (C); 152.87 (C); 144.77 (CH=CH); 142.13 (C); 140.12 (C); 129.85 (C); 125.47 (C); 117.27 (CH=CH); 106.78 (CH arom.); 105.24 (CH arom.); 65.13 (CH_2); 62.15 (CH_2); 60.87 (OCH_3); 60.82 (OCH_3); 57.92 (CH_2); 56.19 (OCH_3); 56.10 (OCH_3); 55.69 (CH_2); 42.66 (NCH_3); 29.16 (CH_2); 28.65 (CH_2); 27.28 (CH_2); 27.08 (CH_2); 25.93 (CH_2) ppm.
Hydrochloride: mp 106-108 °C**. Anal:** $C_{32}H_{46}ClNO_{10}$ (C, H, N).

5.1.6.15. ***(E)-2-(Methyl-(7-((3-(3,4,5-trimethoxyphenyl)acryloyl)oxy)heptyl)amino)ethyl anthracene-9-carboxylate 15***

Procedure B, starting from **67** and anthracene-9-carboxylic acid.
Free base: chromatographic eluent: CH_2Cl_2/MeOH/NH_4OH 98:2:0.2. Yield: 56.4.%.
^{1}H-NMR ($CDCl_3$) δ: 8.47 (s, 1H, CH arom.); 8.15 (d, J=8.4 Hz, 2H, CH arom.); 7.97 (d, J=8.4 Hz, 2H, CH arom.); 7.58 (d, J=16.0 Hz, 1H, *CH*=CH); 7.53-7.44 (m, 4H, CH arom.); 6.73 (s, 2H, CH arom.); 6.34 (d, J=16.0 Hz, 1H, CH=*CH*); 4.72 (t, J=5.6 Hz, 2H, CH_2O); 4.15 (t, J=6.8 Hz, 2H, CH_2O); 3.87 (s, 3H, OCH_3); 3.84 (s, 6H, OCH_3); 2.85 (t, J=6.0 Hz, 2H, NCH_2); 2.46 (t, J=7.2 Hz, 2H, NCH_2); 2.36 (s, 3H, NCH_3); 1.64-1.60 (m, 2H, CH_2); 1.52-1.48 (m, 2H, CH_2); 1.35-1.20 (m, 6H, CH_2) ppm. ^{13}C APT NMR ($CDCl_3$) δ: 169.51 (C=O); 167.04 (C=O); 153.42 (C); 144.56 (CH=CH); 140.04 (C); 130.97 (C); 129.96 (C); 129.32 (CH arom.); 128.56 (CH arom.); 128.48 (C); 127.98 (C); 126.87 (CH arom.); 125.44 (CH arom.); 125.29 (CH arom.); 117.51 (CH=CH); 105.19 (CH arom.); 64.66 (CH_2); 63.17 (CH_2); 60.97 (OCH_3); 58.00 (CH_2); 56.13 (OCH_3); 56.09 (CH_2); 42.47 (NCH_3); 29.23 (CH_2); 28.69 (CH_2); 27.32 (CH_2); 27.29 (CH_2); 25.93 (CH_2) ppm.
Hydrochloride: low melting solid**. Anal:** $C_{37}H_{44}ClNO_7$ (C, H, N).

5.1.6.16. ***(E)-7-(Methyl-(2-((3-(3,4,5-trimethoxyphenyl)acryloyl)oxy)ethyl)amino)heptyl anthracene-9-carboxylate 16***

Procedure A, starting from **69** and (*E*)-3-(3,4,5-trimethoxyphenyl)acrylic acid.

Free base: chromatographic eluent: CH_2Cl_2/MeOH/NH_4OH 98:2:0.2. Yield: 33.8.%.
^{1}H-NMR ($CDCl_3$) δ: 8.49 (s, 1H, CH arom.); 8.03 (d, J=8.8 Hz, 2H, CH arom.); 7.99 (d, J=8.4 Hz, 2H, CH arom.); 7.60 (d, J=16.0 Hz, 1H, *CH*=CH); 7.54-7.45 (m, 4H, CH arom.); 6.73 (s, 2H, CH arom.); 6.38 (d, J=16.0 Hz, 1H, CH=*CH*); 4.59 (t, J=6.8 Hz, 2H, CH_2O); 4.30 (t, J=6.0 Hz, 2H, CH_2O); 3.86 (s, 3H, OCH_3); 3.84 (s, 6H, OCH_3); 2.69 (t, J=5.6 Hz, 2H, NCH_2); 2.41 (t, J=7.2 Hz, 2H, NCH_2); 2.30 (s, 3H, NCH_3); 1.90-1.83 (m, 2H, CH_2); 1.52-1.25 (m, 8H, CH_2) ppm. ^{13}C APT NMR ($CDCl_3$) δ: 169.72 (C=O); 166.95 (C=O); 153.43 (C); 144.83 (CH=CH); 140.16 (C); 131.00 (C); 129.90 (C); 129.20 (CH arom.); 128.61 (CH arom.); 128.38 (C); 128.18 (C); 126.90 (CH arom.); 125.45 (CH arom.); 125.01 (CH arom.); 117.33 (CH=CH); 105.28 (CH arom.); 65.86 (CH_2); 62.20 (CH_2); 60.95 (OCH_3); 57.98 (CH_2); 56.14 (OCH_3); 55.71 (CH_2); 42.68 (NCH_3); 29.17 (CH_2); 28.73 (CH_2); 27.32 (CH_2); 27.07 (CH_2); 26.06 (CH_2) ppm.
Hydrochloride: mp 71-73 °C**. Anal:** $C_{37}H_{44}ClNO_7$ (C, H, N).

5.1.6.17. ***(E)-4-(Methyl-(6-((3-(3,4,5-trimethoxyphenyl)acryloyl)oxy)hexyl)amino)butyl 3,4,5-trimethoxybenzoate 17***

Procedure B, starting from **61** and 3,4,5-trimethoxybenzoic acid.
Free base: chromatographic eluent: CH_2Cl_2/MeOH/NH_4OH 97:3:0.3. Yield: 65.6%.
^{1}H-NMR ($CDCl_3$) δ: 7.56 (d, J=16.0 Hz, 1H, *CH*=CH); 7.26 (s, 2H, CH arom.); 6.72 (s, 2H, CH arom.); 6.31 (d, J=16.0 Hz, 1H, *CH*=CH); 4.30 (t, J=6.8 Hz, 2H, CH_2O); 4.16 (t, J=6.4 Hz, 2H, CH_2O); 3.87 (s, 9H, OCH_3); 3.85 (s, 6H, OCH_3); 3.84 (s, 3H, OCH_3); 2.36 (t, J=7.6 Hz, 2H, NCH_2,); 2.31 (t, J=7.6 Hz, 2H, NCH_2); 2.19 (s, 3H, NCH_3); 1.81-1.74 (m, 2H, CH_2); 1.70-1.65 (m, 2H, CH_2); 1.61-1.55 (m, 2H, CH_2); 1.49-1.28 (m; 6H, CH_2) ppm. ^{13}C APT NMR ($CDCl_3$) δ: 166.98 (C=O); 166.21 (C=O); 153.42 (C); 152.90 (C); 144.56 (CH=CH); 142.20 (C); 140.11 (C); 129.93 (C); 125.43 (C); 117.45 (CH=CH); 106.83 (CH arom.); 105.24 (CH arom.); 65.05 (CH_2); 64.55 (CH_2); 60.92 (OCH_3); 60.87 (OCH_3); 57.80 (CH_2); 57.31 (CH_2); 56.23 (OCH_3); 56.14 (OCH_3); 42.14 (NCH_3); 28.72 (CH_2); 27.21 (CH_2); 26.77 (CH_2); 25.95 (CH_2); 23.83 (CH_2) ppm.
Hydrochloride: mp 64-66 °C**. Anal:** $C_{34}H_{49}ClNO_{10}$ (C, H, N).

5.1.6.18. ***(E)-6-(Methyl-(4-((3-(3,4,5-trimethoxyphenyl)acryloyl)oxy)butyl)amino)hexyl 3,4,5-trimethoxybenzoate 18***

Procedure A, starting from **60** and 3,4,5-trimethoxybenzoic acid.
Free base: chromatographic eluent: CH_2Cl_2/MeOH/NH_4OH 98:2:0.2. Yield: 50.3%.
^{1}H-NMR ($CDCl_3$) δ: 7.58 (d, J=16.0 Hz, 1H, *CH*=CH); 7.28 (s, 2H, CH arom.); 6.74 (s, 2H, CH arom.); 6.33 (d, J=16.0 Hz, 1H, CH=*CH*); 4.29 (t, J=6.8 Hz, 2H, CH_2O); 4.20 (t, J=6.4 Hz, 2H, CH_2O); 3.89 (s, 9H, OCH_3); 3.87 (s, 6H, OCH_3); 3.86 (s, 3H, OCH_3); 2.39-2.32 (m, 4H, NCH_2); 2.21 (s, 3H, NCH_3); 1.80-1.67 (m, 4H, CH_2); 1.62-1.56 (m, 2H, CH_2); 1.53-1.42 (m, 4H, CH_2); 1.41-1.34 (m, 2H, CH_2) ppm. ^{13}C APT NMR ($CDCl_3$) δ: 166.78 (C=O); 166.27 (C=O); 153.42 (C); 152.92 (C); 144.86 (CH=CH); 142.13 (C); 140.07 (C); 129.87 (C); 125.45 (C); 117.22 (CH=CH); 106.76 (CH arom.); 105.20 (CH arom.); 65.05 (CH_2); 64.05 (CH_2); 60.98 (OCH_3); 60.93 (OCH_3); 57.37 (CH_2); 56.91 (CH_2); 56.26 (OCH_3); 56.17 (OCH_3); 41.54 (NCH_3); 28.69 (CH_2); 27.04 (CH_2); 26.62 (CH_2); 26.35 (CH_2); 25.87 (CH_2); 23.08 (CH_2) ppm.
Hydrochloride: mp 79-81 °C**. Anal:** $C_{34}H_{49}ClNO_{10}$ (C, H, N).

5.1.6.19. ***(E)-4-(Methyl-(6-((3-(3,4,5-trimethoxyphenyl)acryloyl)oxy)hexyl)amino)butyl anthracene-9-carboxylate 19***

Procedure B, starting from **61** and anthracene-9-carboxylic acid.
Free base: chromatographic eluent: CH_2Cl_2/MeOH/NH_4OH 98:2:0.2. Yield: 35.4%.
^{1}H-NMR ($CDCl_3$) δ: 8.50 (s, 1H, CH arom.); 8.04-7.99 (m, 4H, CH arom.); 7.58 (d, J=16.0 Hz, 1H, *CH*=CH); 7.54-7.45 (m, 4H, CH arom.); 6.73 (s, 2H, CH arom.); 6.33 (d, J=16.0 Hz, 1H, CH=*CH*); 4.63 (t, J=6.4 Hz, 2H, CH_2O); 4.18 (t, J=6.4 Hz, 2H, CH_2O); 3.87 (s, 3H, OCH_3); 3.86 (s, 6H, OCH_3); 2.41 (t, J=7.2 Hz, 2H, NCH_2); 2.32 (t, J=7.6 Hz, 2H, NCH_2); 2.20 (s, 3H, NCH_3); 1.93-1.86 (m, 2H, CH_2); 1.72-1.63 (m, 4H, CH_2); 1.51-1.31 (m, 6H, CH_2) ppm. ^{13}C APT NMR ($CDCl_3$) **δ:** 169.71 (C=O); 167.03 (C=O); 153.43 (C); 144.58 (CH=CH); 140.11 (C); 131.00 (C); 129.96 (C); 129.24 (CH arom.); 128.62 (CH arom.); 128.38 (C); 126.92 (CH arom.); 125.46 (CH arom.);

125.00 (CH arom.); 117.49 (CH=CH); 105.25 (CH arom.); 65.78 (CH_2); 64.60 (CH_2); 60.96 (OCH_3); 57.70 (CH_2); 57.18 (CH_2); 56.15 (OCH_3); 42.13 (NCH_3); 28.74 (CH_2); 27.19 (CH_2); 26.81 (CH_2); 25.95 (CH_2); 23.82 (CH_2) ppm.
Hydrochloride: mp 68-69 °C**. Anal:** $C_{38}H_{46}ClNO_7$ (C, H, N).

5.1.6.20. ***(E)-6-(Methyl-(4-((3-(3,4,5-trimethoxyphenyl)acryloyl)oxy)butyl)amino)hexyl anthracene-9-carboxylate 20***

Procedure B, starting from **60** and anthracene-9-carboxylic acid.
Free base: chromatographic eluent: CH_2Cl_2/MeOH/NH_4OH 98:2:0.2. Yield: 63.4%.
^{1}H-NMR ($CDCl_3$) δ: 8.50 (s, 1H, CH arom.); 8.02 (t, J=9.2 Hz, 4H, CH arom.); 7.59 (d, J=15.6 Hz, 1H, *CH*=CH); 7.56-7.44 (m, 4H, CH arom.); 6.73 (s, 2H, CH arom.); 6.34 (d, J=15.6 Hz, 1H, CH=*CH*); 4.61 (t, J=6.8 Hz, 2H, CH_2O); 4.21 (t, J=6.4 Hz, 2H, CH_2O); 3.87 (s, 3H, OCH_3); 3.86 (s, 6H, OCH_3); 2.38-2.29 (m, 4H, NCH_2); 2.20 (s, 3H, NCH_3); 1.93-1.84 (m, 2H, CH_2); 1.73-1.66 (m, 2H, CH_2); 1.62-1.46 (m, 6H, CH_2); 1.43-1.37 (m, 2H, CH_2) ppm. ^{13}C APT NMR ($CDCl_3$) δ: 169.75 (C=O); 167.01 (C=O); 153.42 (C); 144.64 (CH=CH); 131.00 (C); 129.93 (C); 129.22 (CH arom.); 128.62 (CH arom.); 128.37 (C); 128.15 (C); 126.92 (CH arom.); 125.46 (CH arom.); 125.00 (CH arom.); 117.44 (CH=CH); 105.20 (CH arom.); 65.86 (CH_2); 64.46 (CH_2); 60.97 (OCH_3); 57.76 (CH_2); 57.35 (CH_2); 56.14 (OCH_3); 42.14 (NCH_3); 28.76 (CH_2); 27.19 (CH_2); 26.79 (CH_2); 26.08 (CH_2); 23.83 (CH_2) ppm.
Hydrochloride: mp 80-81 °C**. Anal:** $C_{38}H_{46}ClNO_7$ (C, H, N).

5.1.6.21. ***(E)-3-(Methyl-(7-((3-(3,4,5-trimethoxyphenyl)acryloyl)oxy)heptyl)amino)propyl 3,4,5-trimethoxybenzoate 21***

Procedure B, starting from **62** and 3,4,5-trimethoxybenzoic acid.
Free base: chromatographic eluent: CH_2Cl_2/MeOH/NH_4OH 98:2:0.2. Yield: 72.6%.
^{1}H-NMR ($CDCl_3$) δ: 7.55 (d, J=15.6 Hz, 1H, *CH*=CH); 7.26 (s, 2H, CH arom.); 6.72 (s, 2H, CH arom.); 6.31 (d, J=15.6 Hz, 1H, CH=*CH*); 4.32 (t, J=6.4 Hz, 2H, CH_2O); 4.15 (t, J=6.8 Hz, 2H, CH_2O); 3.87 (s, 9H, OCH_3); 3.85 (s, 6H, OCH_3); 3.84 (s, 3H, OCH_3); 2.46 (t, J=7.2 Hz, 2H, NCH_2); 2.31 (t, J=7.2 Hz, 2H, NCH_2); 2.20 (s, 3H, NCH_3); 1.94-1.87 (m, 2H, CH_2); 1.67-1.60 (m, 2H, CH_2); 1.46-1.20 (m, 8H, CH_2) ppm. ^{13}C APT NMR ($CDCl_3$) δ: 167.00 (C=O); 166.16 (C=O); 153.41 (C); 152.90 (C); 144.54 (CH=CH); 142.17 (C); 140.06 (C); 129.94 (C); 125.41 (C); 117.47 (CH=CH); 106.79 (CH arom.); 105.21 (CH arom.); 64.60 (CH_2); 63.58 (CH_2); 60.92 (OCH_3); 60.87 (OCH_3); 57.79 (CH_2); 56.21 (OCH_3); 56.13 (OCH_3); 54.20 (CH_2); 42.21 (NCH_3); 29.22 (CH_2); 28.69 (CH_2); 27.37 (CH_2); 27.30 (CH_2); 26.69 (CH_2); 25.93 (CH_2) ppm.
Hydrochloride: mp 77-79 °C**. Anal:** $C_{33}H_{48}ClNO_{10}$ (C, H, N).

5.1.6.22. ***(E)-7-(Methyl-(3-((3-(3,4,5-trimethoxyphenyl)acryloyl)oxy)propyl)amino)heptyl 3,4,5-trimethoxybenzoate 22***

Procedure B, starting from **63** and (*E*)-3-(3,4,5-trimethoxyphenyl)acrylic acid.
Free base: chromatographic eluent: CH_2Cl_2/MeOH/NH_4OH 98:2:0.2. Yield: 53.7.%.
^{1}H-NMR ($CDCl_3$) δ: 7.56 (d, J=16.0 Hz, 1H, *CH*=CH); 7.26 (s, 2H, CH arom.); 6.72 (s, 2H, CH arom.); 6.31 (d, J=16.0 Hz, 1H, CH=*CH*); 4.27 (t, J=6.8 Hz, 2H, CH_2O); 4.22 (t, J=6.8 Hz, 2H, CH_2O); 3.88 (s, 6H, OCH_3); 3.87 (s, 3H, OCH_3); 3.86 (s, 6H, OCH_3); 3.85 (s, 3H, OCH_3); 2.43 (t, J=7.2 Hz, 2H, NCH_2); 2.31 (t, J=7.2 Hz, 2H, NCH_2); 2.20 (s, 3H, NCH_3); 1.89-1.82 (m, 2H, CH_2); 1.77-1.70 (m, 2H, CH_2); 1.50-1.23 (m, 8H, CH_2) ppm. ^{13}C APT NMR ($CDCl_3$) δ: 166.91 (C=O); 166.23 (C=O); 153.43 (C); 152.91 (C); 144.65 (CH=CH); 142.19 (C); 140.17 (C); 129.90 (C); 125.51 (C); 117.36 (CH=CH); 106.84 (CH arom.); 105.28 (CH arom.); 65.19 (CH_2); 63.03 (CH_2); 60.92 (OCH_3); 60.86 (OCH_3); 57.74 (CH_2); 56.23 (OCH_3); 56.15 (OCH_3); 54.26 (CH_2); 42.13 (NCH_3); 29.22 (CH_2); 28.69 (CH_2); 27.38 (CH_2); 27.24 (CH_2); 26.70 (CH_2); 25.97 (CH_2) ppm.
Hydrochloride: mp 89-90 °C**. Anal:** $C_{33}H_{48}ClNO_{10}$ (C, H, N).

5.1.6.23. ***(E)-3-(Methyl-(7-((3-(3,4,5-trimethoxyphenyl)acryloyl)oxy)heptyl)amino)propyl anthracene-9-carboxylate 23***

Procedure B, starting from **62** and anthracene-9-carboxylic acid.
Free base: chromatographic eluent: CH_2Cl_2/MeOH/NH_4OH 98:2:0.2. Yield: 68.5%.

^{1}H-NMR ($CDCl_3$) δ: 8.49 (s, 1H, CH arom.); 8.04 (d, J=8.4 Hz, 2H, CH arom.); 7.98 (d, J=8.4 Hz, 2H, CH arom.); 7.59 (d, J=16.0 Hz, 1H, *CH*=CH); 7.55-7.43 (m, 4H, CH arom.); 6.73 (s, 2H, CH arom.); 6.34 (d, J=16.0 Hz, 1H, CH=*CH*); 4.67 (t, J=6.4 Hz, 2H, CH_2O); 4.18 (t, J=6.8 Hz, 2H, CH_2O); 3,87 (s, 3H, OCH_3); 3,84 (s, 6H, OCH_3); 2.52 (t, J=7.2 Hz, 2H, NCH_2); 2.33 (t, J=7.6 Hz, 2H, NCH_2); 2.23 (s, 3H, NCH_3); 2.09-2.00 (m, 2H, CH_2); 1.72-1.63 (m, 2H, CH_2); 1.49-1.43 (m, 2H, CH_2); 1.39-1.29 (m, 6H, CH_2) ppm. ^{13}C APT NMR ($CDCl_3$) δ: 169.67 (C=O); 167.04 (C=O); 153.41 (C); 144.56 (CH=CH); 140.04 (C); 130.98 (C); 129.96 (C); 129.25 (CH arom.); 128.62 (CH arom.); 126.38 (C); 128.10 (C); 126.92 (CH arom.); 125.46 (CH arom.); 125.02 (CH arom.); 117.51 (CH=CH); 105.19 (CH arom.); 64.66 (CH_2); 64.25 (CH_2); 63.25 (CH_2); 60.96 (OCH_3); 57.88 (CH_2); 56.12 (OCH_3); 54.23 (CH_2); 42.19 (NCH_3); 29.24 (CH_2); 28.73 (CH_2); 27.39 (CH_2); 27.29 (CH_2); 26.70 (CH_2); 25.96 (CH_2) ppm.

Hydrochloride: mp 61-63°C**. Anal:** $C_{38}H_{46}ClNO_7$ (C, H, N).

5.1.6.24. ***(E)-7-(Methyl-(3-((3-(3,4,5-trimethoxyphenyl)acryloyl)oxy)propyl)amino)heptyl anthracene-9-carboxylate 24***

Procedure B, starting from **64** and (*E*)-3-(3,4,5-trimethoxyphenyl)acrylic acid.

Free base: chromatographic eluent: CH_2Cl_2/MeOH/NH_4OH 98:2:0.2. Yield: 42.8.%.

^{1}H-NMR ($CDCl_3$) δ: 8.51 (s, 1H, CH arom.); 8.04-8.00 (m, 4H, CH arom.); 7.59 (d, J=16.0 Hz, 1H, *CH*=CH); 7.55-7.45 (m, 4H, CH arom.); 6.74 (s, 2H, CH arom.); 6.33 (d, J=16.0 Hz, 1H, CH=*CH*); 4.60 (t, J=6.8 Hz, 2H, CH_2O); 4.24 (t, J=6.4 Hz, 2H, CH_2O); 3.87 (s, 3H, OCH_3); 3.86 (s, 6H, OCH_3); 2.48 (t, J=7.2 Hz, 2H, NCH_2); 2.36 (t, J=7.6 Hz, 2H, NCH_2); 2.24 (s, 3H, NCH_3); 1.93-1.83 (m, 4H, CH_2); 1.53-1.48 (m, 4H, CH_2); 1.47-1.38 (m, 2H, CH_2); 1.37-1.30 (m, 2H, CH_2) ppm. ^{13}C APT NMR ($CDCl_3$) δ: 169.73 (C=O); 166.94 (C=O); 153.45 (C); 144.73 (CH=CH); 140.18 (C); 131.01 (C); 129.90 (C); 129.20 (CH arom.); 128.61 (CH arom.); 128.39 (C); 126.90 (CH arom.); 125.45 (CH arom.); 125.01 (CH arom.); 117.33 (CH=CH); 105.30 (CH arom.); 65.88 (CH_2); 62.97 (CH_2); 60.96 (OCH_3); 57.65 (CH_2); 56.17 (OCH_3); 54.22 (CH_2); 42.01 (NCH_3); 29.16 (CH_2); 28.72 (CH_2); 27.35 (CH_2); 27.01 (CH_2); 26.56 (CH_2); 26.07 (CH_2) ppm.

Hydrochloride: low melting solid**. Anal:** $C_{38}H_{46}ClNO_7$ (C, H, N).

5.1.6.25. ***(E)-2-(Methyl-(8-((3-(3,4,5-trimethoxyphenyl)acryloyl)oxy)octyl)amino)ethyl 3,4,5-trimethoxybenzoate 25***

Procedure A, starting from **70** and 3,4,5-trimethoxybenzoic acid.

Free base: chromatographic eluent: CH_2Cl_2/MeOH/NH_4OH 96:4:0.4. Yield: 44.5%.

^{1}H-NMR ($CDCl_3$) δ: 7.58 (d, J=16.0 Hz, 1H, *CH*=CH); 7.29 (s, 2H, CH arom.); 6.74 (s, 2H, CH arom.); 6.34 (d, J=16.0 Hz, 1H, CH=*CH*); 4.40 (t, J=6.0 Hz, 2H, CH_2O); 4.18 (t, J=6.8 Hz, 2H, CH_2O); 3.89 (s, 9H, OCH_3); 3.87 (s, 6H, OCH_3); 3.86 (s, 3H, OCH_3); 2.76 (t, J=6.0 Hz, 2H, NCH_2); 2.42 (t, J=7.6 Hz, 2H, NCH_2); 2.33 (s, 3H, NCH_3); 1.71-1.64 (m, 2H, CH_2); 1.53-1.42 (m, 2H, CH_2); 1.41-1.22 (m, 8H, CH_2) ppm. ^{13}C APT NMR ($CDCl_3$) δ: 167.01 (C=O); 166.15 (C=O); 153.40 (C); 152.88 (C); 144.54 (CH=CH); 142.17 (C); 140.02 (C); 129.94 (C); 125.25 (C); 117.47 (CH=CH); 106.84 (CH arom.); 105.17 (CH arom.); 64.64 (CH_2); 63.14 (CH_2); 60.93 (OCH_3); 60.88 (OCH_3); 58.08 (CH_2); 56.18 (OCH_3); 56.12 (OCH_3); 55.62 (CH_2); 42.82 (NCH_3); 29.45 (CH_2); 29.23 (CH_2); 28.72 (CH_2); 27.41 (CH_2); 27.33 (CH_2); 25.91 (CH_2) ppm.

Hydrochloride: mp 90-93 °C**. Anal:** $C_{33}H_{48}ClNO_{10}$ (C, H, N).

5.1.6.26. ***(E)-8-(Methyl-(2-((3-(3,4,5-trimethoxyphenyl)acryloyl)oxy)ethyl)amino)octyl 3,4,5-trimethoxybenzoate 26***

Procedure A, starting from **71** and (*E*)-3-(3,4,5-trimethoxyphenyl)acrylic acid.

Free base: chromatographic eluent: CH_2Cl_2/MeOH/NH_4OH 95:5:0.5. Yield: 44.2%.

^{1}H-NMR ($CDCl_3$) δ: 7.56 (d, J=16.0 Hz, 1H, *CH*=CH); 7.24 (s, 2H, CH arom.); 6.70 (s, 2H, CH arom.); 6.33 (d, J=16.0 Hz, 1H, CH=*CH*); 4.28-4.22 (m, 4H, CH_2O); 3.85 (s, 6H, OCH_3); 3.84 (s, 3H, OCH_3); 3.83 (s, 6H, OCH_3); 3.82 (s, 3H, OCH_3); 2.68 (t, J=5.6 Hz, 2H, NCH_2); 2.39 (t, J=7.6 Hz, 2H, NCH_2); 2.29 (s, 3H, NCH_3); 1.73-1.66 (m, 2H, CH_2); 1.50-1.19 (m, 10H, CH_2) ppm. ^{13}C APT NMR ($CDCl_3$) δ: 166.87 (C=O); 166.24 (C=O); 153.41 (C); 152.89 (C); 144.99 (CH=CH); 142.10 (C); 140.12 (C); 129.85 (C); 125.51 (C); 117.16 (CH=CH); 106.75 (CH arom.); 105.23 (CH

arom.); 65.21 (CH_2); 61.84 (CH_2); 60.95 (OCH_3); 60.90 (OCH_3); 57.90 (CH_2); 56.23 (OCH_3); 56.14 (OCH_3); 55.53 (CH_2); 42.53 (NCH_3); 29.43 (CH_2); 29.22 (CH_2); 28.71 (CH_2); 27.32 (CH_2); 26.85 (CH_2); 25.94 (CH_2) ppm.
Hydrochloride: mp 77-78°C**. Anal:** $C_{33}H_{48}ClNO_{10}$ (C, H, N).

5.1.6.27. ***(E)-2-(Methyl-(8-((3-(3,4,5-trimethoxyphenyl)acryloyl)oxy)octyl)amino)ethyl anthracene-9-carboxylate 27***

Procedure B, starting from **70** and anthracene-9-carboxylic acid.
Free base: chromatographic eluent: CH_2Cl_2/MeOH/NH_4OH 98:2:0.2. Yield: 47.2%.
^{1}H-NMR ($CDCl_3$) δ: 8.51 (s, 1H, CH arom.); 8.15 (d, J=8.8 Hz, 2H, CH arom.); 8.01 (d, J=8.0 Hz, 2H, CH arom.); 7.59 (d, J=16.0 Hz, 1H, *CH*=CH); 7.54-7.46 (m, 4H, CH arom.); 6.74 (s, 2H, CH arom.); 6.34 (d, J=16.0 Hz, 1H, CH=*CH*); 4.72 (t, J=5.6 Hz, 2H, CH_2O); 4.17 (t, J=6.4 Hz, 2H, CH_2O); 3.88 (s, 3H, OCH_3); 3.87 (s, 6H, OCH_3); 2.86 (t, J=5.6 Hz, 2H, NCH_2); 2.46 (t, J=7.6 Hz, 2H, NCH_2); 2.36 (s, 3H, NCH_3); 1.71-1.61 (m, 2H, CH_2); 1.60-1.40 (m, 2H, CH_2); 1.39-1.24 (m, 8H, CH_2) ppm. ^{13}C APT NMR ($CDCl_3$) δ: 167.06 (C=O); 153.43 (C); 144.55 (CH=CH); 131.00 (C); 129.97 (C); 129.29 (CH arom.); 128.54 (CH arom.); 126.84 (CH arom.); 125.43 (CH arom.); 125.31 (CH arom.); 117.53 (CH=CH); 105.22 (CH arom.); 64.71 (CH_2); 63.29 (CH_2); 60.98 (OCH_3); 58.09 (CH_2); 56.16 (OCH_3); 56.12 (CH_2); 42.53 (NCH_3); 29.49 (CH_2); 29.25 (CH_2); 28.74 (CH_2); 27.40 (CH_2); 25.92 (CH_2) ppm.
Hydrochloride: mp 64-66 °C**. Anal:** $C_{38}H_{46}ClNO_7$ (C, H, N).

5.1.6.28. ***(E)-8-(Methyl-(2-((3-(3,4,5-trimethoxyphenyl)acryloyl)oxy)ethyl)amino)octyl anthracene-9-carboxylate 28***

Procedure A, starting from **72**and (*E*)-3-(3,4,5-trimethoxyphenyl)acrylic acid.
Free base: chromatographic eluent: cyclohexane/ethyl acetate 10:90. Yield: 51.9%.
^{1}H-NMR ($CDCl_3$) δ: 8.52 (s, 1H, CH arom.); 8.03 (d, J=8.8 Hz, 2H, CH arom.); 8.01 (d, J=6.8 Hz, 2H, CH arom.); 7.60 (d, J=16.0 Hz, 1H, *CH*=CH); 7.55-7.46 (m, 4H, CH arom.); 6.74 (s, 2H, CH arom.); 6.38 (d, J=16.0 Hz, 1H, CH=*CH*); 4.60 (t, J=6.8 Hz, 2H, CH_2O); 4.30 (t, J=6.0 Hz, 2H, CH_2O); 3.87 (s, 3H, OCH_3); 3.86 (s, 6H, OCH_3); 2.70 (t, J=5.6 Hz, 2H, NCH_2); 2.40 (t, J=7.2 Hz, 2H, NCH_2); 2.31 (s, 3H, NCH_3); 1.90-1.82 (m, 2H, CH_2); 1.55-1.40 (m, 4H, CH_2); 1.39-1.23 (m, 6H, CH_2) ppm. ^{13}C APT NMR ($CDCl_3$) **δ:** 168.28 (C=O); 166.08 (C=O); 153.44 (C); 144.81 (CH=CH); 140.09 (C); 131.01 (C); 129.93 (C); 129.20 (CH arom.); 128.61 (CH arom.); 128.39 (C); 126.92 (CH arom.); 125.45 (CH arom.); 125.03 (CH arom.); 117.37 (CH=CH); 105.25 (CH arom.); 65.91 (CH_2); 62.86 (CH_2); 60.97 (OCH_3); 57.86 (CH_2); 56.15 (OCH_3); 54.72 (CH_2); 42.13 (NCH_3); 29.27 (CH_2); 28.76 (CH_2); 27.38 (CH_2); 27.11 (CH_2); 26.56 (CH_2); 26.05 (CH_2) ppm.
Hydrochloride: mp 58-60 °C**. Anal:** $C_{38}H_{46}ClNO_7$ (C, H, N).

5.2. Biology.

5.2.1. Cell lines and cultures. The K562 is an undifferentiated erythroleukemia cell line originally derived from a patient with chronic myelogenous leukemia [29]. The K562 leukemia cells and the P-gp over-expressing K562/DOX cells were obtained from Prof. J.P. Marie (Hopital Hotel-Dieu, Paris, France). The cells were cultured following a previously reported protocol [30].
MDCK-MDR1, MDCK-MRP1 and MDCK-BCRP cells are a gift of Prof. P. Borst, NKI-AVL Institute, Amsterdam, Nederland. MDCK cells were grown in DMEM high glucose supplemented with 10% fetal bovine serum, 2 mM glutamine, 100 U/mL penicillin, 100 μg/mL streptomycin, in a humidified incubator at 37 °C with a 5 % CO2 atmosphere. Caco-2 cells were a gift of Dr. Aldo Cavallini and Dr. Caterina Messa from the Laboratory of Biochemistry, National Institute for Digestive Diseases, "S. de Bellis", Bari (Italy).

5.2.2. Drugs and chemicals.
Purified verapamil and pirarubicin were purchased by Sigma-Aldrich (Milan - Italy). Concentrations were determined by diluting stock solutions to approximately 10^{-5} M and using ε_{480} = 11500 M^{-1} cm^{-1}. Stock solutions were prepared just before use. Buffer solutions were HEPES

buffer containing 5 mM HEPES, 132 mM NaCl, 3.5 mM $CaCl_2$, 5 mM glucose, at pH 7.3. Rhodamine-123 was purchased by Sigma-Aldrich (Milan - Italy). Cell culture reagents were purchased from Celbio s.r.l. (Milano, Italy). CulturePlate 96/wells plates were purchased from PerkinElmer Life Science; Calcein-AM, bisBenzimide H 33342 trihydrochloride were obtained from Sigma-Aldrich (Milan, Italy).

5.2.3. P-glycoprotein expression

5.2.3.1. Flow cytometric P-glycoprotein expression

For flow cytometric detection of P-glycoprotein expression, JSB-1 (Millipore) monoclonal antibody was used at 1 µg per 5 x 10^5 cells, the cells were fixed with 70% methanol for 1 min at room temperature, then washed twice with PBS/BSA 1% prior to staining. Primary antibody was incubated for 30 min at room temperature, then detected using fluorescein isothiocyanate (FITC)-conjugated anti- mouse Ig (Life Technologies, Monza, Italy). Isotype control was used at identical concentrations to the P-glycoprotein antibody.

At the end of incubation time, cells were sedimented, washed twice with ice-cold PBS, placed on ice, and kept in the dark until flow cytometric analysis. Samples were analyzed on a FACScanto flow cytometer (Becton Dickinson, San Jose CA, USA) equipped with two lasers at 488/633 nm and FACSDIVA software. The green fluorescence of conjugate JSB-1 antibody was collected by a 530-nm band pass filter. Samples were gated on forward scatter versus side scatter to exclude cell debris and at least 20,000 events were acquired. The fluorescence curves were analyzed by software FCS express 5. For each sample, the amount of P-gp was expressed by the fluorescence ratio between the median fluorescence intensity value of stained sample and negative sample.

Percentage of positive cells was also calculated.

5.2.3.2. Reverse transcript and Real-Time PCR

Total RNA from the cell lines was isolated using Trizol Reagent (Life Technologies, Monza, Italy). One µg of RNA was retro transcribed using iScript (Bio-Rad Milan Italy). PCR amplification was carried out by means of SsoAdvancedTM Universal SYBR® Green Supermix (Bio-Rad, USA) according to manual instruction using the RotorGene 3000 Instrument (Qiagen Germany). Forward and reverse specific primers for MDR1 were used: CAGCTATTCGAAGAGTGGGCACAAAC and GCCTCTGCATCAGCTGGACTGTTG respectively. Ribosomal 18s rRNA was used as the normalizer, FW CGG CTA CCA CAT CCA AGG AA; RV GCT GGA ATT ACC GCG GCT.

Quantitative PCR was performed using the following procedure: 98°C for 1 min, 40 cycles of 98°C for 5 sec, 60°C for 10 sec. The program was set to reveal the melting curve of each amplicon from 60°C to 95°C with a read every 0.5°C.

5.2.4 Modulation of pirarubicin uptake

The uptake of pirarubicin in cells was followed by monitoring the decrease in the fluorescence signal at 590 nm (λ_{ex} = 480 nm) according to the previously described method [43,44].

5.2.5. Inhibition of P-gp-mediated rhodamine-123 (Rhd 123) efflux.

The inhibition of P-gp activity was evaluated by measuring the efflux of the P-gp substrate rhodamine 123 (Rhd 123) in K562/DOX cells, in the absence or in the presence of compounds **17**, **19-21** and **23-28** by a flow cytometric test. Briefly, K562/DOX cells were sedimented and diluted to obtain a cell suspension at 5 10^5 cells/mL in complete RPMI 1640 medium containing rhodamine-123 at a final concentration of 5.0 µM. Cells were loaded with the fluorochrome for 30 min at 37 °C in a humidified atmosphere with 5% CO2 in the presence of the tested compounds at 1.0 µM concentration, or of the reference compound verapamil at 3.0 µM concentration. An aliquot of cells (control) was incubated with the fluorochrome in the absence of inhibitors. All compounds were added 15 min before rhodamine-123. After the accumulation period (30 min), efflux initiated after Rhd 123 washout by sedimentation at 1200 rpm and resuspension in rhodamine-free medium with

or without the modulators (control). The efflux was carried out at 37 °C with 5% CO_2 for 10 min. At the end of both the accumulation and efflux periods, cells were sedimented, washed twice in ice-cold PBS, placed in PBS on ice, and kept in the dark until flow cytometric analysis. Samples were analyzed on a FACScanto flow cytometer (Becton Dickinson, San Jose CA, USA) equipped with two lasers at 488/633 nm and FACSDIVA software. The green fluorescence of rhodamine-123 was collected by a 530-nm band pass filter. Samples were gated on forward scatter versus side scatter to exclude cell debris and at least 20,000 events were acquired.
For each sample, the intracellular amount of Rhd 123 after the efflux time was expressed by the fluorescence ratio, that is the ratio between the median fluorescence intensity value acquired at the end of the efflux phase and that acquired at the end of the uptake phase, expressed as percentage; the same ratio was calculated in the control sample in the absence of the compounds.
The histograms were generated by program GraphPad Prism 5 (GraphPad Prism software, Inc. CA).

5.2.6. Immunoblotting analysis of P-gp, MRP1 and BCRP expression in MDCK, MDCK-MDR1, MDCK-MRP1 and MDCK-BCRP cells.
All MDCK cells were rinsed with lysis buffer (50 mM Tris-HCl, 1 mM EDTA, 1 mM EGTA, 150 mM NaCl, 1% v/v Triton-X100; pH 7.4), supplemented with the protease inhibitor cocktail III (Cabiochem, La Jolla, CA), sonicated and clarified at 13000×g, for 10 min at 4°C. Protein extracts (20 μg) were subjected to SDS-PAGE and probed with the following antibodies: anti-P-glycoprotein (P-gp; 1:250, rabbit polyclonal, #sc-8313, Santa Cruz Biotechnology Inc., Sanat Cruz, CA), anti-multidrug resistant protein 1 (MRP1; 1:500, mouse clone MRPm5, Abcam, Cambridge, UK), anti-breast cancer resistance protein (BCRP; 1:500, mouse clone BXP-21, Santa Cruz Biotechnology Inc.), anti-β-tubulin (1:1000, mouse clone D10, Santa Cruz Biotechnology Inc.), followed by the horseradish peroxidase-conjugated secondary antibodies (Bio-Rad). The membranes were washed with Tris-buffered saline (TBS)/Tween 0.01% v/v. Proteins were detected by enhanced chemiluminescence (Bio-Rad Laboratories).

5.2.7. Calcein-AM experiments
These experiments were carried out as previously described by Teodori et al. with minor modifications [41]. Each cell line (30,000 cells per well) was seeded into black CulturePlate 96/wells plate with 100 μL medium and allowed to become confluent overnight. 100 μL of test compounds were solubilized in culture medium and added to monolayers, with final concentrations ranging from 0.1 to 100 μM. 96/Wells plate was incubated at 37 °C for 30 min. Calcein-AM was added in 100 μL of Phosphate Buffered Saline (PBS) to yield a final concentration of 2.5 μM and plate was incubated for 30 min. Each well was washed 3 times with ice cold PBS. Saline buffer was added to each well and the plate was read with Victor3 (PerkinElmer) at excitation and emission wavelengths of 485 nm and 535 nm, respectively. In these experimental conditions Calcein cell accumulation in the absence and in the presence of tested compounds was evaluated and fluorescence basal level was estimated with untreated cells. In treated wells the increase of fluorescence with respect to basal level was measured. EC_{50} values were determined by fitting the fluorescence increase percentage versus log[dose].

5.2.8. Hoechst 33342 experiment
These experiments were carried out as described by Teodori et al. [41]. Each cell line (30,000 cells per well) was seeded into black CulturePlate 96/wells plate with 100 μL medium and allowed to become confluent overnight. 100 μL of test compounds were solubilized in culture medium and added to monolayers, with final concentrations ranging from 0.1 to 100 μM. 96/Wells plate was incubated at 37 °C for 30 min. Hoechst 33342 was added in 100 μl of Phosphate Buffered Saline (PBS) to yield a final concentration of 8 μM and plate was incubated for 30 min. The supernatants were drained, and the cells were fixed for 20 min under light protection using 100 μL per well of a 4% PFA solution. Each well was washed 3 times with ice cold PBS. Saline buffer was added to

each well and the plate was read with Victor3 (PerkinElmer) at excitation and emission wavelengths of 340/35 nm and 485/20 nm, respectively. In these experimental conditions, Hoechst 33342 accumulation in the absence and in the presence of tested compounds was evaluated and fluorescence basal level was estimated with untreated cells. In treated wells the increase of fluorescence with respect to basal level was measured. EC_{50} values were determined by fitting the fluorescence increase percentage versus log[dose].

5.2.9. ATPlite assay

The MDCK-MDR1 cells were seeded into 96-well microplate in 100 μL of complete medium at a density 2 × 104 cells/well. The plate was incubated overnight (O/N) in a humidified atmosphere 5% CO_2 at 37 °C. The medium was removed and 100 μL of complete medium either alone or containing different concentrations of test compounds was added. The plate was incubated for 2h in a humidified 5% CO_2 atmosphere at 37 °C. 50 μL of mammalian cell lysis solution was added to all wells and the plate shaked for five minutes in an orbital shaker. 50 μL of substrate solution was added to all wells and the plate shaked for five minutes in an orbital shaker. The plate was dark adapted for ten minutes and the luminescence was measured.

5.2.10. Permeability Experiments

5.2.10.1. Preparation of Caco-2 monolayer

Caco-2 cells were seeded onto a Millicell® assay system (Millipore), where a cell monolayer is set in between a filter cell and a receiver plate, at a density of 10,000 cells/well.[14] The culture medium was replaced every 48 h and the cells kept for 21 days in culture. The Trans Epithelial Electrical Resistance (TEER) of the monolayers was measured daily, before and after the experiment, using an epithelial volt-ohmmeter (Millicell® -ERS). Generally, TEER values greater than 1000 Ω for a 21 day culture, are considered optimal.

5.2.10.2. Drug transport experiment

After 21 days of Caco-2 cell growth, the medium was removed from filter wells and from the receiver plate, which were filled with fresh HBSS buffer (Invitrogen). This procedure was repeated twice, and the plates were incubated at 37 °C for 30 min. After incubation time, the HBSS buffer was removed and drug solutions and reference compounds were added to the filter well at the concentration of 100 μM, while fresh HBSS was added to the receiver plate. The plates were incubated at 37 °C for 120 min. Afterwards, samples were removed from the apical (filter well) and basolateral (receiver plate) side of the monolayer to measure the permeability.

The apparent permeability (Papp), in units of nm/second, was calculated using the following equation:

$$P_{app} = \left(\frac{V_A}{\text{Area} \times \text{time}} \right) \times \left(\frac{[\text{drug}]_{\text{acceptor}}}{[\text{drug}]_{\text{initial}}} \right)$$

VA = the volume (in mL) in the acceptor well;
Area = the surface area of the membrane (0.11 cm^2 of the well);
time = the total transport time in seconds (7200 sec);
[drug]acceptor = the concentration of the drug measured by U.V. spectroscopy;
[drug]initial = the initial drug concentration (1 × 10-4 M) in the apical or basolateral wells.

5.3. Molecular modeling

The crystal structure of human P-gp with in the ATP-bound, outward-facing conformation (PDB ID: 6C0V) [35], and the mouse P-gp complexed with BDE100 inhibitor (PDB code 4XWK) [37], were downloaded from PDB database [45]. The molecular structures of synthetized compounds

were optimized prior to docking procedure, by using the Dock Prep application [46], The program performs optimization of ligand structures and conversion of them from 2D to 3D, also providing correction of improper bond distances, bond orders, adding hydrogens and assigning Gasteiger partial charges. Before Docking simulation, a Steepest descent minimization (100 steps at 0.02 Å step size) was taken to remove highly unfavourable clashes, followed by 10 steps of conjugate gradient minimization (0.02 Å step size) to further minimize the energy of the structure, and the "minimize structure UCSF Chimera tool" of UCSF Chimera package [47] was used to analyse their molecular graphics. In order to prepare the ligands and receptor for docking calculation, AutoDock/VinaXB was used [34], then for each compound, the molecular docking study was carried out by the software. The grid box was set to 20Å × 20 Å × 28 Å with a grid space value of 1 Å. The binding box was centred at the previously reported helix TM4 (W232), TM5 (R296, I299, I306), TM6 (Y310, F336), TM7 (F928), TM8 (F303, Y307, F770) and TM12 (M986, Q990, F994), involved in the substrate-binding region [33]. By default, a maximum of 10 poses per ligand were collected. For Autodock/VinaXB program, the parameters used were default. Within the P-gp we performed the Docking simulations on the compounds detailed in Table 1. Docking systems were set up and the results were analysed using PyMOL v2.0 [48]. To identify the network of interaction we used Ligplot+ v.1.4.5 [49] and Protein-Ligand Interaction Profiler [50], all the sets were by default.

5.4. Stability test

5.4.1. Chemicals

Acetonitrile (Chromasolv), formic acid and ammonium formate (MS grade), NaCl, KCl, Na_2HPO_4 $2H_2O$, KH_2PO_4 (Reagent grade) and verapamil hydrochloride (analytical standard, used as internal standard), ketoprofen (analytical standard) were purchased by Sigma-Aldrich (Milan, Italy). Ketoprofen Ethyl Ester (KEE) was obtained by Fisher's reaction from ketoprofen and ethanol.
MilliQ water 18 MΩ cm^{-1} was obtained from Millipore's Simplicity system (Milan - Italy).
Phosphate buffer solution (PBS) was prepared by adding 8.01 g L^{-1} of NaCl, 0.2 g L^{-1} of KCl, 1.78 g L^{-1} of Na_2HPO_4 $2H_2O$ and 0.27 g L^{-1} of KH_2PO_4. Human plasma was collected from healthy male volunteer and kept at -80 °C until use.

5.4.2. Sample preparation

Each sample was prepared adding 10 µL of working solution 1 to 100 µL of tested matrix (PBS or human plasma) in microcentrifuge tubes. The obtained solutions correspond to 1 µM of analyte.
Each set of samples was incubated in triplicate at four different times, 0, 30, 60 and 120 min. at 37 °C. Therefore, the degradation profile of each analyte was represented by a batch of 12 samples (4 incubation times x 3 replicates). After the incubation, the samples were added with 300 µL of ISTD solution and centrifuged (room temperature for 5 min at 10000 rpm). The supernatants were transferred in autosampler vials and dried under a gentle stream of nitrogen.
The dried samples were dissolved in 1.0 mL of 5 mM of ammonium formate and 10 mM formic acid in mQ water: acetonitrile 70:30 (v/v) solution. The obtained sample solutions were analysed by LC-MS/MS methods described in the Supplementary Data section.

Aknowledgements

The authors thank Dr. Cristina Bellucci for her excellent technical assistance. This work was supported by grants from the University of Florence (Fondo Ricerca Ateneo RICATEN16 and RICATEN17).

Supplementary data

Supplementary data related to this article can be found in the online version.

References

[1] L.A. Mitcher, S.P. Pillai, E.J. Gentry, D.M. Shankel, Multiple Drug Resistance, Med. Res. Rev. 19 (1999) 477-496.

[2] R. Callaghan, F. Luk, M. Bebawy, Inhibition of the multidrug resistance P-glycoprotein: time for a change in strategy?, Drug Metab. Dispos. 42 (2014) 623-631.

[3] A.J. Horsey, M.H. Cox, S. Sarwat, I.D. Kerr, The multidrug transporter ABCG2: still more questions than answers. Biochem. Soc. Trans. 44 (2016) 824-830.

[4] E. Baiceanu, K.A. Nguyen, L. Gonzalez-Lobato, R. Nasr, H. Baubichon-Cortay, F. Loghin, M. Le Borgne, L. Chow, A. Boumendjel, M. Peuchmaur, P. Falson, 2-Indolylmethylenebenzofuranones as first effective inhibitors of ABCC2. Eur. J. Med. Chem. 122 (2016) 408–418.

[5] R.H. Ho, R.B. Kim, Transporters and drug therapy: implications for drug disposition and disease, Clin. Pharmacol. Ther. 78 (2005) 260-277.

[6] S. Li, W. Zhang, X. Yin, S. Xing, H.Q. Xie, Z. Cao, B. Zhao, Mouse ATP-Binding cassette (ABC) transporters conferring multi-drug resistance, Anticancer Agents Med. Chem. 15 (2015) 423-432.

[7] W. Li, H. Zhang, Y. G. Assaraf, K. Zhao, X. Xu, J. Xie, D.-H. Yang, Z.-S. Chen, Overcoming ABC transporter-mediated multidrug resistance: molecular mechanisms and novel therapeutic drug strategies. Drug Resist. Updates 27 (2016) 14-29.

[8] R.J. Kathawala, P. Gupta, C.R. Ashb, Jr, Z.S. Chen, The modulation of ABC transporter-mediated multidrug resistance in cancer: A review of the past decade, Drug Resist. Updat. 18 (2015) 1-17.

[9] A. Palmeira, E. Sousa, M.H. Vasconcelos, M.M. Pinto, Three decades of P-gp inhibitors: skimming through several generations and scaffolds, Curr. Med. Chem. 19 (2012) 1946-2025.

[10] D. Waghray, Q. Zhang, Inhibit or evade multidrug resistance P-glycoprotein in cancer treatment, J. Med. Chem. 61 (2018) 5108-5121.

[11] R.A. Darby, R. Callaghan, R.M. McMahon, P-glycoprotein inhibition: the past, the present and the future Curr. Drug Metab. 12 (2011) 722-731.

[12] H.M. Coley, Overcoming multidrug resistance in cancer: clinical studies of P-glycoprotein inhibitors, Methods Mol. Biol. 596 (2010) 341-358.

[13] S. Modok, H.R. Mellor, R. Callaghan, Modulation of multidrug resistance efflux pump activity to overcome chemoresistance in cancer, Curr. Opin. Pharmacol. 6 (2006) 350-354.

[14] G. Szakács, M.D. Hall, M.M. Gottesman, A. Boumendjel, R. Kachadourian, B.J. Day, H. Baubichon-Cortay, A. Di Pietro, Targeting the Achilles heel of multidrug-resistant cancer by exploiting the fitness cost of resistance. Chem Rev. 114 (2014) 5753-74.

[15] T. Wanek, S. Mairinger, O. Langer, Radioligands targeting P-glycoprotein and other drug efflux proteins at the blood-brain barrier. J Labelled Comp. Radiopharm. 56 (2013) 68-77.

[16] R.M. Raaphorst, A.D. Windhorst, P.H. Elsinga, N.A. Colabufo, A.A. Lammertsma, G. Luurtsema, Radiopharmaceuticals for assessing ABC transporters at the blood-brain barrier. Clin. Pharmacol. Ther. 97 (2015) 362-371.

[17] M.A. Schumacher, M.C. Miller, R.G. Brennan, Structural mechanism of the simultaneous binding of two drugs to a multidrug binding protein. EMBO J. 23 (2004) 2923-2930.

[18] E. Teodori, S. Dei, A. Garnier-Suillerot, F. Gualtieri, D. Manetti, C. Martelli, M.N. Romanelli, S. Scapecchi, P. Sudwan, M. Salerno, Exploratory chemistry toward the identification of a new class of multidrug resistance reverters inspired by pervilleine and verapamil models. J. Med. Chem. 48 (2005) 7426-7436.

[19] E. Teodori, C. Martelli, M. Salerno, N. Darghal, S. Dei, A. Garnier-Suillerot, F. Gualtieri, D. Manetti, S. Scapecchi, M. N. Romanelli, Isomeric *N*,*N*-bis(cyclohexanol)amine aryl esters: the discovery of a new class of highly potent Pgp-dependent MDR inhibitors. J. Med. Chem. 50 (2007) 599-602.

[20] M.M. Pires, D. Emmert, C.A. Hrycyna, J. Chmielewski, Inhibition of P-glycoprotein-mediated paclitaxel resistance by reversibly linked quinine homodimers, Mol. Pharmacol. 75 (2009) 92-100.

[21] Z.E. Sauna, M.B. Andrus, T.M. Turner, S.V. Ambudkar, Biochemical basis of polyvalency as a strategy for enhancing the efficacy of P-glycoprotein (ABCB1) modulators: stipiamide homodimers separated with defined-length spacers reverse drug efflux with greater efficacy. Biochemistry 43 (2004) 2262-2271.

[22] K.-F. Chan, I.L.K. Wong, J.W. Kan, C.S.W. Yan, L.M.C. Chow, T.H. Chan, Amine linked flavonoid dimers as modulators for P-glycoprotein-based multidrug resistance: structure-activity relationship and mechanism of modulation. J Med Chem. 55 (2012) 1999−2014.

[23] C. Martelli, M. Coronnello, S. Dei, D. Manetti, F. Orlandi, S. Scapecchi, M.N. Romanelli M. Salerno, E. Mini, E. Teodori, Structure-activity relationships studies in a series of N,N-bis(alkanol)amine aryl esters as P-glycoprotein (Pgp) dependent multidrug resistance (MDR) inhibitors. J. Med. Chem. 53 (2010) 1755-1762.

[24] S. Dei, M. Coronnello, E. Floriddia, G. Bartolucci, C. Bellucci, L. Guandalini, D. Manetti, M. N. Romanelli, M. Salerno, I. Bello, E. Mini, E. Teodori Multidrug Resistance (MDR) reversers: high activity and efficacy in a series of asymmetrical *N*,*N*-bis(arylalkanol)amine aryl esters Eur. J. Med. Chem. 87 (2014) 398-412.

[25] C.B. Lozzio, B.B. Lozzio, Human chronic myelogenous leukemia cell line positive philadelphia chromosome, Blood 45 (1975) 321-334.

[26] J. Vergote, J.L. Moretti, E.G.E. De Vries, A. Garnier-Suillerot, Comparison of the kinetics of active efflux of ^{99m}Tc-MIBI in cells with P-glycoprotein-mediated and multidrug-resistance protein-associated multidrug-resistance phenotype, Eur. J. Biochem. 252 (1998) 140-146.

[27] P. Reungpatthanaphong, C. Marbeuf-Gueye, L. Le Moyec, M. Salerno, A. Garnier-Suillerot, Decrease of P-glycoprotein activity in K562/ADR cells by MβCD and filipin and lack of effect induced by cholesterol oxidase indicate that this transporter is not located in rafts, J. Bioenerg. Biomembr. 36 (2004) 533-543.

[28] T. Saeki, T. Tsuruo, W. Sato, K. Nishikawa Drug resistance in chemotherapy for breast cancer, Cancer Chemother. Pharmacol. 56 (2005) Suppl 1, 84-89.

[29] L. Yalçintepe, E. Halis, S. Ulku, Effect of CD38 on the multidrug resistance of human chronic myelogenous leukemia K562 cells to doxorubicin, Oncol Lett. 11 (2016) 2290–2296.

[30] E. Teodori, S. Dei, M. Coronnello, E. Floriddia, G. Bartolucci, D. Manetti, D. Santo Domingo Porqueras, M. Salerno, *N*-alkanol-*N*-cyclohexanol amine aryl esters: Multidrug resistance (MDR) reversing agents with high potency and efficacy. Eur J Med Chem. 127 (2017) 586-598.

[31] E. Pereira, A. Garnier-Suillerot, Correlation between the short-term measurements of drug accumulation in living cells and the long-term growth inhibition, Biochem Pharmacol. 47 (1994) 1851-1857.

[32] O. Spiga, A. Bernini, M. Scarselli, A. Ciutti, L. Bracci, L. Lozzi, B. Lelli, D. Di Maro, D. Calamandrei, N. Niccolai. Peptide-protein interactions studied by surface plasmon and nuclear magnetic resonances. FEBS Lett. 511 (2002) 33-35.

[33] A. Bernini, O. Spiga, V. Venditti, F. Prischi, L. Bracci, J. Huang, J.A. Tanner, N. Niccolai. Tertiary structure prediction of SARS coronavirus helicase. Biochem Biophys Res Commun. 343 (2006) 1101-1104.

[34] M.R. Koebel, G. Schmadeke, R.G. Posner, S. Sirimulla, AutoDock VinaXB: implementation of XBSF, new empirical halogen bond scoring function, into AutoDock Vina. J. Cheminform. (2016) 8-27.

[35] Y. Kim, J. Chen Molecular structure of human P-glycoprotein in the ATP-bound, outward-facing conformation. Science 359 (2018) 915-919.

[36] J.W. McCormick, P.D. Vogel, J.G. Wise, Multiple Drug Transport Pathways through Human P-Glycoprotein, Biochemistry 54 (2015) 4374-4390.

[37] S.C. Nicklisch, S.D. Rees, A.P. McGrath, T. Gökirmak, L.T. Bonito, L.M. Vermeer, C. Cregger, G. Loewen, S. Sandin, G. Chang, A. Hamdoun, Global marine pollutants inhibit P-glycoprotein: Environmental levels, inhibitory effects, and cocrystal structure, Sci. Adv. 2 (2016) 2(4): e1600001.

[38] A. Daina, O. Michielin, V. Zoete, SwissADME: a free web tool to evaluate pharmacokinetics, drug-likeness and medicinal chemistry friendliness of small molecules, Sci. Rep. 7 (2017) 42717.

[39] H. Pajouhesh, G.R. Lenz, Medicinal Chemical Properties of Successful Central Nervous System Drugs NeuroRx. 2 (2005) 541–553.

[40] L. Chang, M. Xiao, L. Yang, S. Wang, SQ Wang, A. Bender, A. Hu, ZS Chen, BY, HM Liu, Discovery of a non-toxic [1,2,4]triazolo[1,5-a]pyrimidin-7-one (WS-10) that modulates ABCB1-mediated multidrug resistance (MDR), Bioorg. Med. Chem. 26 (2018) 5974-5985.

[41] E. Teodori, S. Dei, G. Bartolucci, M.G. Perrone, D. Manetti, M.N. Romanelli, M. Contino, N.A. Colabufo. Structure-Activity Relationship Studies on 6,7-dimethoxy-2-phenethyl-1,2,3,4-tetrahydroisoquinoline derivatives as Multidrug Resistance (MDR) reversers, ChemMedChem. 12 (2017) 1369-1379.

[42] J.W. Polli, S.A. Wring, J.E. Humphreys, L. Huang, J.B. Morgan, L.O. Webster, C.S. Serabjit-Singh, Rational use of in vitro P-glycoprotein assays in drug discovery. J. Pharmacol. Exp. Ther. 299 (2001) 620-628.

[43] S. Mankhetkorn, A. Garnier-Suillerot, The ability of verapamil to restore intracellular accumulation of anthracyclines in multidrug resistant cells depends on the kinetics of their uptake, Eur J Pharmacol. 343 (1998) 313-321.

[44] C. Marbeuf-Gueye, M. Salerno, P. Quidu, A. Garnier-Suillerot, Inhibition of the P-glycoprotein- and multidrug resistance protein-mediated efflux of anthracyclines and calceinacetoxymethyl ester by PAK-104P. Eur J Pharmacol. 391 (2000) 207-216.

[45] H.M. Berman, J. Westbrook, Z. Feng, G. Gilliland, T.N. Bhat, H. Weissig, I.N. Shindyalov, P.E. Bourne. The Protein Data Bank, Nucleic Acids Res. 28 (2000) 235-242.

[46] P.T. Lang, S.R. Brozell, S. Mukherjee, E.F. Pettersen, E.C. Meng, V. Thomas, R.C. Rizzo, D.A. Case, T.L. James, I.D. Kuntz, RNA 15 (2009) 1219-30.

[47] Chimera is developed by the Resource for Biocomputing, Visualization, and Informatics at the University of California, San Francisco (supported by NIGMS P41-GM103311).

[48] The PyMOL Molecular Graphics System, Version 2.0 Schrödinger, LLC.

[49] A.C. Wallace, R.A. Laskowski, J.M. Thornton. LIGPLOT: a program to generate schematic diagrams of protein-ligand interactions, Protein Eng. 8 (1995) 127–134.

[50] S. Salentin, S. Schreiber, V.J. Haupt, M.F. Adasme, M. Schroeder, PLIP: fully automated protein–ligand interaction profiler. Nucleic Acids Res. (2015) W443–W447.

Highlights

- A new series of *N*,*N*-bis(alkanol)amine aryl esters was designed and synthesized
- The compounds were tested on K562/DOX cells in the pirarubicin uptake assay
- *In silico* studies and stability tests in PBS and human plasma were also performed
- Further experiments confirmed that they are P-gp-dependent MDR reversers
- A different selectivity *vs* sister proteins MRP1 and BCRP was highlighted.